

AN ABSTRACT OF THE THESIS OF

Seung-Ho Hong for the degree of Master of Science in Mechanical Engineering  
presented on April 14, 1994.

Title : Monte Carlo Simulation of Radiation Heat Transfer in a Three-Dimensional  
Enclosure Containing a Circular Cylinder

Redacted for Privacy

Abstract approved :

James R. Welty

The distribution of radiation heat flux within an enclosure containing a horizontal circular pipe, which also contains a medium which has absorbing, emitting and isotropic scattering characteristics was studied using the Monte Carlo method. The MCHO3D Monte Carlo code was developed for this three-dimensional geometry.

This study consisted of three parts. First, a comparison with results of previous work in one- and two-dimensional cases was conducted to validate the MCHO3D Monte Carlo code. The other two parts were conducted for the three-dimensional enclosure for the case without and with an absorbing and scattering medium present.

The bottom surface of the square enclosure was considered a uniform-heat flux surface and the other surfaces were considered cold. Enclosure surfaces were treated as black walls. A circular pipe was located in the center of the enclosure; its length varied with enclosure depth. In the second part of this study (cases 1, 2), different configurations were used with an optically thin ( $\tau \ll 1$ ) medium in the enclosure, and for part 3 different optical thicknesses were used with a range of enclosure size.

The amount of radiative energy transferred to the enclosed pipe depends on its location, the optical thickness of the participating medium, and enclosure depth. For the optically thin cases ( $\tau \ll 1$ ) the Monte Carlo solution calculates view factors which are generally applicable for geometric descriptions.

**MONTE CARLO SIMULATION OF RADIATION HEAT  
TRANSFER IN A THREE - DIMENSIONAL ENCLOSURE  
CONTAINING A CIRCULAR CYLINDER**

by

Seung - Ho Hong

A THESIS

Submitted to

Oregon State University

in partial fulfillment of  
the requirements for the  
degree of

Master of Science

Completed April 14, 1994

Commencement June 1994

APPROVED

Redacted for Privacy

---

Professor of Mechanical Engineering in charge of major

Redacted for Privacy

---

Head Department of Mechanical Engineering

Redacted for Privacy

---

Dean of Graduate School

Date thesis is presented April 14, 1994

Typed by Seung-Ho Hong

## **ACKNOWLEDGMENTS**

I am especially thankful to my major professor, Dr. James R. Welty, for his encouragement and guidance throughout the course of this study.

Thanks to my parents, brother and sister for their love and encouragement.

## TABLE OF CONTENTS

Chapter	Page
<b>1. INTRODUCTION</b>	1
<b>2. MONTE CARLO METHOD</b>	4
<b>2.1 Introduction and Definition</b>	4
<b>2.2 Review of the Monte Carlo method in Radiative Heat Transfer Analysis</b>	5
<b>2.3 Advantages and Disadvantages of Monte Carlo method</b>	6
<b>2.4 Monte Carlo method in Radiative Heat Transfer</b>	8
<b>2.4.1 Probability Distributions</b>	8
<b>2.4.2 Random Number Relations</b>	9
<b>2.4.2.1 Emission Points of Bundle</b>	10
<b>2.4.2.2 Choosing the Direction of Emission</b>	11
<b>2.4.2.3 Absorption and Reflection</b>	12
<b>2.4.2.4 Directions for Emission from within Medium</b>	12
<b>2.4.2.5 Path Length of Bundle within Medium</b>	13
<b>2.5 Equations for Solutions</b>	16
<b>2.5.1 Net Heat Transfer to surfaces</b>	16
<b>2.5.2 Gas Emissive Power Distribution</b>	17
<b>3. NUMERICAL ANALYSIS</b>	19
<b>3.1 Algorithm of MCHO3D</b>	20
<b>4. MODEL PARAMETERS</b>	29
<b>5. RESULTS AND DISCUSSION</b>	32
<b>5.1 Comparison with other methods</b>	32
<b>5.2 Geometric Variations</b>	37
<b>5.3 Optical Thickness Effects</b>	39
<b>6. CONCLUSIONS</b>	74
<b>BIBLIOGRAPHY</b>	75

**APPENDICES**

78

**Appendix 1 Radiative heat flux between perpendicular  
surface**

79

**Appendix 2 Program listing for MCHO3D**

80

## LIST OF FIGURES

Figure	Page
1. Geometrical configuration	3
2. Comparison of Monte Carlo and conventional solution techniques	7
3. Inclosure composed of n discrete surface areas and filled with uniform gas with radiation mode	16
4. Numerical model configuration	19
5. Trajectory of bundle	21
6. Reflection mode on wall surface	22
7. Flow chart of MCHO3D	26
8. Geometrical configuration	30
9. Heat transfer between infinite parallel gray plates containing a gray medium	35
10. Distribution of emissive power in gray medium with no source	35
11. Incident radiation of medium along the vertical center line at $x = X/2$	36
12. Variation of view factors with enclosure depth and pipe location (--- refers to $Y/X = \infty$ )	42
13. Variation of view factors with enclosure depth (--- refers to $Y/X = \infty$ )	42
(a) $Dz = 2.0$	
(b) $Dz = 4.0$	
(c) $Dz = 5.0$	
(d) $Dz = 6.0$	
(e) $Dz = 8.0$	

14. Distribution of radiation heat flux around pipe at  $y = Y/2$  with enclosure depth 45
- (a)  $Dz = 2.0$
  - (b)  $Dz = 4.0$
  - (c)  $Dz = 5.0$
  - (d)  $Dz = 8.0$
15. Distribution of radiation heat flux to center line of side walls,  $y = Y/2$  47
- (a)  $Dz = 2.0$
  - (b)  $Dz = 4.0$
  - (c)  $Dz = 5.0$
  - (d)  $Dz = 8.0$
16. Distribution of radiation heat flux to center line of top surface ,  $y = Y/2$  49
- (a)  $Dz = 4.0$
  - (b)  $Dz = 5.0$
  - (c)  $Dz = 6.0$
  - (d)  $Dz = 8.0$
17. Variation of view factors  $F_{1,j}$  with enclosure depth and pipe diameter (--- refers to  $Y/X = \infty$  ) 51
18. Variation of view factors with enclosure depth (--- refers to  $Y/X = \infty$  ) 51
- (a)  $D = 2.0$
  - (b)  $D = 5.0$
  - (c)  $D = 8.0$
  - (d)  $D = 10.0$
19. Variation of radiation heat transfer rate on pipe with enclosure depth and optical thickness 54
20. Variation of radiation heat transfer rates with enclosure depth ( $\tau = 0.1, 0.5, 1.0, 3.0, 5.0, 10.0$  ) 55
- (a)  $\tau = 0.1$
  - (b)  $\tau = 0.5$
  - (c)  $\tau = 1.0$

- (d)  $\tau = 3.0$   
 (e)  $\tau = 5.0$   
 (f)  $\tau = 10.0$
21. Distribution of radiation heat flux around pipe  
 at  $y = Y/2$  with optical thickness 58
22. Distribution of radiation heat flux to center line of  
 bottom surface at  $y = Y/2$  with optical thickness 58
23. Distribution of radiation heat flux to center line of  
 top surface at  $y = Y/2$  with optical thickness 59
24. Distribution of radiation heat flux to center line of  
 side wall at  $y = Y/2$  with optical thickness 59
25. Distribution of radiation heat flux around pipe  
 surface ( $\tau = \ll 1, 0.5, 1.0, 3.0, 5.0, 10.0$ ) 60
- (a)  $\tau \ll 1$   
 (b)  $\tau = 0.5$   
 (c)  $\tau = 1.0$   
 (d)  $\tau = 3.0$   
 (e)  $\tau = 5.0$   
 (f)  $\tau = 10.0$
26. Distribution of radiation heat flux on bottom surface  
 ( $\tau = 0.5, 1.0, 3.0, 5.0, 10.0$ ) 63
- (a)  $\tau = 0.5$   
 (b)  $\tau = 1.0$   
 (c)  $\tau = 3.0$   
 (d)  $\tau = 5.0$   
 (e)  $\tau = 10.0$
27. Distribution of radiation heat flux on top surface  
 ( $\tau = \ll 1, 0.5, 1.0, 3.0, 5.0, 10.0$ ) 65
- (a)  $\tau \ll 1$   
 (b)  $\tau = 0.5$   
 (c)  $\tau = 1.0$   
 (d)  $\tau = 3.0$   
 (e)  $\tau = 5.0$

28. Distribution of radiation heat flux on side walls  
( $\tau = \ll 1, 0.5, 1.0, 3.0, 5.0, 10.0$ )

68

- (a)  $\tau \ll 1$
- (b)  $\tau = 0.5$
- (c)  $\tau = 1.0$
- (d)  $\tau = 3.0$
- (e)  $\tau = 5.0$
- (f)  $\tau = 10.0$

29. Distribution of radiation heat flux on wall 5,6  
( $\tau = \ll 1, 0.5, 1.0, 3.0, 5.0, 10.0$ )

71

- (a)  $\tau \ll 1$
- (b)  $\tau = 0.5$
- (c)  $\tau = 1.0$
- (d)  $\tau = 3.0$
- (e)  $\tau = 5.0$
- (f)  $\tau = 10.0$

## NOMENCLATURE

$a_n$	scattering phase function coefficients
$A_i$	area of surface $i$ of enclosure
$D$	diameter of pipe
$E$	emissive power
$E_b$	blackbody emissive power
$G$	incident radiation
$I$	intensity of radiation
$L$	path length
$N$	number of emitted bundles per unit volume or area
$N_{total}$	total number of bundle emitted from wall 1
$P$	probability function
$P_n$	Legendre polynomials
$Q_1$	emissive power of wall 1
$\hat{r}$	unit vector into a given direction
$R$	random number
$s$	path length
$SN_i$	total number of absorptions in given area element
$T$	Temperature
$\Delta V$	volume element
$x$	horizontal direction
$X$	horizontal length of enclosure
$y$	direction in enclosure depth
$Y$	depth of enclosure
$z$	vertical direction
$Z$	vertical length of enclosure
$\alpha$	absorptance or absorptivity
$\beta$	extinction coefficient

$\epsilon$	emittance or emissivity
$\theta$	polar angle
$\kappa$	absorption coefficient
$\sigma$	Stefan - Boltzmann constant
$\sigma_s$	scattering coefficient
$\tau$	optical thickness
$\phi$	azimuthal angle
$\omega$	energy per photon bundle
$\omega$	single scattering albedo
$\Phi$	scattering phase function
$\Phi_p, \Phi_b$	dimensionless temperature in medium
$\varphi_p$	dimensionless emissive power in medium
$\Psi_p$	dimensionless radiative heat flux
$\Omega'$	solid angle

### Subscriptions

i	incident, incoming
e	emitted, outgoing
g	gas, medium
p	medium increment index
1,2,x,y,z	in a given direction
$\lambda$	at a given wavelength, or per unit wavelength
$\lambda$	wavelength dependent
$\theta, \phi$	in a given direction

### Superscripts

/	directional quantity or dummy variable
*	dummy variable

**MONTE CARLO SIMULATION OF RADIATION HEAT  
TRANSFER IN A THREE-DIMENSIONAL ENCLOSURE  
CONTAINING A CIRCULAR CYLINDER**

**CHAPTER 1**

**INTRODUCTION**

In any process involving high temperatures such as heat treatment, power generation, and other large-scale industrial applications, radiation heat transfer is an important mechanism in addition to convection and conduction. Many investigators have studied radiation heat transfer problems over the past several decades.

Early radiation research was confined to one-dimensional cases involving absorbing, emitting, and/or isotropic scattering media [1,2,3]. As one-dimensional analyses of radiative heat transfer are often inadequate, it has been necessary to broaden the research to include multidimensional geometries. In recent years many studies have dealt with multidimensional enclosures with absorbing, emitting, and scattering media present. Most of these studies were focused on solving the radiative transfer equation with few parametric studies on design factors in simple enclosures. It has been the purpose of the present study to determine appropriate parameters to describe radiant transfer in a geometry of practical interest.

A variety of computational tools for analyzing radiative heat transfer

problems have been proposed in the past several decades. Each of the methods developed has been successfully applied to simple one-dimensional gray problems. However, no single method is now accepted as being the best for all complicated problems. One of the more popular current methods is the Monte Carlo method [4,5,6,7,8], a statistical method in which the history of large numbers of photon bundles is traced. The Monte Carlo method has the advantage that almost any problem of arbitrary complexity can be addressed with relative ease, but has the disadvantages of statistical scatter in the results and its large appetite for computer time. With the developments in computer technology the second disadvantage is disappearing, and we can expect more accurate and faster results from these kinds of simulations.

In this paper a square duct with a centered, circular pipe as shown in figure 1, was examined, and the relevant heat exchange between surfaces was determined using the Monte Carlo method. The bottom surface of the square enclosure was considered a uniform-heat flux surface; it radiated to walls considered cool enough so their emission was small, with their surfaces rough and soot-covered so they were treated as black walls. A circular pipe was located in the enclosure and its length varied with enclosure depth.

In cases 1 and 2, different configurations were used with an optically thin medium in the enclosure. In cases 3 and 4, different optical thicknesses were used for a range of enclosure depths. Through these simulations useful design factors were obtained and presented parametrically.

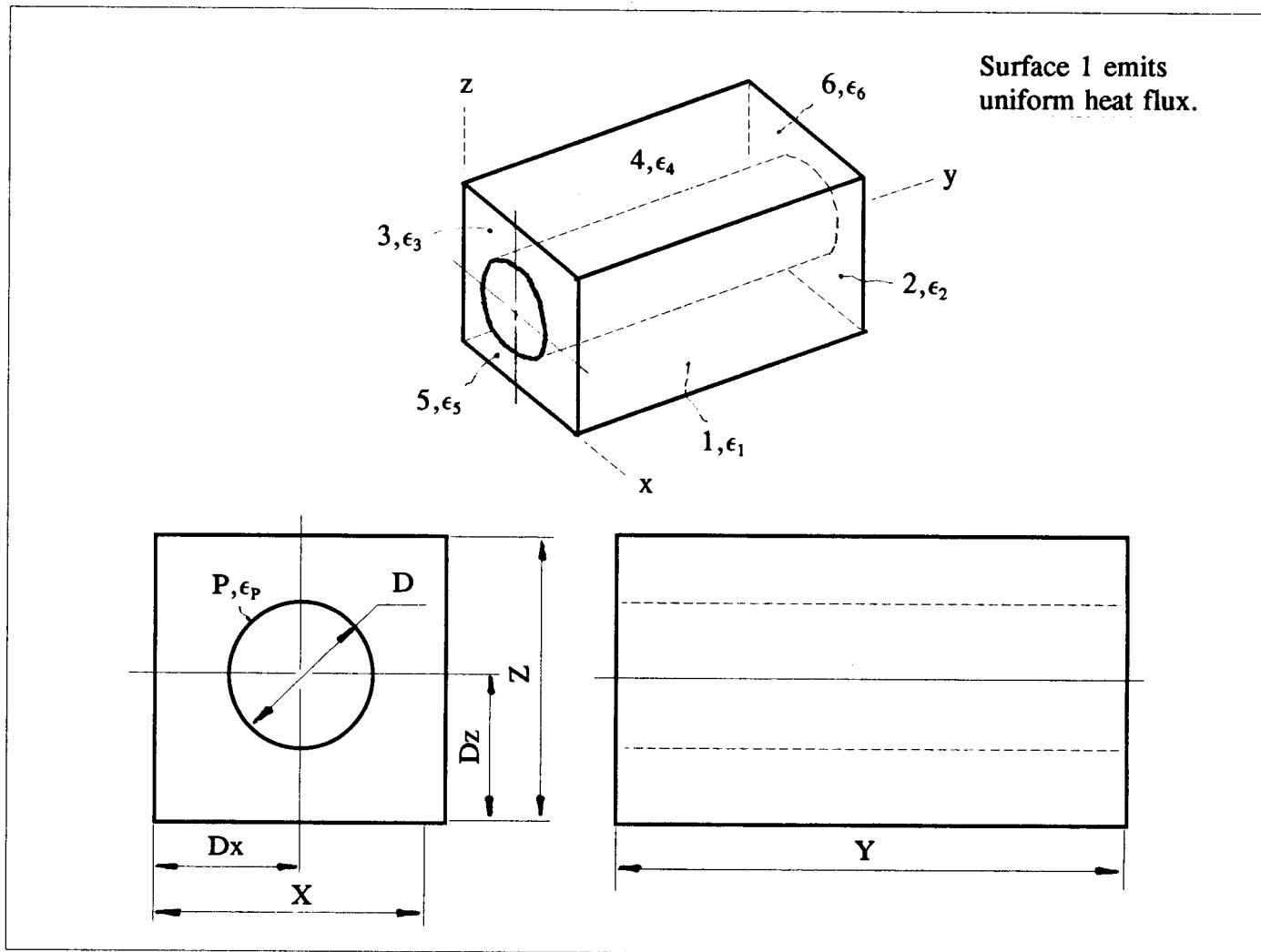


Figure 1. Geometrical configuration.

## CHAPTER 2

### MONTE CARLO METHOD

#### 2.1. Introduction and Definition

There are several different computational methods with which radiative heat transfer problems may be analyzed. One of the more popular ones is the Monte Carlo method, a statistical method in which the history of large numbers of photon bundles is traced.

A good definition for the Monte Carlo method has been given by Kahn [9], who wrote " The expected score of a player in any reasonable game of chance, however complicated, can in principle be estimated by averaging the results of a large number of plays of the game. Such estimation can be rendered more efficient by various devices which replace the game with another known to have the same expected score. The new game may lead to a more efficient estimate by being less erratic, that is, having a score of lower variance or by being cheaper to play with the equipment on hand. There are obviously many problems about probability that can be viewed as problems of calculating the expected score of a game. Still more, there are problems that do not concern probability but are none the less equivalent for some purposes to the calculation of an expected score. The Monte Carlo method refers simply to the exploitation of these remarks."

This definition also gives us a good opportunity to apply this method to

other areas. Indeed what must be done for a specific problem is to set up a game or model that obeys the same behavior and hence is expected to produce the same outcome as the physical problem which the model simulates; make the game as simple and fast to play as possible; then play the game many times and find the average outcome. After some remarks on previous uses of the method, this formalism will be applied to the given application in radiative heat transfer.

## **2. 2. Review of the Monte Carlo method in Radiative Heat Transfer Analyses**

Like several other radiative heat transfer models, the Monte Carlo method was first employed in the field of neutron transport, for the development of the atomic bomb during World War II. The first radiative heat transfer papers using this method were published by Howell and Perlmutter [2], and Perlmutter and Howell [10]. They treated radiation through gases in simple geometries such as plane walls and concentric cylinders. Subsequently many investigators, Fleck [11], Howell et al [12], for example, have used the method to solve more practical problems.

Recent applications of the Monte Carlo method have appeared that exploit its flexibility and power to examine difficult problems. A few of these can be cited to give the overall flavor of these applications. Slater et al.[13], Bernes [14], Meier and Lee [15], Katkovskii et al.[16], and Vlasov and Titarchuk [17] all have used Monte Carlo approaches to solve problems in which the medium was not assumed to be in local thermodynamic equilibrium (LTE). Carter et al.[18] used

the method to include the effects of polarization on radiative transfer. Egan and Hilgeman[19] examined the spectral reflectance of particulates. Dunn [20] has applied the method to nonhomogeneous media. Gupta et al.[21] included anisotropic scattering in their Monte Carlo analysis of coal furnaces with fly-ash. Lewis and Miller [22] and Meier et al.[23] have presented valuable information on Monte Carlo applications in scattering problems.

### **2.3. Advantages and Disadvantages of the Monte Carlo method**

The advantage of the Monte Carlo method is in its flexibility. It is extremely useful when (1) there is no other convenient method, (2) a simple procedure is needed to check the validity of a new method, and (3), in some instances, a computationally faster procedure is needed[Haji-Sheikh,8]. Indeed, it is refreshing to see that Monte Carlo program complexity increases roughly in proportion to problem complexity for radiative interchange problems. As the complexity of the problem increases, however, the complexity of formulation and the solution effort increase much more rapidly for conventional techniques. For problems beyond a certain complexity, the Monte Carlo solution will be preferable, as schematically indicated in Figure 2 [Modest, 7]. As mentioned by Modest, there is no way to determine a priori precisely where this crossover point in complexity lies.

Another disadvantage of Monte Carlo methods is that, as with other statistical methods, the results calculated fluctuate around the real answer, similar

to the unavoidable error associated with experimental measurements, because the method is a repetitive experiment using a mathematical model in place of the actual physical situation. The uncertainty can be found by applying standard statistical tests; the uncertainty can be reduced in the same manner as experimental error,

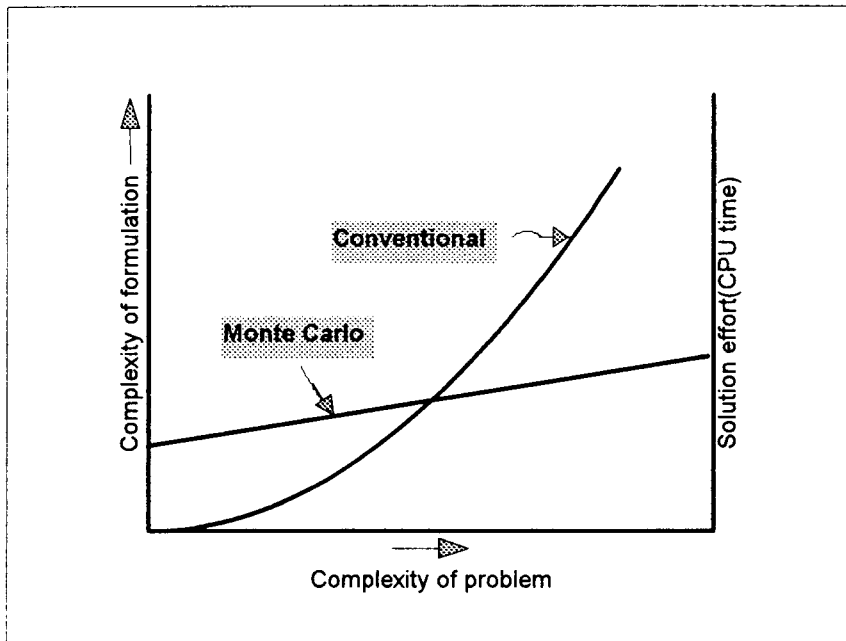


Figure 2. Comparison of Monte Carlo and conventional solution techniques [Modest, 7].

that is, by averaging over more tests (bundle histories in radiative problems).

No rigorous criteria exist to guarantee the convergence of Monte Carlo results to a valid solution; however, convergence has not as yet been a difficulty in thermal radiation problems. It would be immediately evident that convergence to invalid solutions was occurring because of the limiting solutions and physical

constraints that are known for most radiative problems. It should be noted that the latter fault is common to many methods when complex problems are being treated because rigorous mathematical criteria to guarantee convergence to a solution is available only in certain cases.

## 2.4. Monte Carlo method in Radiative Heat Transfer

### 2.4.1. Probability Distributions

In order to follow the history of radiative energy bundles in a statistically meaningful way, the points, directions and wavelengths of emission, reflective behavior, etc. must be chosen according to probability distributions.

As an example, consider the total radiative heat flux being emitted from a surface, i.e., the total emissive power,

$$E = \int_0^{\infty} E_{\lambda} d\lambda = \int_0^{\infty} \epsilon_{\lambda} E_{b\lambda} d\lambda \quad (1)$$

Between the wavelengths of  $\lambda$  and  $\lambda + d\lambda$  the emitted heat flux is  $E_{\lambda} d\lambda = \epsilon_{\lambda} E_{b\lambda} d\lambda$  and the fraction of energy emitted over this wavelength range is

$$P(\lambda) d\lambda = \frac{E_{\lambda} d\lambda}{\int_0^{\infty} E_{\lambda} d\lambda} = \frac{E_{\lambda}}{E} d\lambda \quad (2)$$

We may think of all the photons leaving the surface as belonging to a set of  $N$  energy bundles of equal energy (each consisting of many photons of a single

wavelength). Then each bundle carries the amount of energy ( $E/N$ ) with it, and the probability that any particular bundle has a wavelength between  $\lambda$  and  $\lambda + d\lambda$  is given by the probability density function  $P(\lambda)$ . The fraction of energy emitted over all wavelengths between 0 and  $\lambda$  is then

$$R(\lambda) = \int_0^\infty P(\lambda) d\lambda = \frac{\int_0^\lambda E_\lambda d\lambda}{\int_0^\infty E_\lambda d\lambda} \quad (3)$$

It is immediately obvious that  $R(\lambda)$  is also the probability that any given energy bundle has a wavelength between 0 and  $\lambda$ , and it is known as the cumulative distribution function. The probability that a bundle has a wavelength between 0 and  $\infty$  is, of course,  $R(\lambda \rightarrow \infty) = 1$ , a certainty. Equation ( 3 ) implies that if we want to simulate emission from a surface with  $N$  energy bundles of equal energy, then the fraction  $R(\lambda)$  of these bundles must have wavelengths smaller than  $\lambda$ .

#### **2.4.2. Random Number Relations**

In the Monte Carlo method a large statistical sample of photon energy bundles are traced from their point of emission to their point of absorption (or their leaving the geometry under investigation). To obtain statistically meaningful results, relations need to be developed between random numbers and points of

emission (from a surface, or from within the medium), direction of emission, wavenumber of emission, distance traveled before absorption (within the medium), distance traveled before scattering, scattering direction, probability of reflection from a surface, and reflection direction.

#### 2.4.2.1. Emission Points of Bundle

In a two dimensional plane-surface system, for example, the relationship between random number,  $R$ , and given length of system,  $X$  or  $Y$ , may be inverted to find the  $x$  or  $y$  location of the emission point. Similar to equation (3) we may write the cumulative distribution function for emission point  $x$ ,  $y$  as

$$R_x = \frac{\int_0^x E_x(x) dx}{\int_0^X E_x(x) dx} \quad (4)$$

$$R_y = \frac{\int_0^y E_y(y) dy}{\int_0^Y E_y(y) dy} \quad (5)$$

respectively. In the simplest case of an isothermal surface with constant emissivity, these relations reduce to

$$x = R_x X, \quad y = R_y Y. \quad (6)$$

### 2.4.2.2. Choosing the Direction of Emission

To choose the direction of emission from an emission point or reflecting point the probability of emission into a particular direction is used. Two angles must be specified, the polar angle  $\theta$  and azimuthal angle  $\phi$ .

The probability density function  $P(\theta)$  over all wavelengths and azimuthal angles is

$$\begin{aligned} P(\theta) d\theta &= d\theta \int_0^{2\pi} \int_0^\lambda P(\lambda, \theta, \phi) d\lambda d\phi \\ &= \frac{2\epsilon'(\theta) \cos\theta \sin\theta d\theta}{\epsilon} \end{aligned} \quad (7)$$

Integrating equation (7) with respect to  $\theta$  between 0 and  $\theta$ , the cumulative probability function is

$$R(\theta) = \int_0^\theta P(\theta^*) d\theta^* = \frac{2 \int_0^\theta \epsilon'(\theta^*) \sin\theta^* \cos\theta^* d\theta^*}{\epsilon} \quad (8)$$

For a diffuse gray emitter equation(8) reduces to

$$\begin{aligned} R(\theta)_{,diffuse} &= 2 \int_0^\theta \sin\theta^* \cos\theta^* d\theta^* \\ &= \sin^2\theta \end{aligned} \quad (9)$$

or

$$\theta = \sin^{-1}(R(\theta)_{,diffuse})^{1/2} \quad (10)$$

Similar arguments apply to the determination of the azimuthal angle,  $\phi$ ,

$$R(\phi) = \frac{\phi}{2\pi} \quad \text{or} \quad \phi = 2\pi R(\phi) \quad (11)$$

#### 2.4.2.3. Absorption and Reflection

When radiative energy impinges on a surface, the fraction  $\alpha'_\lambda$  will be absorbed, which may depend on the wavelength of irradiation, the direction of the incoming rays, and, perhaps, the local temperature. Of many incoming bundles the fraction  $\alpha'_\lambda$  will therefore be absorbed while the rest,  $1 - \alpha'_\lambda$ , will be reflected. This can clearly be simulated by picking a random number,  $R_\alpha$ , and comparing with  $\alpha'_\lambda$  ;

$$\begin{aligned} R(\alpha) \leq \alpha'_\lambda & \quad (\text{absorbed}) \\ R(\alpha) > \alpha'_\lambda & \quad (\text{reflected}) \end{aligned} \quad (12)$$

#### 2.4.2.4. Directions for Emission from within Medium

Under local thermodynamic equilibrium conditions emission within a participation medium is isotropic, i.e., all possible directions are equally likely for the emission of a photon. All possible directions from a point within the medium, are contained within the solid angle of  $4\pi = \int_0^{2\pi} \int_0^\lambda \sin\theta \, d\theta \, d\phi$

The probability distribution for emission corresponding to angle  $\theta$  is given by

$$P(\theta) = \frac{\sin\theta d\theta}{\int_0^\pi \sin\theta d\theta} \quad (13)$$

The cumulative distribution function then becomes

$$R(\theta) = \frac{1}{2} \int_0^\theta \sin\theta^* d\theta^* = \frac{1}{2}(1 - \cos\theta) \quad (14)$$

or, the angle  $\theta$  can be expressed as

$$\theta = \cos^{-1}(1 - 2R(\theta)) \quad (15)$$

Similarly

$$R(\phi) = \frac{\phi}{2\pi} \quad \text{or} \quad \phi = 2\pi R(\phi) \quad (16)$$

Here, the polar angle,  $\theta$ , and azimuthal angle,  $\phi$ , are measured from arbitrary reference coordinates.

#### 2.4.2.5. Path Length of Bundle within Medium

If the medium through which radiative energy travels is participating, then any incident beam will be attenuated by absorption and scattering. Equation (17) gives the absorptivity for the participating medium (for a given path within the medium) as

$$\alpha_\lambda = 1 - \exp\left(-\int_0^S \kappa_\lambda ds\right) \quad (17)$$

Here we can replace  $\alpha_\lambda$  by a random number from 0 to 1. Therefore the path

length of a certain bundle within the absorbing medium is

$$L_{\kappa} = -\frac{1}{\kappa_{\lambda}} \ln[1 - R(\kappa)] \quad (18)$$

Since  $R(s)$  is uniformly distributed between 0 and 1, this relation may as well as written as

$$L_{\kappa} = -\frac{1}{\kappa_{\lambda}} \ln R(\kappa) \quad (19)$$

According to this relation, the bundle is allowed to travel a total distance,  $L_{\kappa}$ , through the medium before being absorbed.

Scattering will also attenuate the bundle intensity. The same relationships apply to the scattering cases as for absorption, thus

$$L_{\sigma} = -\frac{1}{\sigma_{s\lambda}} \ln R(\sigma_s) \quad (20)$$

is the distance a bundle travels in a medium with uniform scattering coefficient before being scattered, or

$$\int_0^l \sigma_{s\lambda} ds < \int_0^L \sigma_{s\lambda} ds = \ln \frac{1}{R(\sigma_s)} \quad (21)$$

for a medium with nonuniform scattering coefficient.

Here, we can use the useful conception, extinction. The total attenuation of the beam by both absorption and scattering is calculated introducing the extinction coefficient which is defined as

$$\beta_{\lambda} = \kappa_{\lambda} + \sigma_{s\lambda} \quad (22)$$

so that equation (17) becomes

$$\alpha_\lambda = 1 - \exp\left[-\int_0^L \beta_\lambda dL\right] \quad (23)$$

and the path length is

$$L_\beta = -\frac{1}{\beta_\lambda} \ln R(\beta) \quad (24)$$

within an absorbing and scattering medium.

For a given geometry there is another useful dimensionless quantity

$$\tau_\lambda(S) = \int_0^S \beta_\lambda(S^*) dS^* \quad (25)$$

The quantity  $\tau(S)$  is the optical thickness or opacity of the layer of given thickness

$S$ . The optical thickness is a measure of the ability of a path length to attenuate radiation of a given wavelength. A large optical thickness means large attenuation.

For a medium with uniform composition and at uniform temperature and pressure equation (25) becomes

$$\tau_\lambda(S) = \beta_\lambda S \quad (26)$$

So that the path length based on given thickness of certain geometry is

$$s_\tau = -\frac{1}{\tau_\lambda(S)} \ln R(\tau) \quad (27)$$

## 2.5. Equations for Solutions

### 2.5.1. Net Heat Transfer to Surfaces

The general solution for different surface temperatures and emissivities is as follows. Referring to figure 3, the energy exchange between surfaces can be written

$$\begin{aligned}
 q_{1,net} &= \sum_{j=1}^n q_{j-1} + q_{g-1} - \sum_{j=1}^n q_{1-j} \\
 &= \sum_{j=1}^n SN_{j-1} \omega_j + SN_{g-1} \omega_g - \sum_{j=1}^n SN_{1-j} \omega_1 \\
 &= \sum_{j=1}^n SN_{j-1} \frac{\epsilon_j Q_{b,j}}{N_j} + SN_{g-1} \frac{\epsilon_g Q_{b,g}}{N_g} - \sum_{j=1}^n SN_{1-j} \frac{\epsilon_1 Q_{b,1}}{N_1}
 \end{aligned} \tag{28}$$

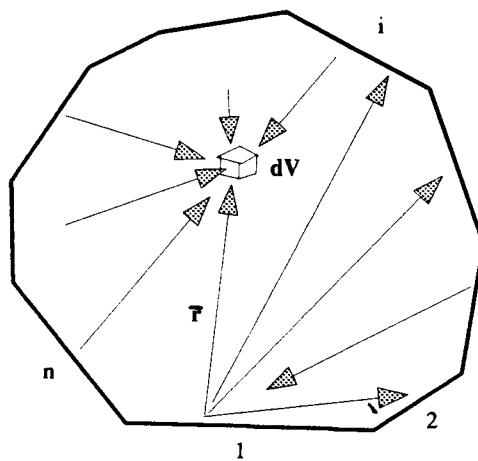


Figure 3. Inclosure composed of n discrete surface areas and filled with uniform gas with radiation mode

If there are no heat sources in the gas and walls except wall 1, the net radiation heat transfer between surface 1 and the other walls is

$$q_{1,net} = - \sum_{j=1}^n SN_{1-j} \frac{\epsilon_1 Q_{b,1}}{N_1} \quad (29)$$

Therefore the dimensionless radiation heat flux for each wall is

$$\frac{q_{i,net}}{q_1} = \frac{SN_i}{N_1} \quad (i=1,2,3,4,5,6,P) \quad (30)$$

### 2.5.2. Gas Emissive Power Distribution

The emissive power distribution for the case of a gas with a uniform heat source, enclosed within walls of different temperatures and emissivities is

$$\begin{aligned} 4\tau\sigma T_{g,r}^A \Delta V &= \omega_g (\Delta V N_g + SN_{g-g,r}) + \sum_{i=1}^n SN_{i-g,r} \omega_i \\ &= \sum_{i=1}^n \frac{SN_{i-g,r} \epsilon_i Q_{b,i}}{N_i} + Q_g \left( \Delta V + \frac{SN_{g-g,r}}{N_g} \right) \end{aligned} \quad (31)$$

where the left hand term,  $4\tau\sigma T_{g,r}^A \Delta V$ , is given by Jakob [30] and  $\omega$  is the energy per bundle.

If there is no heat source in the medium and wall emissivities are equal, equation (31) becomes

$$4\tau\sigma T_{g,\bar{r}}^A \Delta V = \epsilon \sum_{i=1}^n \frac{SN_{i-g,\bar{r}} Q_{b,i}}{N_i} \quad (32)$$

In this work there are no wall heat sources except at wall 1, thus equation (32)

becomes

$$4\tau\sigma T_{g,\bar{r}}^A \Delta V = \frac{SN_{1-g}}{N_1} \epsilon Q_{b,1} \quad (33)$$

### CHAPTER 3

#### NUMERICAL ANALYSIS

The Fortran code, MCHO3D[Appendix 1] was developed for analyzing radiative heat transfer for the configuration shown in figure 1. In chapter 2 details of the Monte Carlo method, as applied to thermal radiation problems, were given. In this chapter, the Monte Carlo solution procedure used in this research will be described.

For the numerical study, the enclosure and circular pipe were subdivided into  $20 \times 20 \times 20$ , and  $20 \times 20$  segments respectively as illustrated in figure 4.

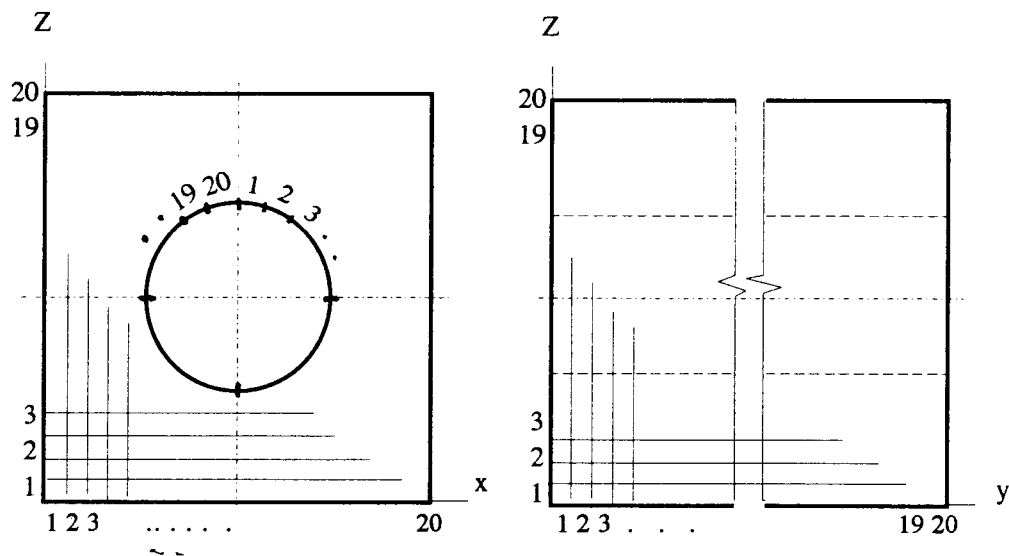


Figure 4. Numerical model configuration

### 3.1 Algorithm of MCHO3D

Steps involved in the code are listed below :

1. Define initial conditions. First, read geometric parameters (X, Y, Z, D), emissivity and specularity of wall surfaces and optical thickness of medium. The enclosure surfaces, pipe and medium are assumed to have uniform radiative surface properties which are specified by the user <1><sup>1</sup>.

2. N bundles are emitted from wall surface 1.

3. Determine the initial direction of bundle from the source. The surfaces of the enclosure are assumed to be gray, diffusely reflecting and emitting walls, so equations (10), and (11) apply

$$\begin{aligned}\theta &= \sin^{-1}(R_1)^{1/2} \\ \phi &= 2\pi R_2\end{aligned}\tag{34}$$

where  $R_1$  and  $R_2$  are random numbers between 0.0 and 1.0 <3>.

4. Determine path length,  $s$ . If radiative energy travels through a medium, then any incident beam will be attenuated by absorbing and scattering. In terms of

---

<sup>1</sup> <> refers to the corresponding block in flow chart (figure 7)

optical thickness the path length,  $s$ , in equation (27) is given by

$$s = -\frac{1}{\tau} \ln R \quad (35)$$

The bundle may be absorbed by the medium before it travels the whole distance,  $s$   $\langle 4 \rangle$ .

5. Determine whether or not the bundle impacts the pipe. From figure 5, a bundle with direction,  $\theta$ , and path length,  $s$ , is emitted from point  $x$ .

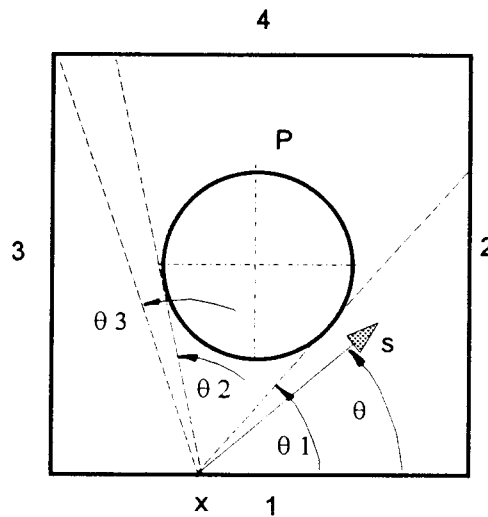


Figure 5. Trajectory of bundle

If  $\theta$  is less than  $\theta_1$  the bundle travels toward wall 2; if the emission angle  $\theta$  exceeds  $\theta_1$ , and is less than  $\theta_2$  the bundle travels toward the pipe; and if path length  $s$  is large enough the bundle will reach either the walls or pipe. Once the impacted wall has been determined, the location of impact is determined by

geometry. If another random number,  $R_e$ , is less than the emissivity the bundle will be absorbed at the impacted wall location. At this point the process is repeated  $\langle 5, 6 \rangle$ .

6. If random number  $R_e$  is larger than the emissivity the bundle will be reflected at the impacted point. Figure 6 shows the reflection mode on the wall surface. The patterns of reflection are determined by comparing random number  $R_{\text{Reflection}}$  with the surface specularity. If  $R_{\text{Reflection}}$  is less than the surface specularity, the bundle is reflected specularly (reflected angle is equal to incident angle,  $\theta_i = \theta_e$ ).

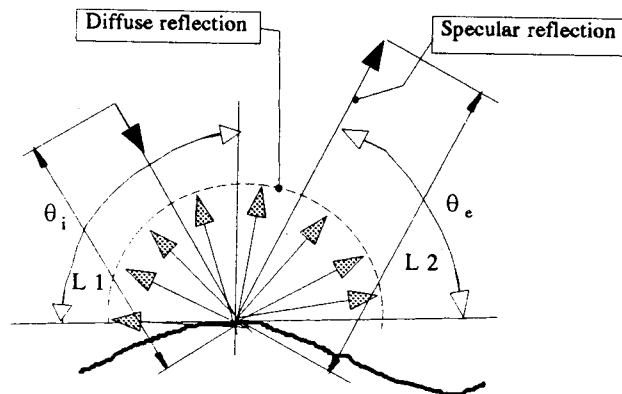


Figure 6. Reflection mode on the wall surface

Otherwise the bundle is reflected diffusely where the diffuse reflection angle will be specified by

$$\theta = \sin^{-1} (R_3)^{1/2} \quad \phi = 2\pi R_4 \quad (36)$$

where  $R_3$  and  $R_4$  are random numbers between 0.0 and 1.0. In these specular and diffuse reflection cases a new path length,  $S_{new}$ , is determined

$$s_{new} = L_2 = s_{old} - L_1 \quad (37)$$

where  $s_{old}$  is the  $s$  determined in step 4 using equation (35). With the new emission location and angle selected, the procedure is repeated until the bundle is absorbed by either the walls or the pipe  $\langle 8,9,10,11,12 \rangle$ .

7. If the path length in a given direction is less than the length necessary to impact a surface, the bundle will be absorbed at distance,  $s$ . To satisfy radiative equilibrium, a bundle which has equal energy with the bundle absorbed is then emitted from the same point.

The energy spontaneously emitted by an isothermal volume element and the temperature can be obtained knowing the number of bundles absorbed and emitted, so that equation (33) becomes

$$Q_{\Delta V} = 4 \tau \sigma T_{\Delta V, P}^A dV = (SN_{\Delta V})_P \omega = \frac{(SN_{\Delta V})_P}{N} Q_1 \quad (38)$$

or

$$T_{\Delta V} = \left[ \frac{\omega (SN_{\Delta V})_P}{4 \tau \sigma dV} \right]^{1/4} \quad (39)$$

If  $\tau$  depends on local temperature  $T_{\Delta V}$ , an iteration is required. In this work  $\tau$  is assumed uniform  $\langle 15,16 \rangle$ . The processes of absorption and emission are

continued until the bundle is absorbed by either the walls or the pipe.

8. Determine a new direction from the medium using

$$\theta = \cos^{-1}(1 - 2R_\theta), \quad \phi = 2\pi R_\phi \quad (40)$$

and also determine a new path length,  $s$ , using equation (35) <17, 18> .

9. A new bundle is emitted, and the process is repeated until all  $N$  bundles have been emitted.

10. Output information is calculated. From equation (30) the dimensionless radiative heat flux reabsorbed at a sub element of wall 1 is determined according to

$$\frac{q_1}{\sigma T_1^4} = \frac{\frac{(SN_1)_p}{(\Delta x \Delta y)_p}}{\frac{N_{total}}{A_1}} \quad (41)$$

Similarly for the other walls we have

$$\frac{q_i}{\sigma T_i^4} = \frac{\frac{(SN_i)_p}{(\Delta A)_p}}{\frac{N_{total}}{A_1}} \quad (42)$$

where  $i$  refers to surface 2,3,4,5,6 or the pipe,P. The temperature at the center of each volume element is found from equation (39) as

$$\begin{aligned}\Phi_{\Delta V,g,P} &= \frac{T_{\Delta V,g,P}}{T_1} = \left[ \frac{\omega (SN_{\Delta V})_{g,P}}{4\tau \sigma \Delta V T_1^4} \right]^{1/4} \\ &= \left[ \frac{(SN_{\Delta V})_{g,P}}{4\tau N_{\Delta V}} \right]^{1/4}\end{aligned}\quad (43)$$

and, finally, the dimensionless emissive power in the medium is given by

$$\varphi_P = \frac{(SN_{\Delta V})_{g,P}}{4\tau N_{\Delta V}} \quad (44)$$

The flow chart for this program sequence is shown in figure 7.

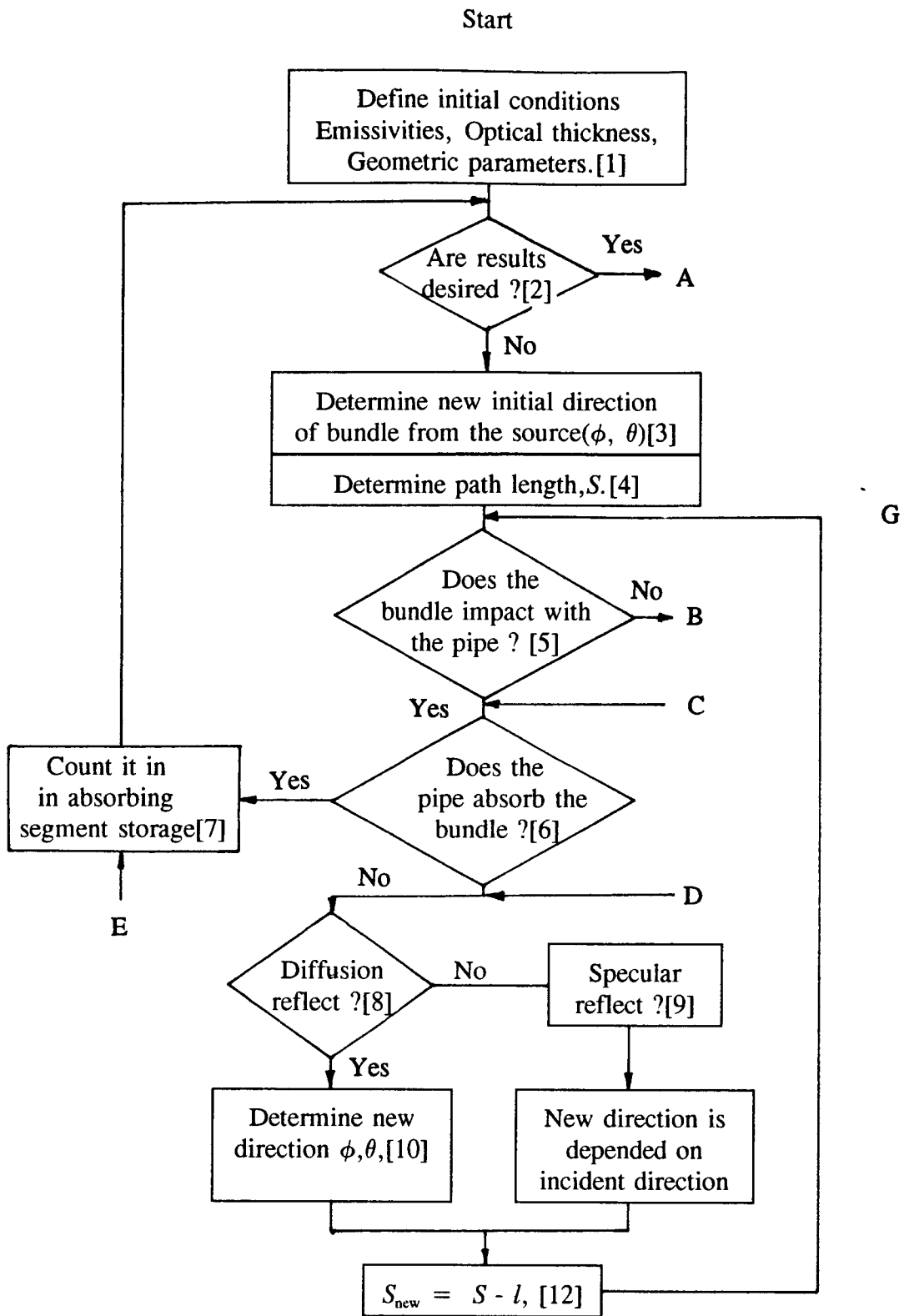


Figure 7. Flow chart of MCHO3D

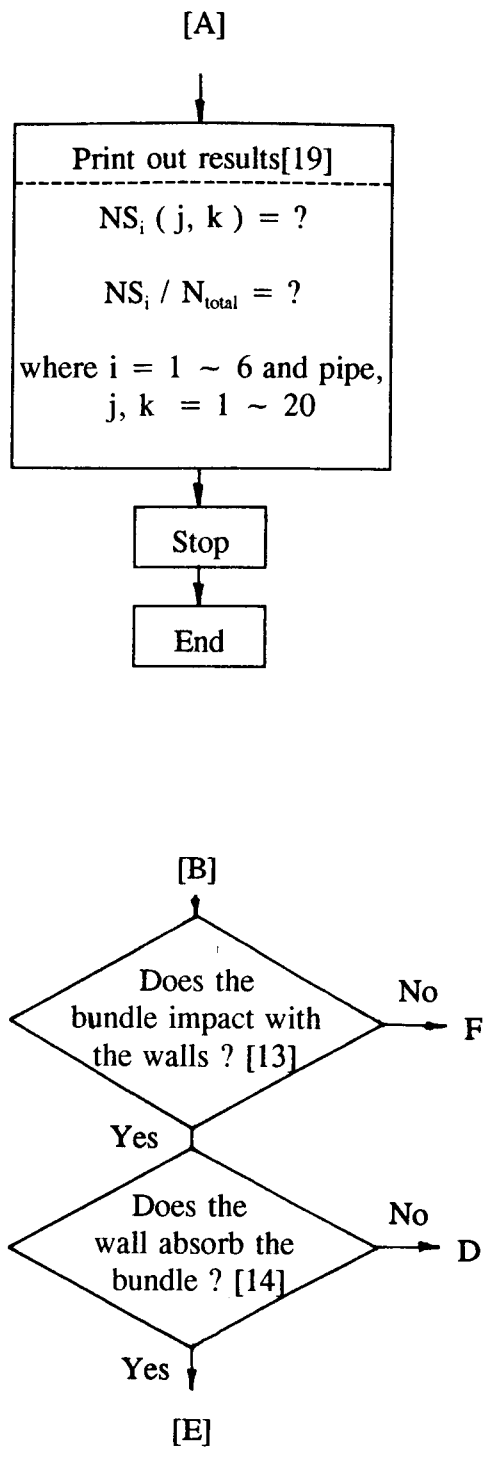


Figure 7. (Continued)

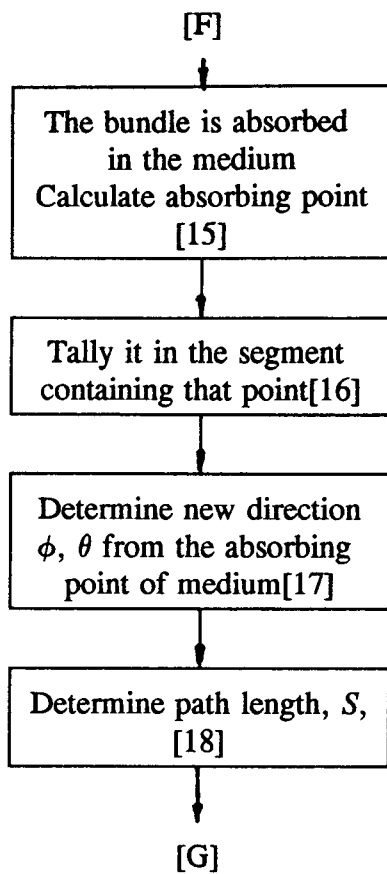


Figure 7. (Continued)

## CHAPTER 4

### MODEL PARAMETERS

The parameters which were used in each of the cases investigated are listed in table 1.

First, to show the validity of the MCHO3D Monte Carlo code, simple problems that have been analyzed by investigators using different methods were selected for comparison.

The first problem to be analyzed was for one-dimensional parallel plates separated by a gray medium. The second was that of a two-dimensional enclosure containing a gray medium. These cases were then been extended to a three-dimensional case with a cylinder running through the enclosure.

Three geometric parameters (dimensions of the enclosure, and size of the pipe) were varied for specific values of optical thickness of the medium and for wall conditions.

Boundaries of the square duct and circular cylinder were considered black and very cold except for the bottom surface which was a uniform-heat-flux emitting surface. To simplify the simulation the participating medium was considered to be an isothermal, absorbing, emitting, and isotropically scattering gray medium. Optical thickness values were varied from 0 to 10.0.

Figure 1, showing geometric parameters, is included again as figure 8 to assist the reader.

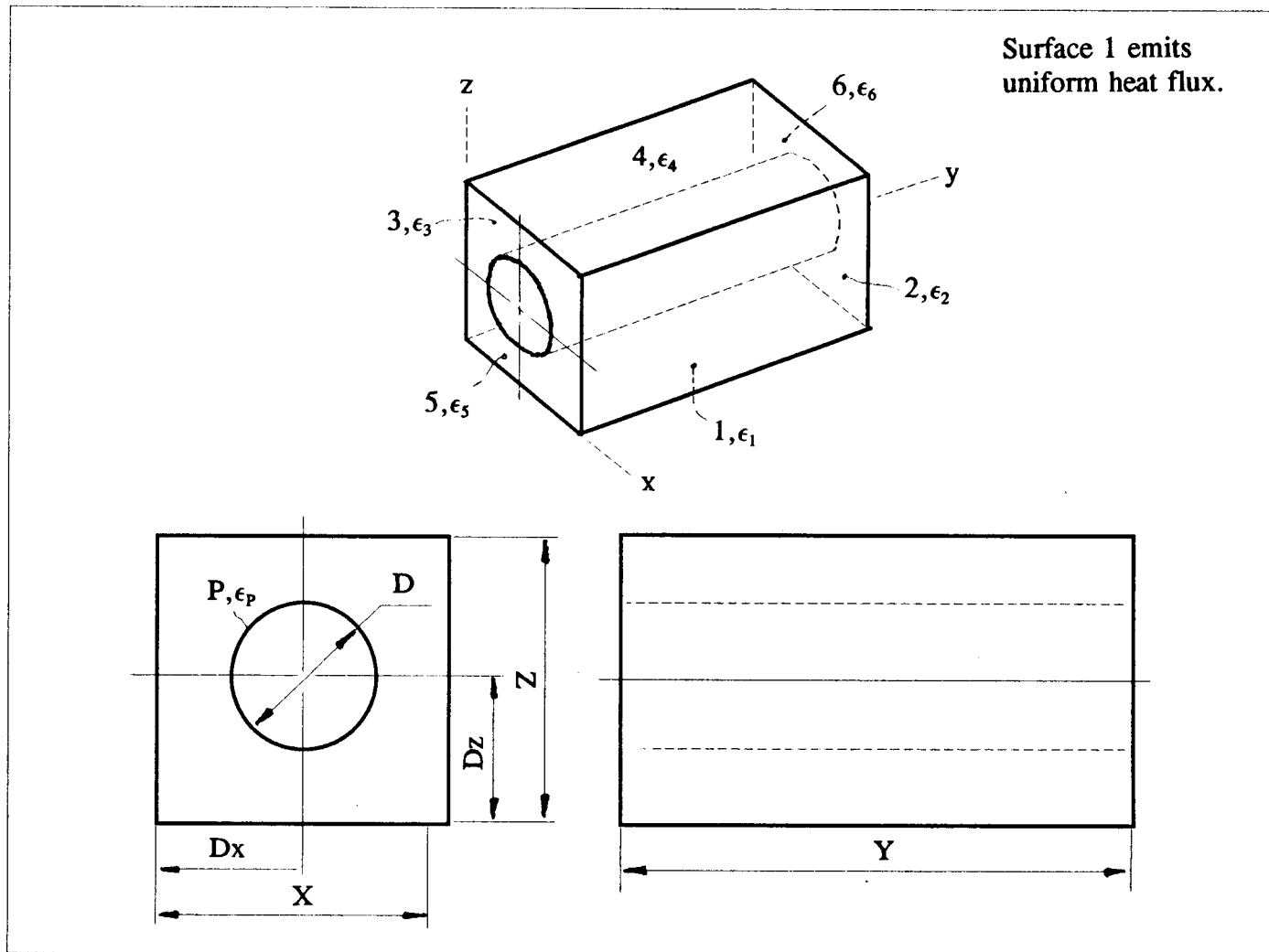


Figure 8. Geometrical configuration.

Table 1. Model parameters.

Case	Geometric shape		$\epsilon_{1-\epsilon, P}$	$\tau$		
One - D	Z = 1.0, X/Z = Y/Z = 200.0 D = 0.0		1.0	0.5		
				2.0		
				10.0		
Two - D	X = 10.0, Z/X = 1.0, Y/X = 200.0		1.0	1.0		
Case 1	X = 10.0 Z/X = 1.0 D/X = 0.4 Dx/X = 0.5	Dz/X	1.0	Y/X	<< 1	
		0.2				0.1, 0.5, 1.0, 1.5, 2.0, 2.5, 3.0, 4.0, 5.0, 10.0, 15.0, 20.0
		0.4				
		0.5				
		0.6				
		0.8				
Case 2	X = 10.0 Z/X = 1.0 Dx/X = 0.5 Dz/X = 0.5	D/X	1.0	Y/X	<< 1	
		0.2				0.1, 2.0, 3.0, 4.0, 5.0, 10.0, 15.0, 20.0
		0.3				
		0.5				
		0.8				
		1.0				
Case 3	X = 10.0 Z/X = 1.0 D/X = 0.4	Dz/X = 0.5	1.0	Y/X	<< 1	
					0.5	
					1.0	
					3.0	
					5.0	
					10.0	
Case 4	X = 10.0 Z/X = 1.0 D/X = 0.4	Dz/X = 0.5	1.0	3.0	//	

## CHAPTER 5

### RESULTS AND DISCUSSION

A numerical investigation involving the effects of radiation in a square duct with a centered, circular pipe has been conducted. The situations considered in this study involve two different parameters, geometrical shape factors and optical thickness. The cases evaluated include a variety of combinations of these parameters. Numerical results are presented graphically.

#### 5.1. Comparison with other methods

The purpose of this section is to describe how the MCHO3D Monte Carlo code, which was developed for a three-dimensional case, compares to known one- and two-dimensional results.

Considering, first, a one-dimensional enclosure with parallel black ( $\epsilon_{1,2} = 1.0$ ) plates separated by an absorbing and emitting gray medium that is in radiative equilibrium, i.e. radiation is the only mode of heat transfer, the universal function for nondimensional radiation heat flux is

$$\Psi_b(\tau) = \frac{q}{n^2 \sigma (T_1^A - T_2^A)} \quad (45)$$

or

$$\Psi_b(\tau) = 1 - 2 \int_0^{\tau_L} \Phi_b(\tau') E_2(\tau') d\tau' \quad (46)$$

and nondimensional emissive power or temperature is

$$\Phi_b(\tau) = \frac{T^A(\tau) - T_2^A}{T_1^A - T_2^A} \quad (47)$$

or

$$\Phi_b(\tau) = \frac{1}{2} \left[ E_2(\tau) + \int_0^{\tau_L} \Phi_b(\tau') E_1(|\tau - \tau'|) d\tau' \right] \quad (48)$$

where  $\tau'$  is a dummy variable [7,26]. The numerical solution to these two equations (46) and (48) was first given by Heaslet and Warming [26]. The solid lines in figures 9 and 10 include the results of numerically solving equations (46) and (48) [26].

To simulate one-dimensional geometry, since MCHO3D was developed for three-dimensions, the geometric ratios were taken to be  $X/Z = 200.0$ ,  $Y/Z = 200.0$  and  $D/Z = 0.0001$ . One emitting source at the center of the bottom wall was used. Had the emitting source points been selected randomly along the x axis it would not have been a one-dimensional case. To examine the validity of choosing these parameters, the numbers of bundles absorbed at walls 2, 3, 5, and 6 were counted. Characteristically fewer than two bundles out of a thousand were absorbed in each case, thus the one-dimensional results are valid. For the one-dimensional case, equations (42) and (44) become

$$\frac{q_4}{q_1} = \frac{SN_4}{N_{total}} \quad (49)$$

and

$$\varphi_P = \frac{\epsilon (SN_{\Delta Z})_P}{4 \tau \Delta Z N_{total}} \quad (50)$$

respectively, and were used to calculate the values which are shown as individual results in figures 9 and 10, with good agreement achieved. The scattering in Monte Carlo results for emissive power distribution evaluated at the lower values of optical thickness is a statistical phenomenon. If the number of bundles were increased less scatter would be obtained.

The next comparison was with two-dimensional enclosure results of a study conducted by Kim and Lee [25]. They solved isotropic and anisotropic scattering cases using the S-N discrete ordinate method. Other results by Thynell and Özisik [27], who achieved a solution for the isotropic scattering case using the Galerkin method [28] were also used for comparison. These two studies were performed with various values of the albedo ( $\omega = \sigma_s / \beta$ ). In the present work the value of the albedo was chosen as  $\omega = 1.0$ . The incident radiation in the medium is the total intensity impinging on a point from all sides defined by the following equation (51)

$$G_\lambda = \int_0^{4\pi} I_\lambda(\bar{r}) d\omega \quad (51)$$

Boundary conditions in both cases include the bottom surface emitting

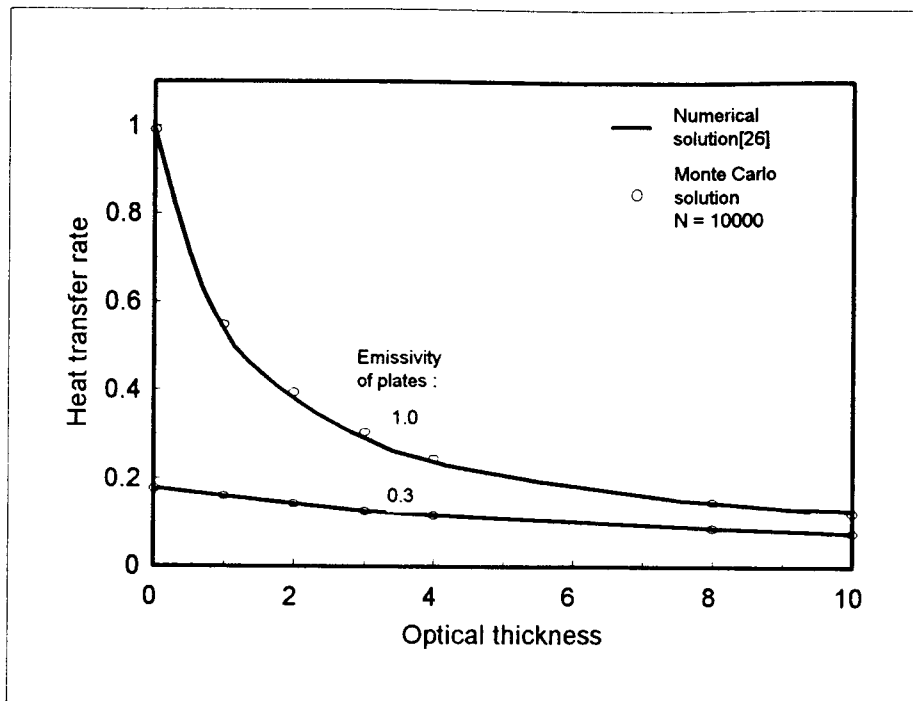


Figure 9. Heat transfer between infinite parallel gray plates containing a gray medium

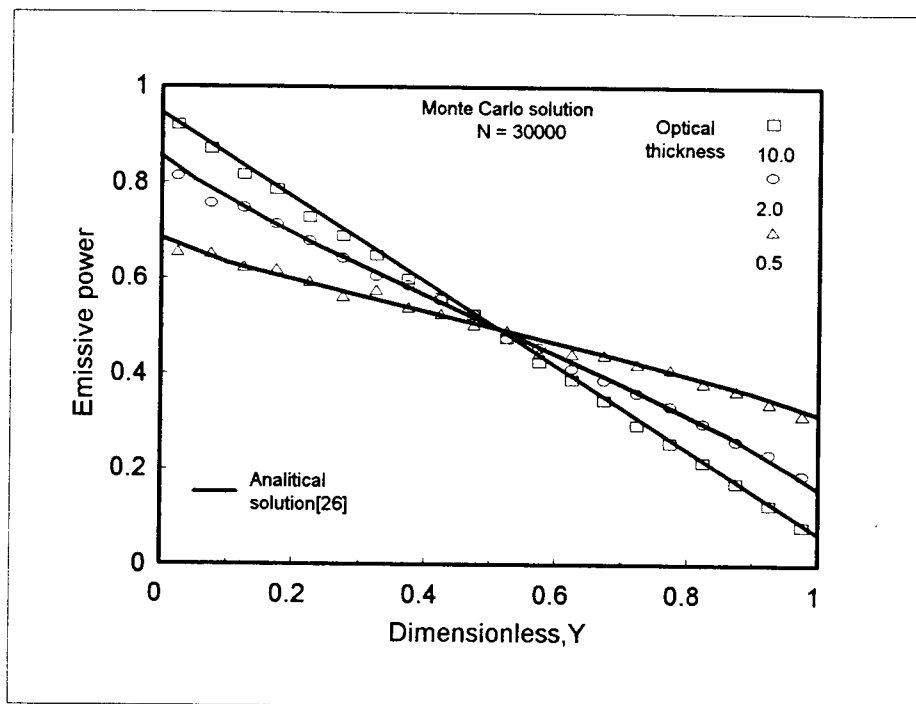


Figure 10. Distribution of emissive power in gray medium with no source

isotropically as a constant flux surface. The remaining three wall surfaces are considered to contain no external energy sources and there was no energy source in the medium. To match geometric similarity the following values were used:  $Z/X = 1.0$ ,  $Y/X = 200.0$ , and  $D/X = 0.0001$ . To establish the base as a uniform energy surface, a line source along  $x$  at  $y = Y/2$  was used. Different grids were used in each case. In MCHO3D the simulation model was subdivided into  $20 \times 20$  grid. In the S-N discrete-ordinate method the enclosure was divided into a  $26 \times 26$  grid. The Galerkin method included seven values ( $z/X = 0.0, 0.1, 0.2, 0.3, 0.5, 0.7, 1.0$ ). Figure 11 is a comparison of the incident radiation distributions of these three methods and shows excellent agreement between them. These two

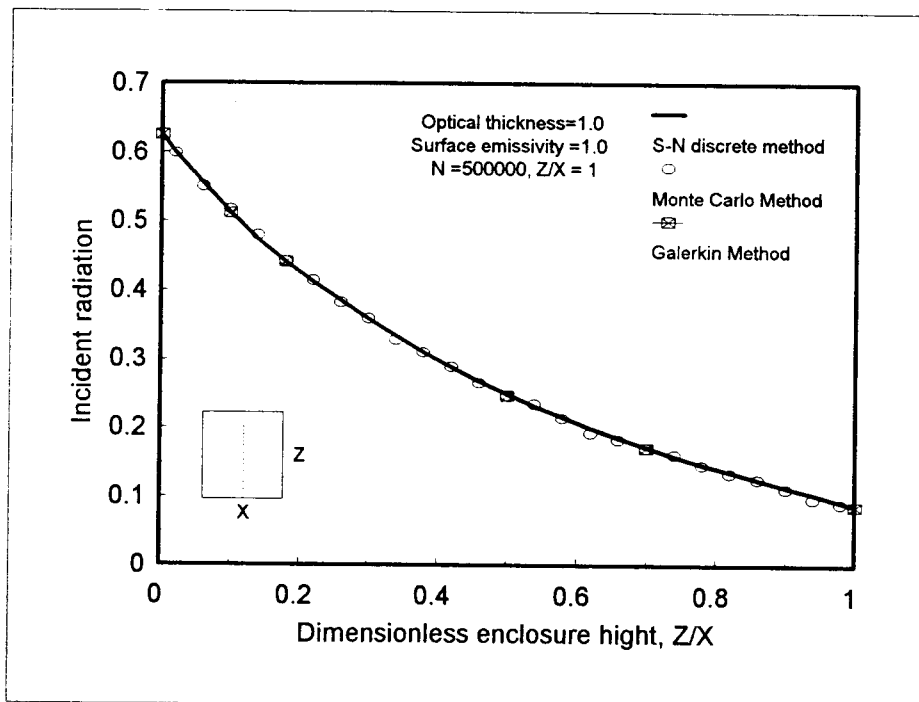


Figure 11. Incident radiation of medium along the vertical center line at  $x = X / 2$ .

comparisons demonstrate that the MCHO3D code is a valid method for evaluating three- or multi-dimensional cases.

## 5.2. Geometric Variations

In cases 1 and 2, heat transfer rates and the distribution of radiative heat flux were examined for a range of geometric shapes, locations of the circular cylinder along the vertical center line, and cylinder diameter. Since the walls are black in this problem, there is no reflected radiation from surfaces, and because the medium is isotropically scattering, the fractional radiative energy in any particular direction incident on surfaces from the entire medium remains unchanged. Also for the case with the optical thickness approaching zero the space between surfaces can be considered as a vacuum and the resulting radiation heat transfer rates are directly related to their view factors and would yield the exact solution for the wall heat flux. For this case equation (42) becomes

$$\frac{q_i}{q_1} = \frac{SN_i}{N_{total}} \quad (i=1,2,3,4,5,6,P) \quad (52)$$

Figure 12 shows the dimensionless radiative heat transfer rate from the bottom surface to the pipe as a function of enclosure depth and pipe location. Figure 13 shows the variation of radiative heat transfer rates at each surface. An inspection of figure 12 reveals that for enclosure depths,  $Y/X$ , greater than 5, the view factor (or radiation heat transfer rate) remains almost unchanged, i.e. it approaches but

never reaches the values of the corresponding two-dimensional case and these trends seem somewhat independent of the location of the pipe. This figure also shows that the radiation heat transfer rates for the pipe are increased at pipe locations close to the bottom surface. The maximum heat transfer (also maximum  $F_{1-p}$ ) between the base (surface 1) and the pipe will occur when the pipe is in contact with the base. For the case shown this maximum is 0.475 of the total. Figure 13 shows that transfer rates for each wall surface show only modest change after  $Y/X=5$ . The results of a study of Wiebelt and Ruo [31], in which they obtained view factors between a finite right-circular cylinder and a parallel rectangular surface using the contour integration method, show similar trends.

The distributions of radiative heat flux around the pipe are shown in figure 14. These cosine-like heat flux profiles were obtained for a lateral line at  $y=Y/2$ . When the pipe is in contact with the base the dimensionless radiative heat flux approaches to 1.0. For each pipe location the maximum radiative heat fluxes are the limiting values for an infinitely long enclosure (the two-dimensional case).

Figure 15 shows the heat flux profiles on both side wall surfaces (2, 3) which are perpendicular to the heated wall (surface 1). The dimensionless radiative heat fluxes approach a value of approximately 0.5 as the vertical location,  $z$ , approaches zero. In figure 15 (d) in which the diagonal lines of the enclosure do not intersect the pipe, the dimensionless radiative heat fluxes approach the value of 0.146 as vertical location,  $z$ , approaches 1.0 and  $Y/X$  approaches infinity. The dimensionless radiative heat flux for an infinitely small element in case 1 can be easily calculated using the crossed-string method [4,7]. It is shown in

Appendix 1 that the radiative heat flux approaches 0.5 when  $n \rightarrow \infty$ .

Figure 16 shows the heat flux distributions along the center line of the upper wall surface of the enclosure. These figures show clearly the effects of pipe location. The radiative heat flux distributions of figures 15 and 16 show there to be a discontinuity at each corner. This radiative heat flux slip (or jump) is a result of geometry and will disappear when heat conduction is present.

The results for case 2 are shown in figures 17 and 18. In this case it is clear that the radiative heat transfer rate to the pipe will increase as the diameter of the pipe is increased as expected. The effect of enclosure depth shows similar trends as for case 1.

From figure 17 we observe that the maximum radiation heat exchange between wall 1 and the enclosed cylinder reaches a maximum value of 78 percent of the total with the remaining 22 percent transferred to the side walls.

The results of the studies of cases 1 and 2 show that, if the optical thickness of the intervening medium is small ( $\tau \ll 1$ ), the geometric view factor,  $F_{i,j}$ , is valid even though boundary conditions may change.

### 5.3 Optical Thickness Effects

The second part of this study was undertaken to answer the question "What happens when the optical thickness of the intervening medium varies from optically-thin to the optically-thick state?" In cases 1 and 2 the optical thickness

was very small (effectively zero), thus the attenuation by absorption and scattering was negligible. In cases 3 and 4 an incident beam was attenuated by absorption and scattering while traversing the enclosure. For isotropic scattering in the case of a gray medium in radiative equilibrium, there is no distinction between absorption and scattering. Any energy absorbed at  $\tau$  must be reemitted isotropically at the same location, i.e., any isotropically scattered energy is simply redirected isotropically.

If a bundle path length is less than the maximum path length the bundle will be absorbed. To satisfy energy equilibrium, a bundle is then reemitted from the same location. The probability that the bundles are absorbed prior to reaching another surface is increased as the optical thickness is increased.

Results of case 3 are shown in figures 19 and 20. Figure 19 shows the effect of optical thickness on dimensionless heat flux to the pipe over a range of with enclosure depth  $Y/X$ . Radiation heat transfer rates to the pipe at small values of optical thickness are larger than for large optical thicknesses for all values of enclosure depth,  $Y/X$ , since the resistance through the medium is relative small.

Figure 20 shows the variation of radiative heat transfer rates at each wall as a function of optical thickness for various enclosure depths,  $Y/X$ . As expected radiation heat transfer rates to each wall decreased as optical thickness increased for all enclosure depths.

In figure 21, radiation heat flux values around the pipe are presented with the optical thickness as the parameter. The total radiation heat transfer rate to the pipe decreased with an increase in optical thickness.

Figure 22 shows the reabsorbing radiation heat-flux distribution at the bottom surface as a function of optical thickness. For parallel plates the distribution would be flat for all optical thicknesses. This figure shows that the effect of side walls was greater for increased optical thickness.

Figure 23 shows the distribution of heat flux at the upper surface of the enclosure. The effect of the pipe is seen to decrease and the heat flux approached zero as the optical thickness increased.

In figure 24 the radiation heat flux distribution along the side walls is also observed to approach zero for large values of optical thickness.

To show the effects of optical thickness for each wall surface and pipe more clearly the distribution of radiative heat flux was plotted in three-dimensions for case 4. Figures 25 through 29 show the distribution of radiative heat flux around the pipe, along walls 2 and 3, wall 4, and walls 5 and 6, respectively. As the optical thickness was increased, the heat flux decreased in all cases except for wall surface 1, the bottom surface.

These results show that radiation heat transfer rates in enclosures filled with an optically thin medium ( $\tau \ll 1$ ) can be accurately predicted using geometric view factors. If, however, the optical thickness of the medium is 0.1 or greater it is necessary to include the effects of participating media in the analysis.

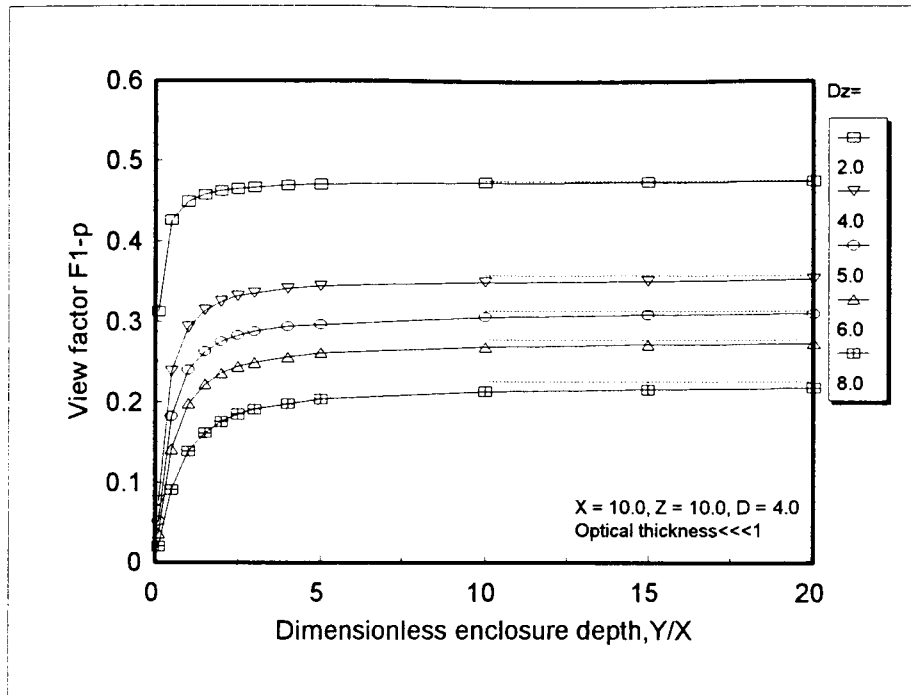
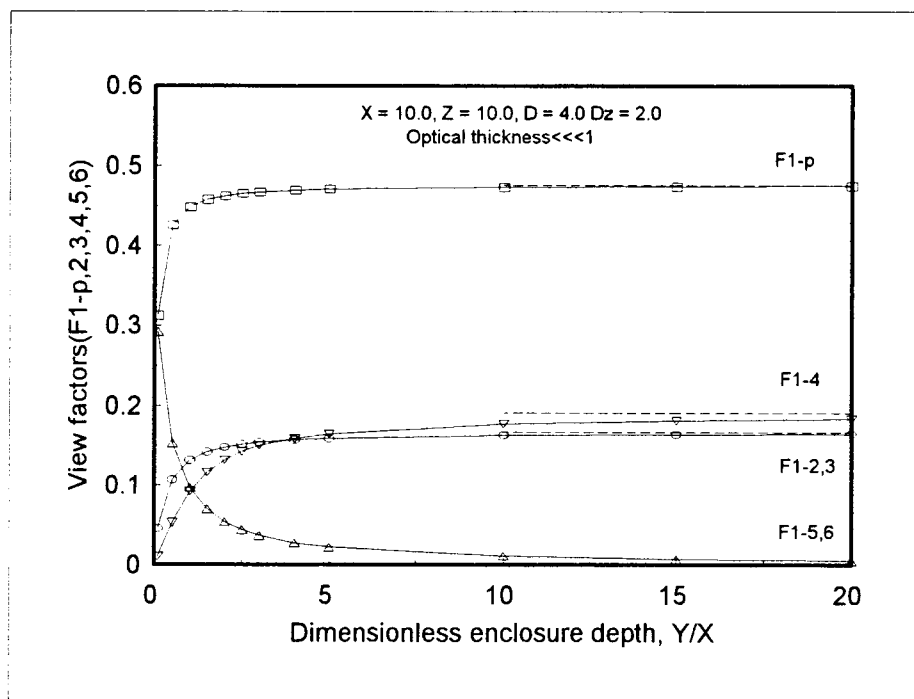
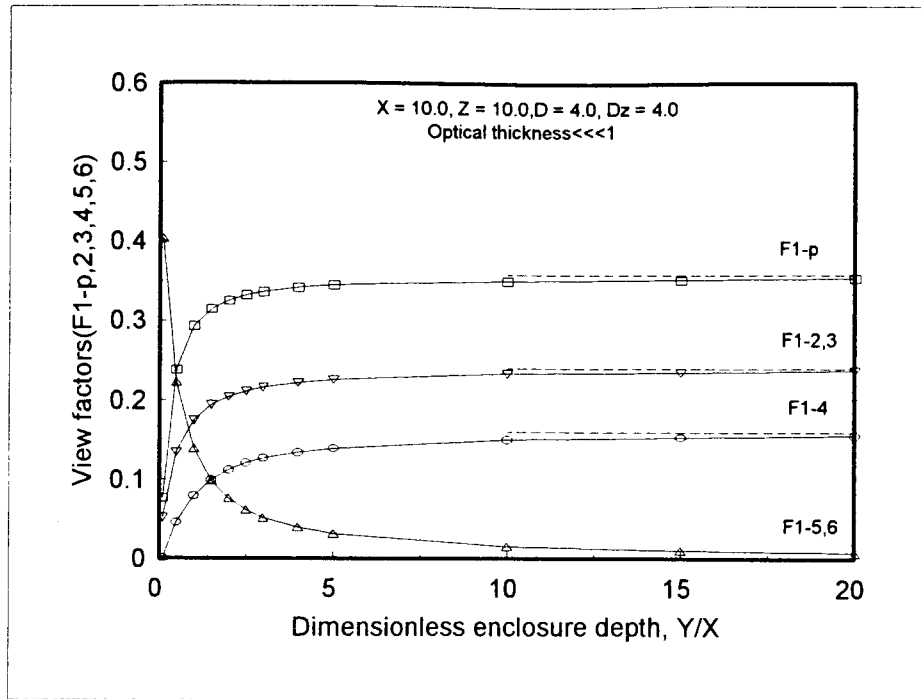


Figure 12. Variation of view factors  $F_{1-p}$  with enclosure depth and pipe location (--- refers to  $Y/X = \infty$ )

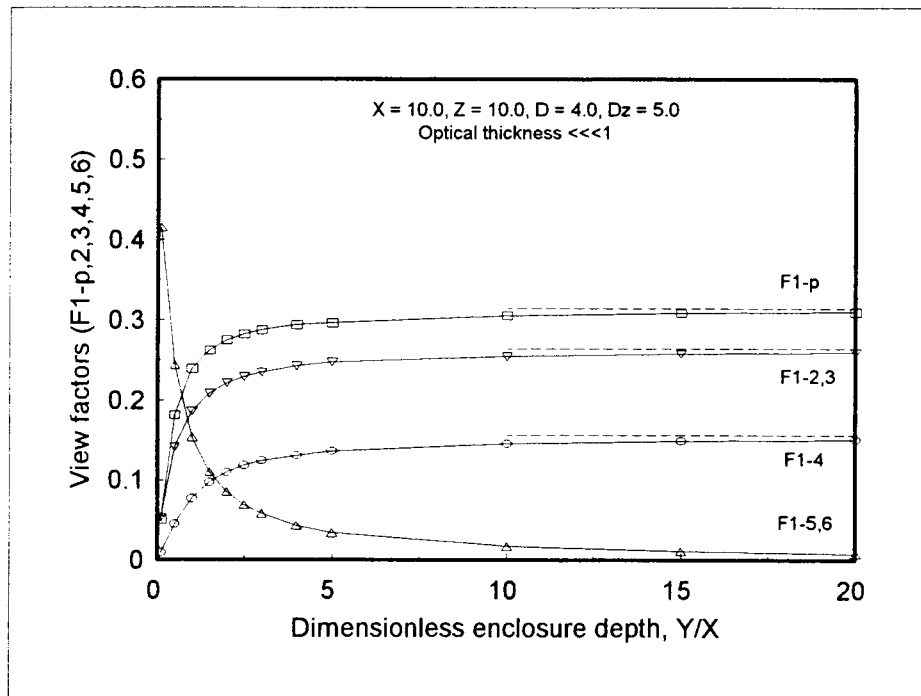


(a)  $Dz = 2.0$

Figure 13. Variation of view factors  $F_{1-j}$  with enclosure depth (--- refers to  $Y/X = \infty$ )



(b)  $Dz = 4.0$



(c)  $Dz = 5.0$

Figure 13. (continued)

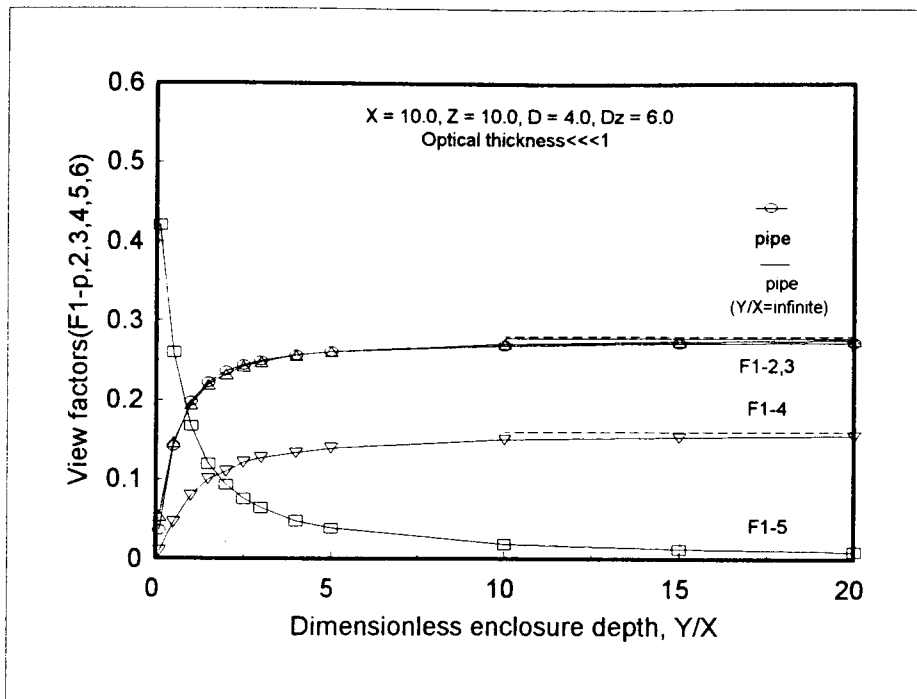
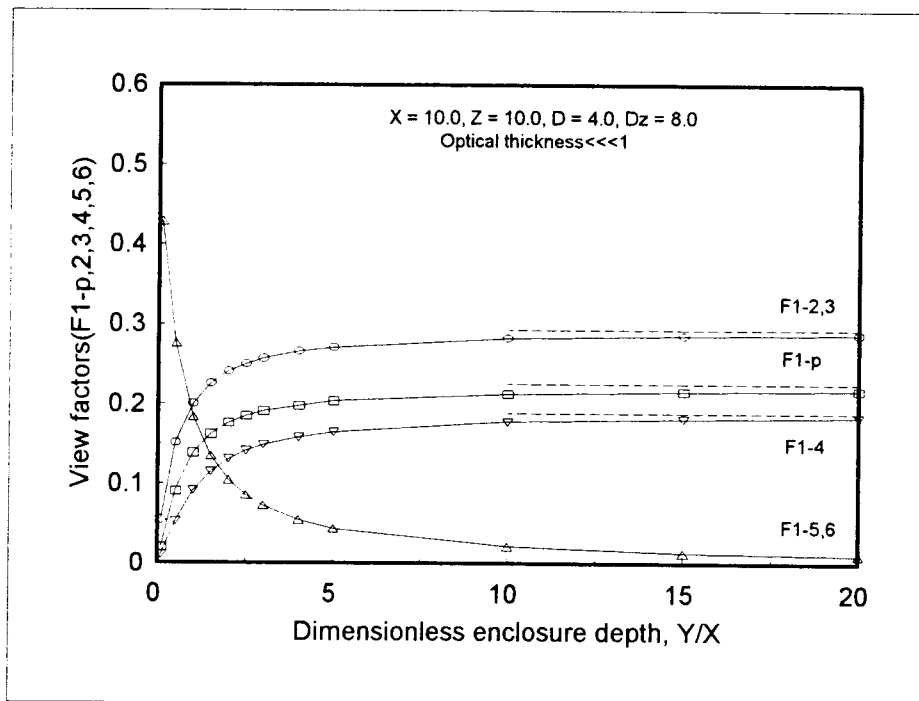
(d)  $Dz = 6.0$ (e)  $Dz = 8.0$ 

Figure 13. (continued)

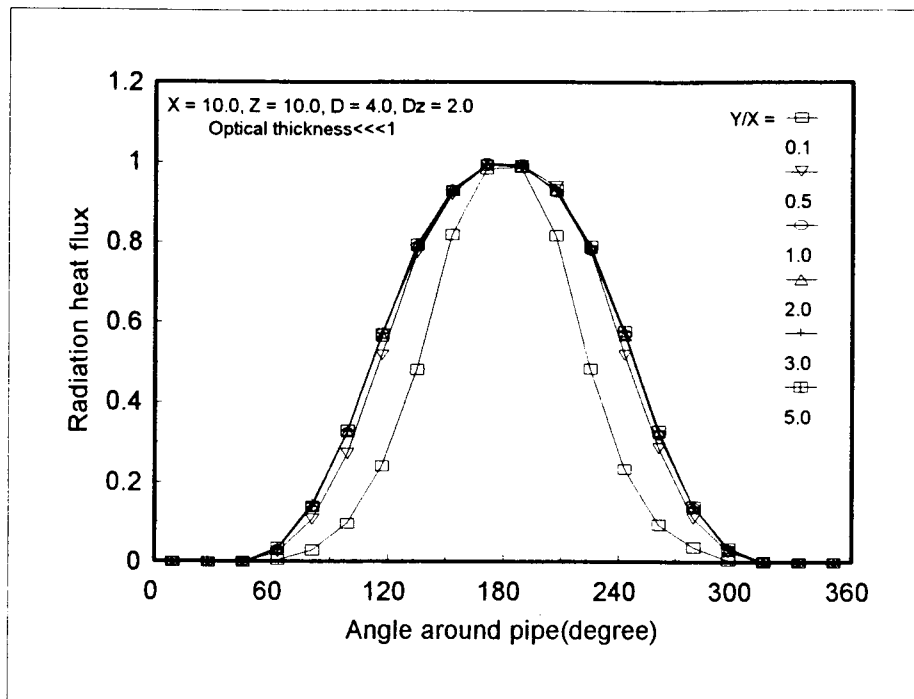
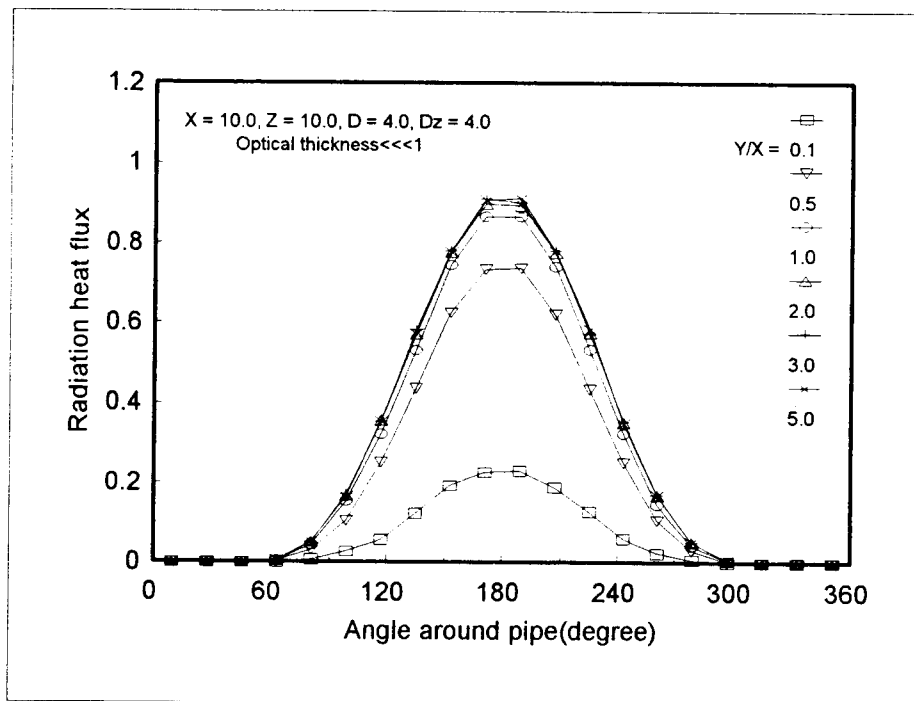
(a)  $Dz = 2.0$ (b)  $Dz = 4.0$ 

Figure 14. Distribution of radiation heat flux around pipe at  $y = Y/2$  with enclosure depth

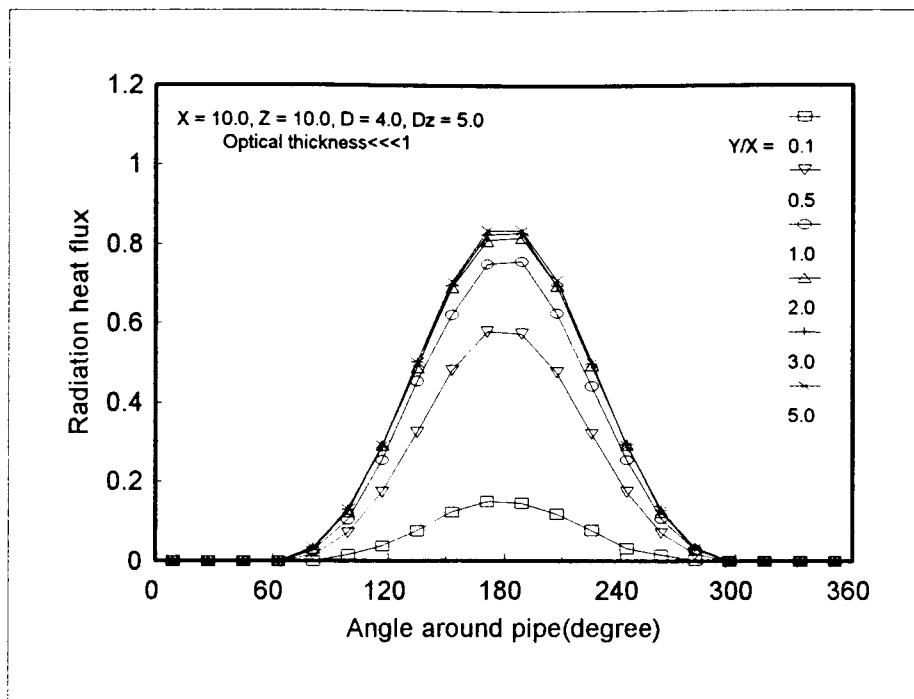
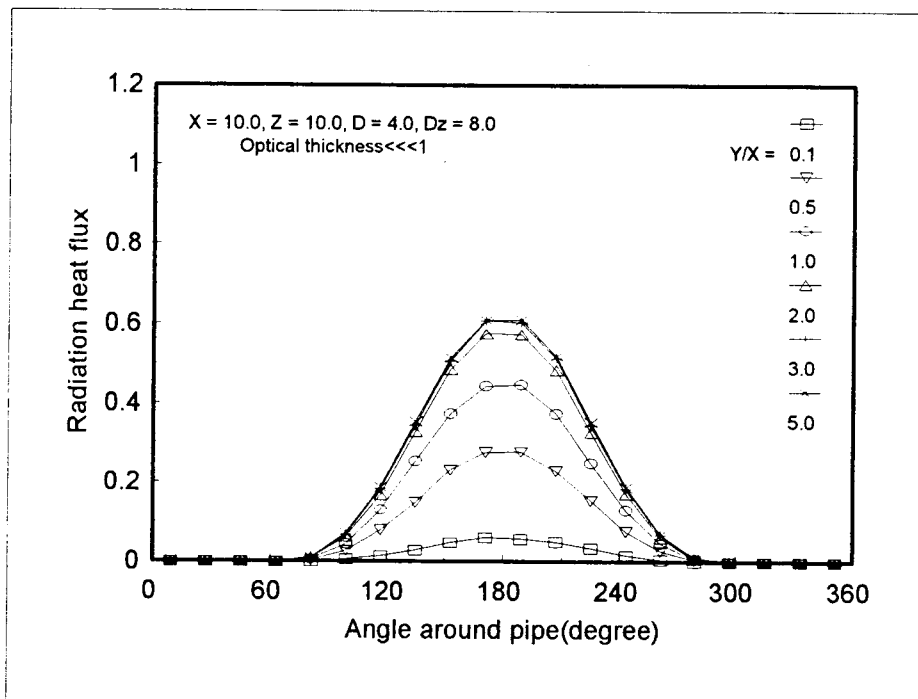
(c)  $Dz = 5.0$ (d)  $Dz = 8.0$ 

Figure 14 (continued)

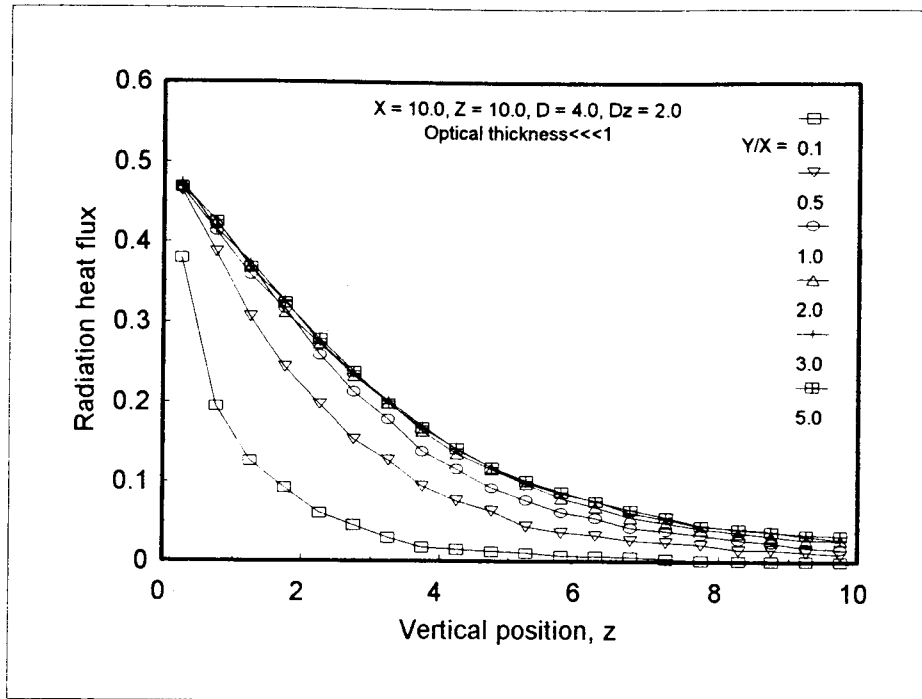
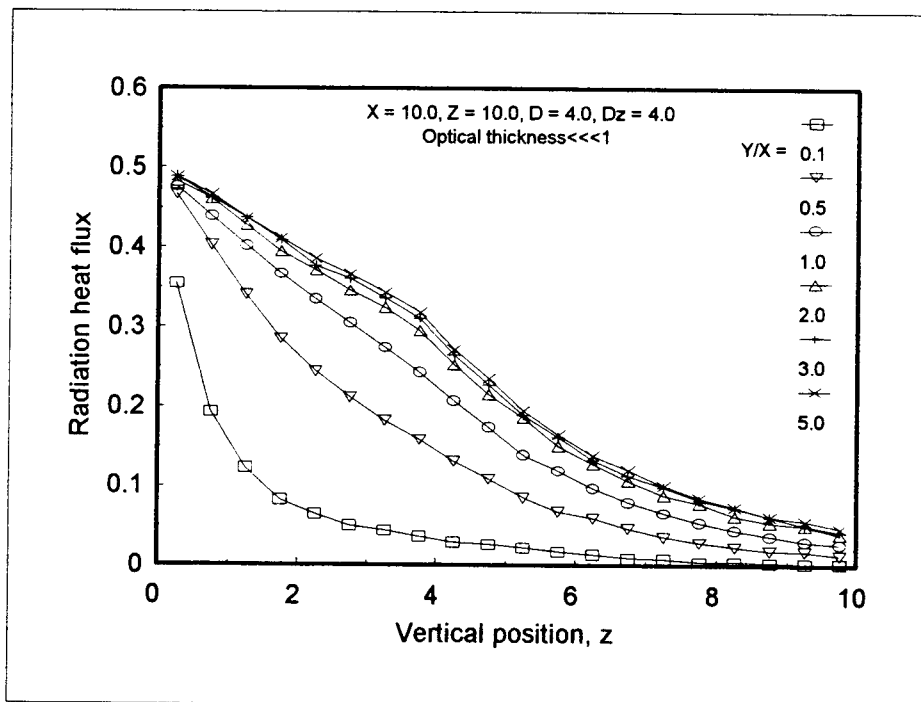
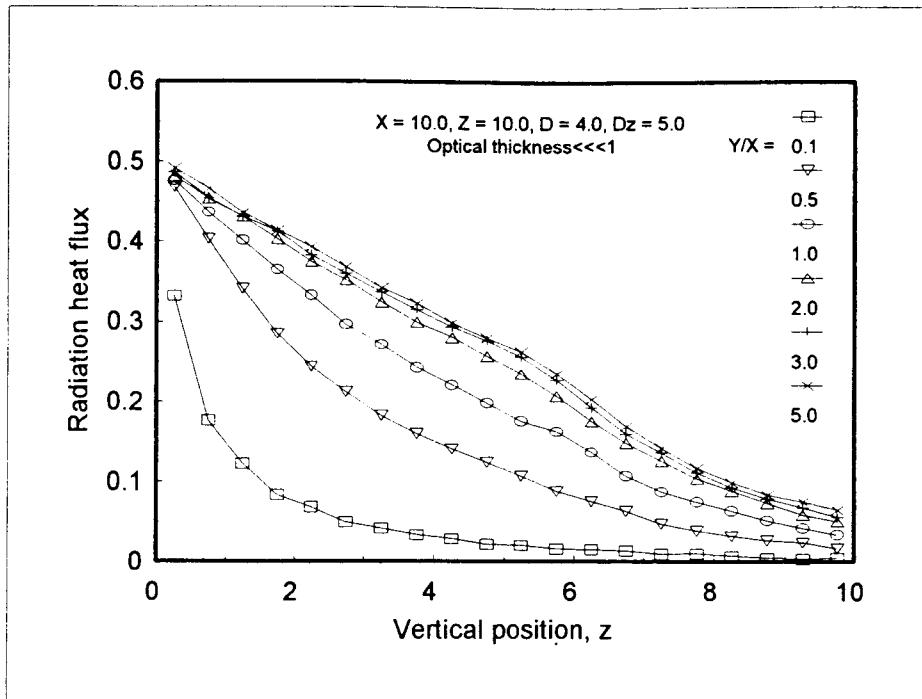
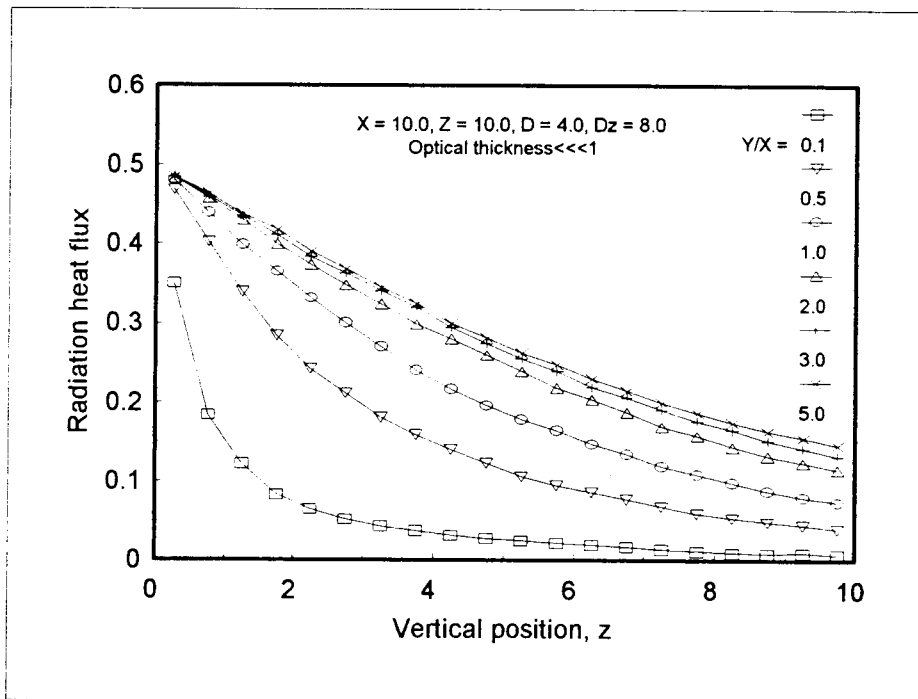
(a)  $Dz = 2.0$ (b)  $Dz = 4.0$ 

Figure 15. Distribution of radiation heat flux to center line of side walls,  $y = Y/2$



(c) Dz = 5.0



(d) Dz = 8.0

Figure 15. (continued)

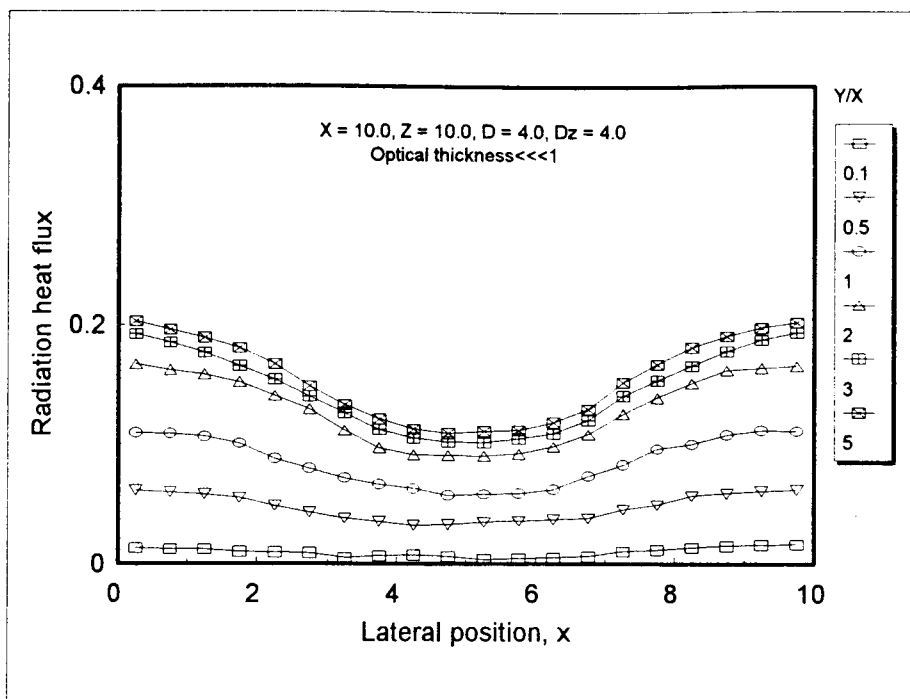
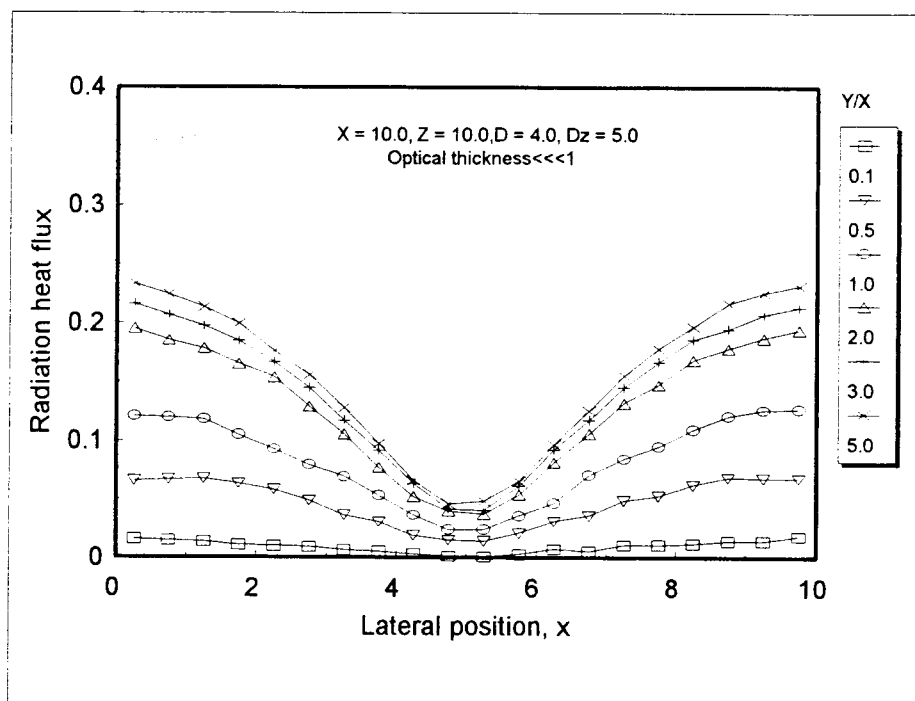
(a)  $Dz = 4.0$ (b)  $Dz = 5.0$ 

Figure 16. Distribution of radiation heat flux to center line of top surface,  $y = Y/2$

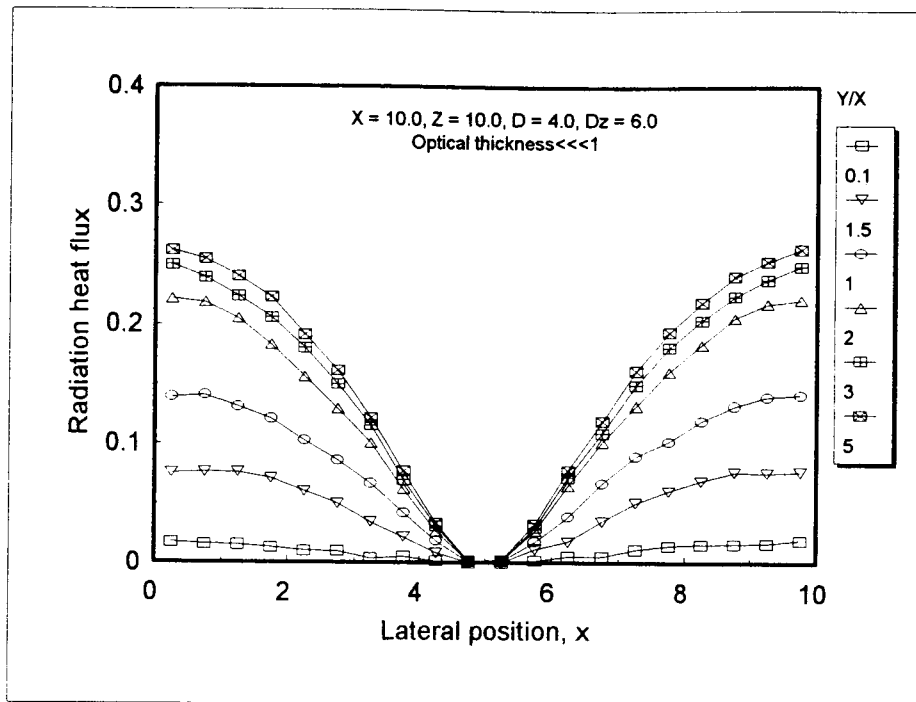
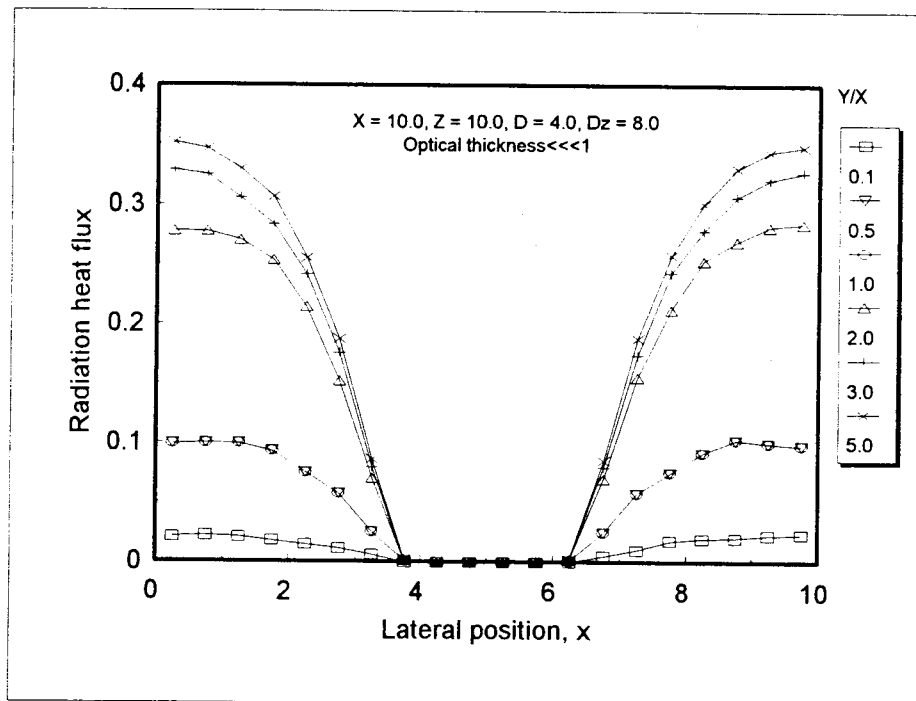
(c)  $Dz = 6.0$ (d)  $Dz = 8.0$ 

Figure 16. (continued)

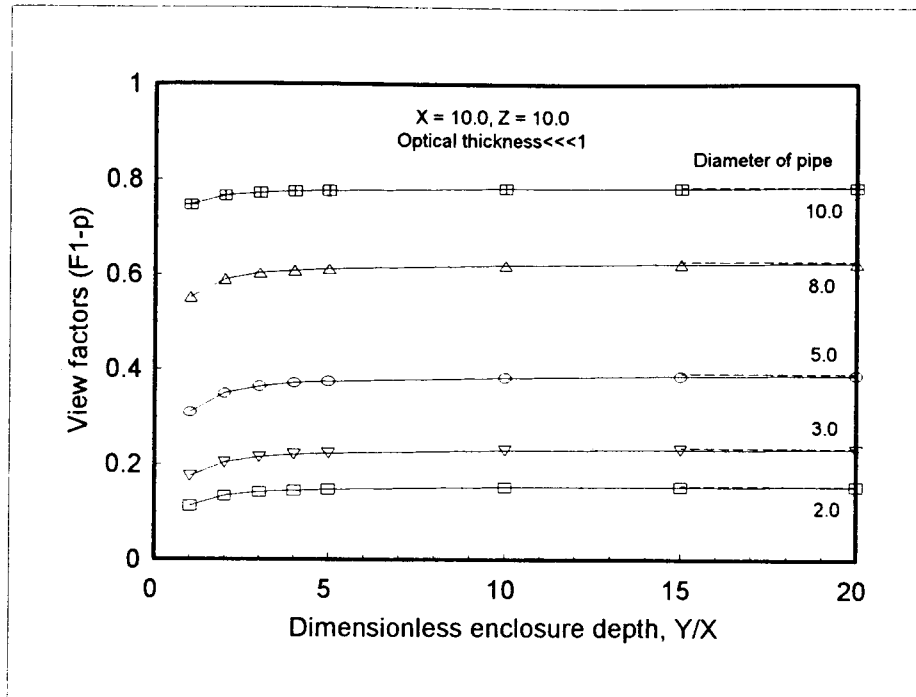
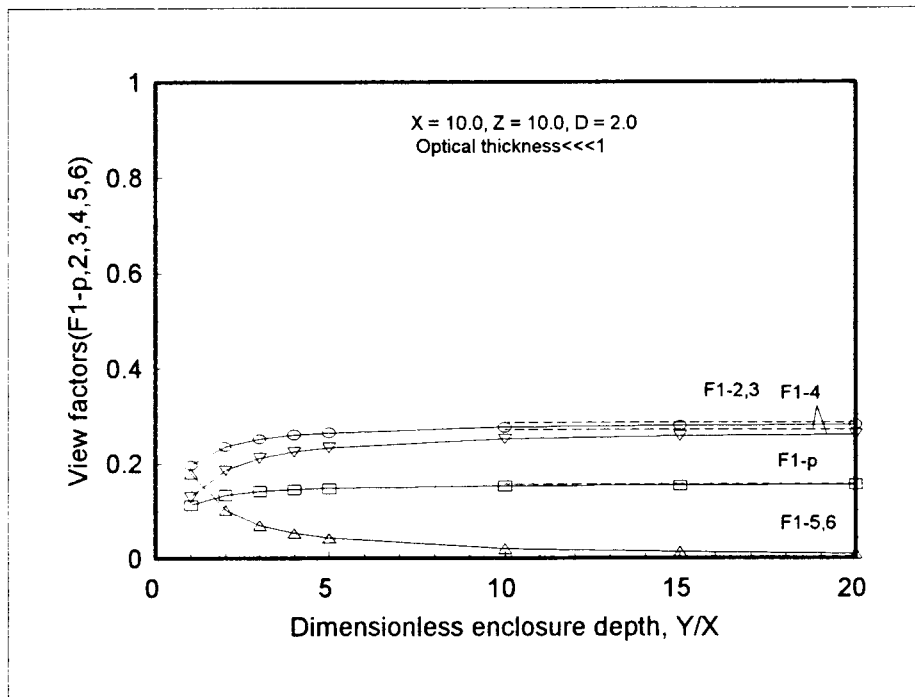


Figure 17. Variation of view factors  $F_{1,p}$  with enclosure depth and pipe diameter (--- refers to  $Y/X = \infty$ )



(a)  $D = 2.0$

Figure 18. Variation of view factors  $F_{1,j}$  with enclosure depth (--- refers to  $Y/X = \infty$ )

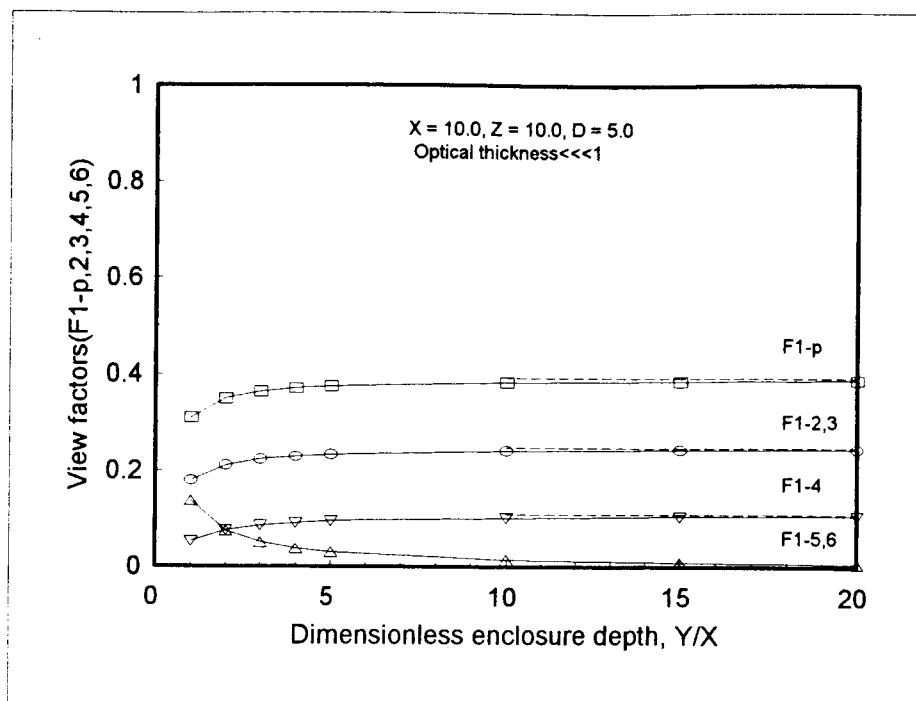
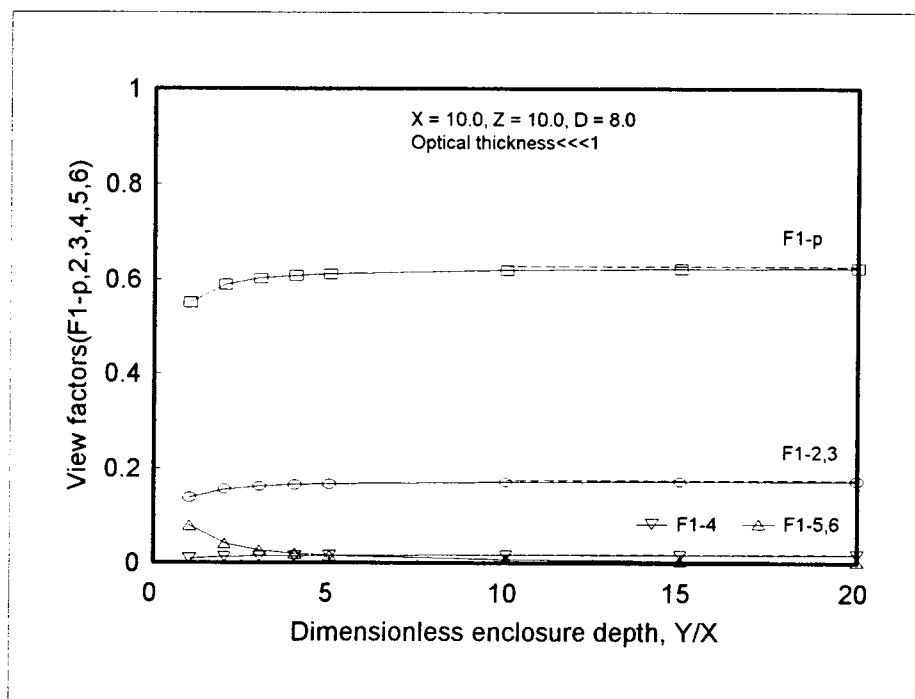
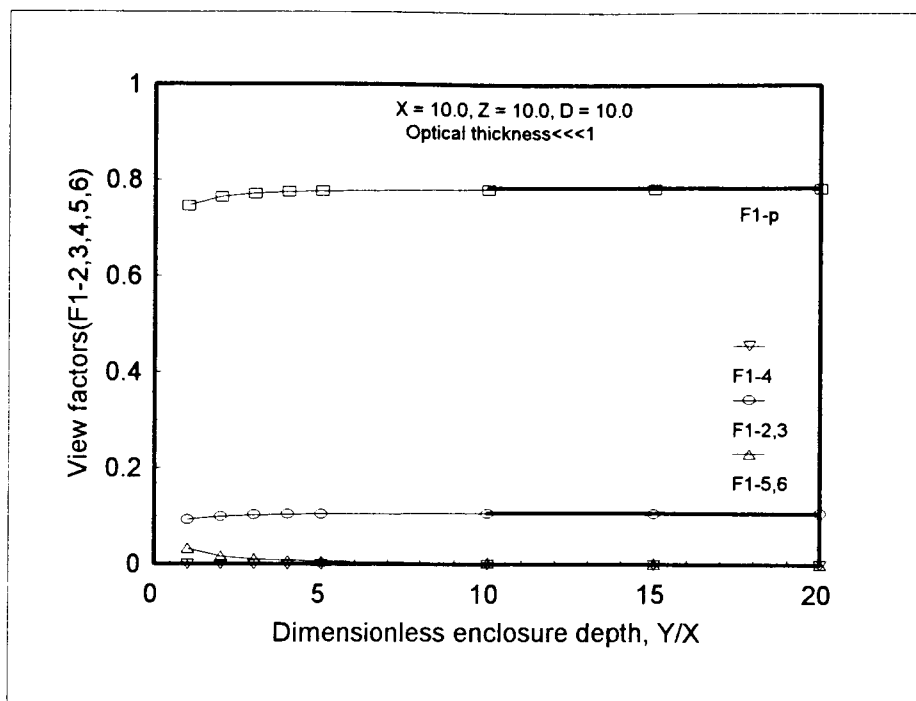
(b)  $D = 5.0$ (c)  $D = 8.0$ 

Figure 18. (continued)



(d)  $D = 10.0$

Figure 18. (continued)

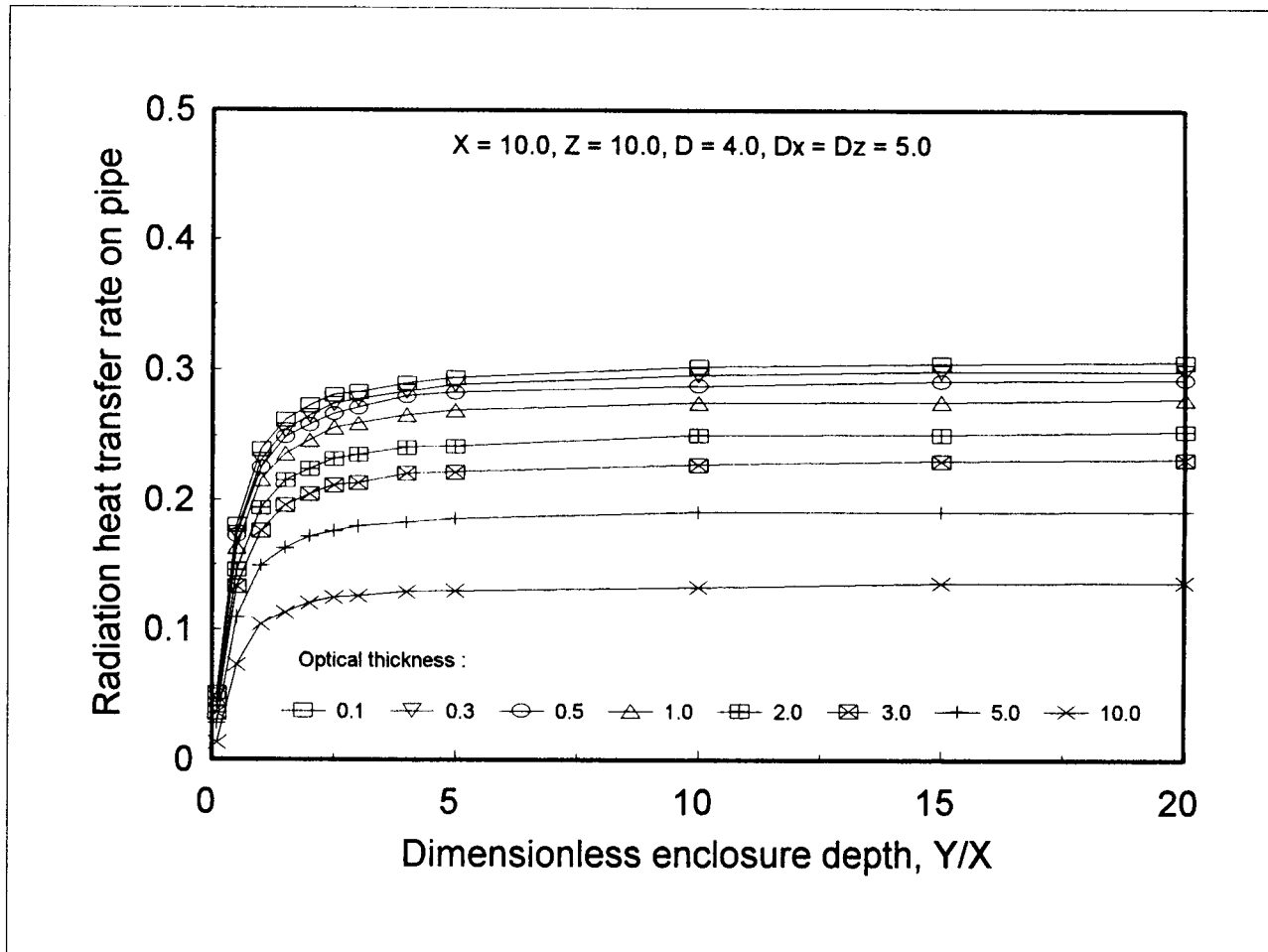


Figure 19. Variation of radiation heat transfer rate on pipe with enclosure depth and optical thickness

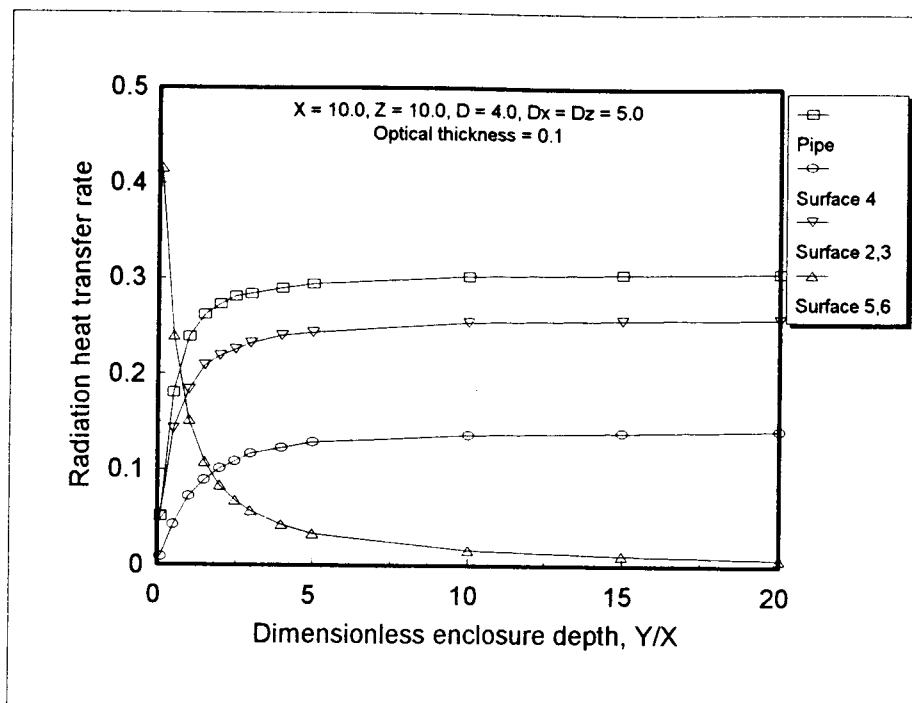
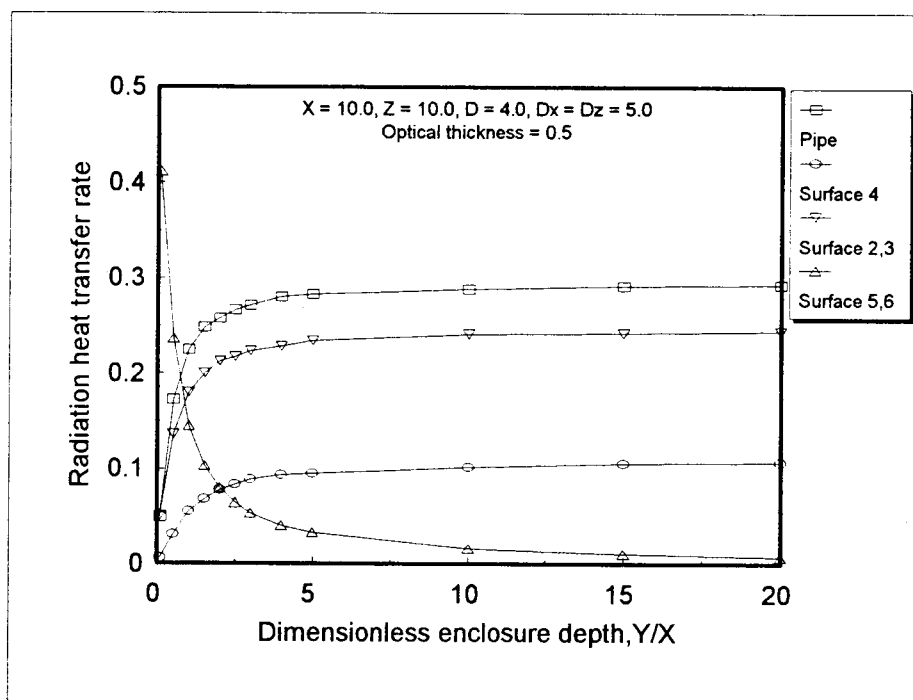
(a)  $\tau = 0.1$ (b)  $\tau = 0.5$ 

Figure 20. Variation of radiation heat transfer rate with enclosure depth ( $\tau = 0.1, 0.5, 1.0, 3.0, 5.0, 10.0$ )

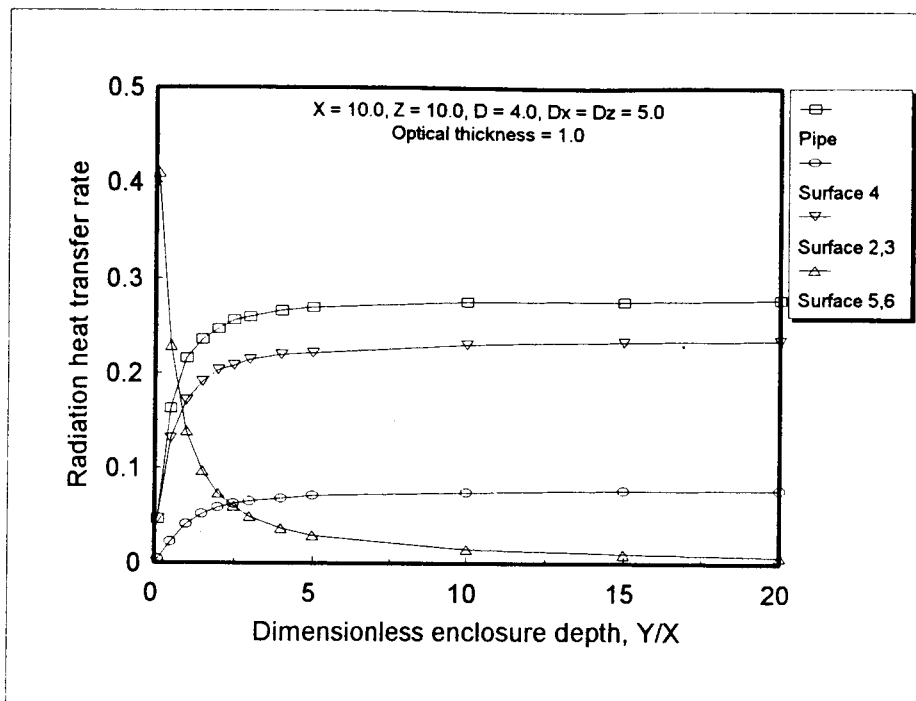
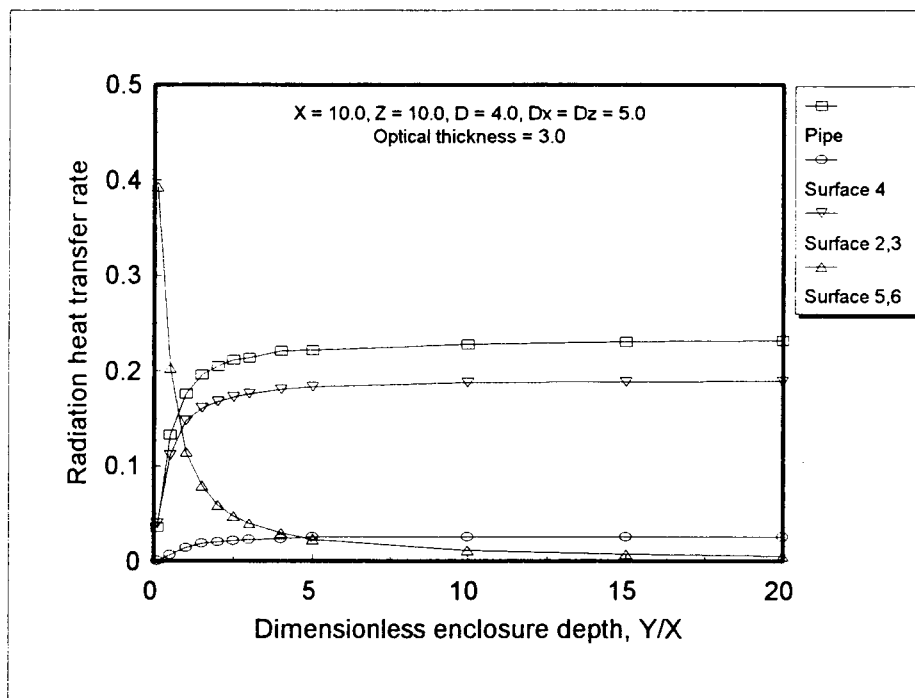
(c)  $\tau = 1.0$ (d)  $\tau = 3.0$ 

Figure 20. (continued)

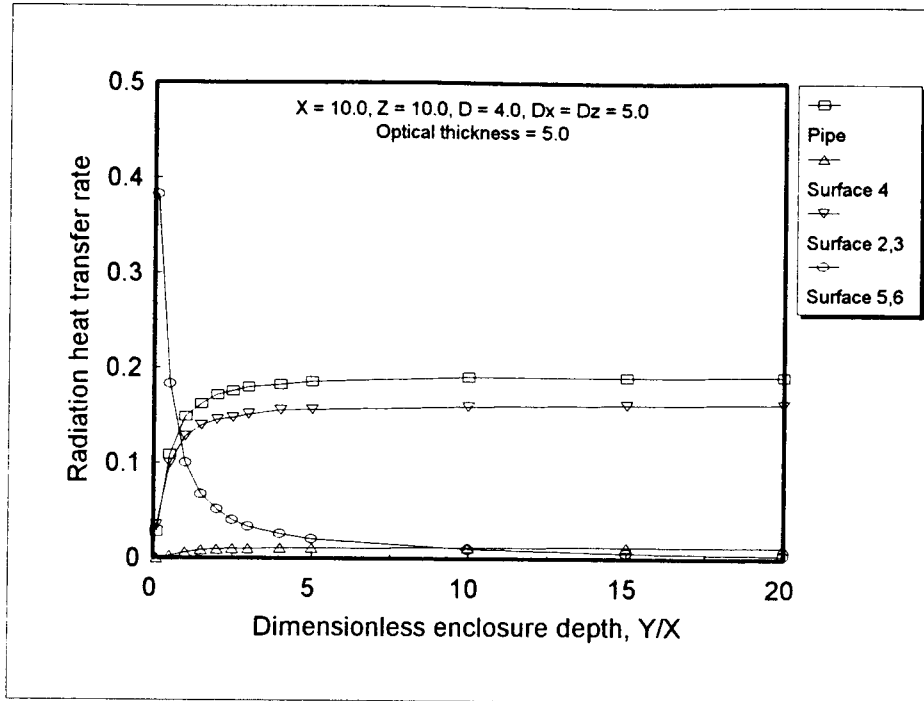
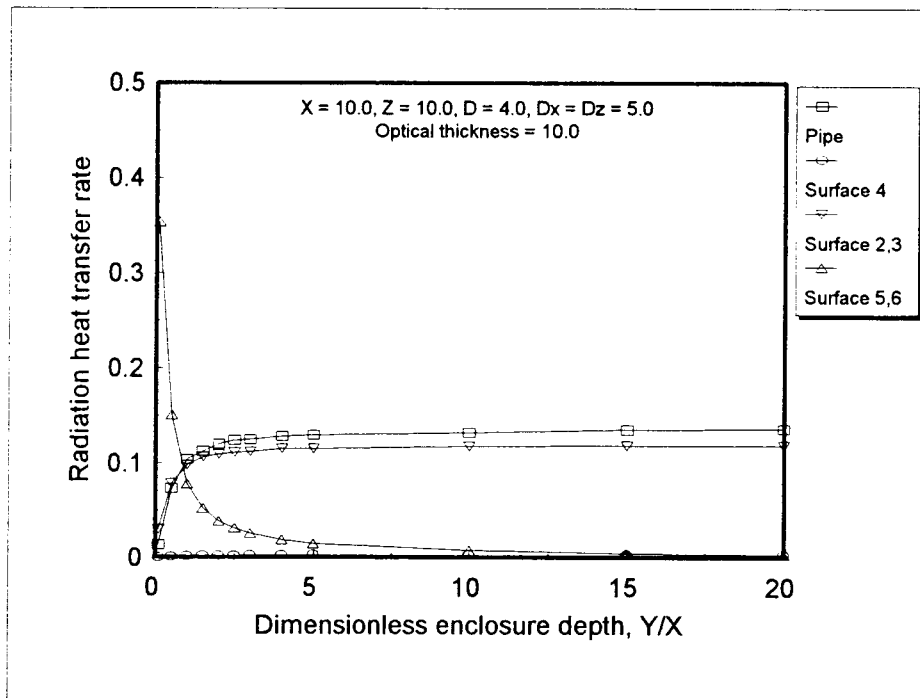
(e)  $\tau = 5.0$ (f)  $\tau = 10.0$ 

Figure 20. (continued)

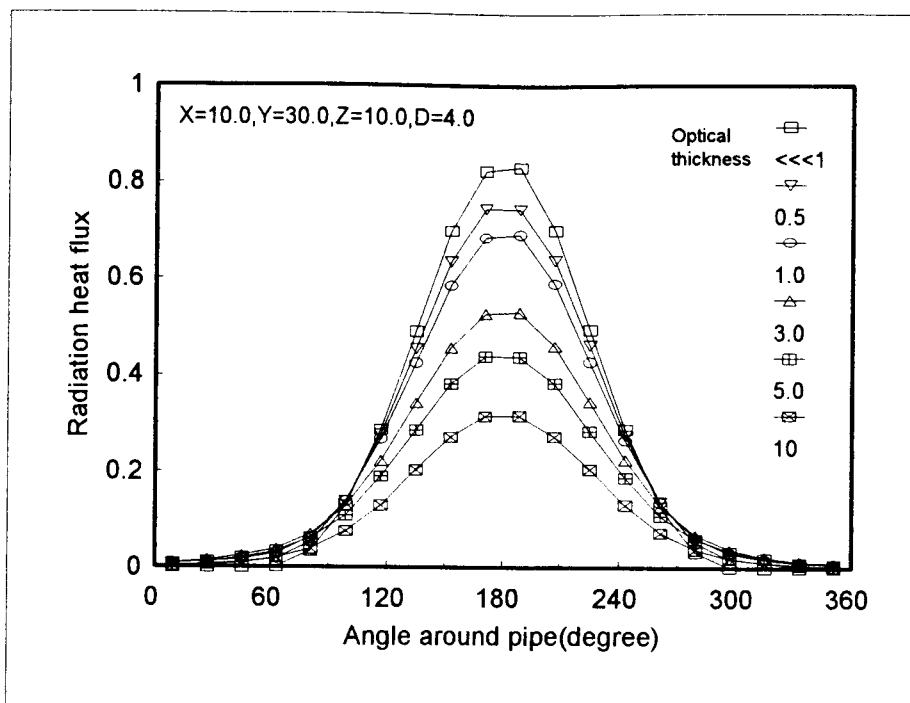


Figure 21. Distribution of radiation heat flux around pipe at  $y = Y/2$  with optical thickness

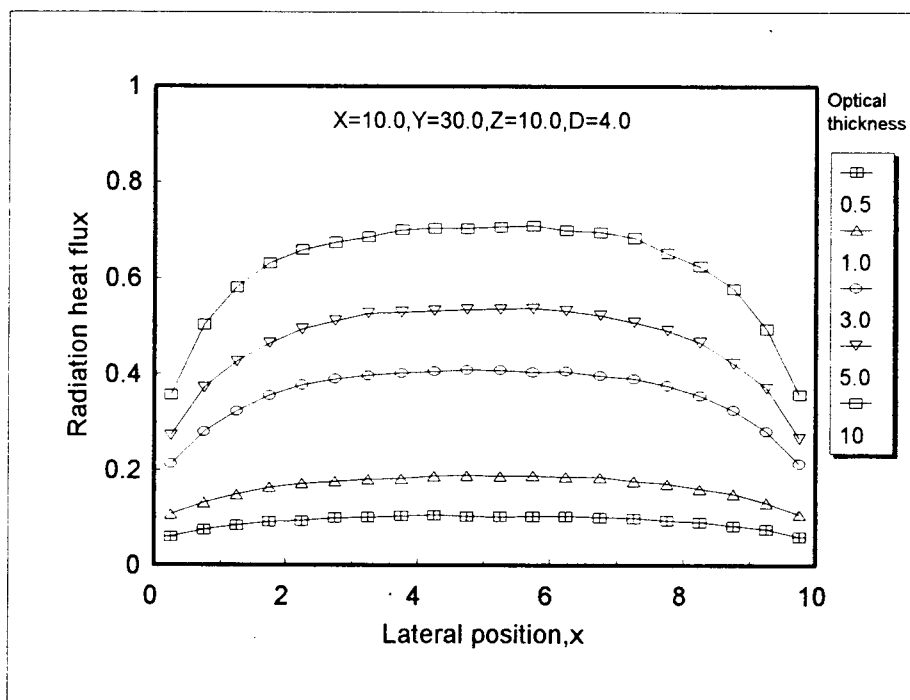


Figure 22. Distribution of radiation heat flux to center line of bottom surface at  $y = Y/2$  with optical thickness

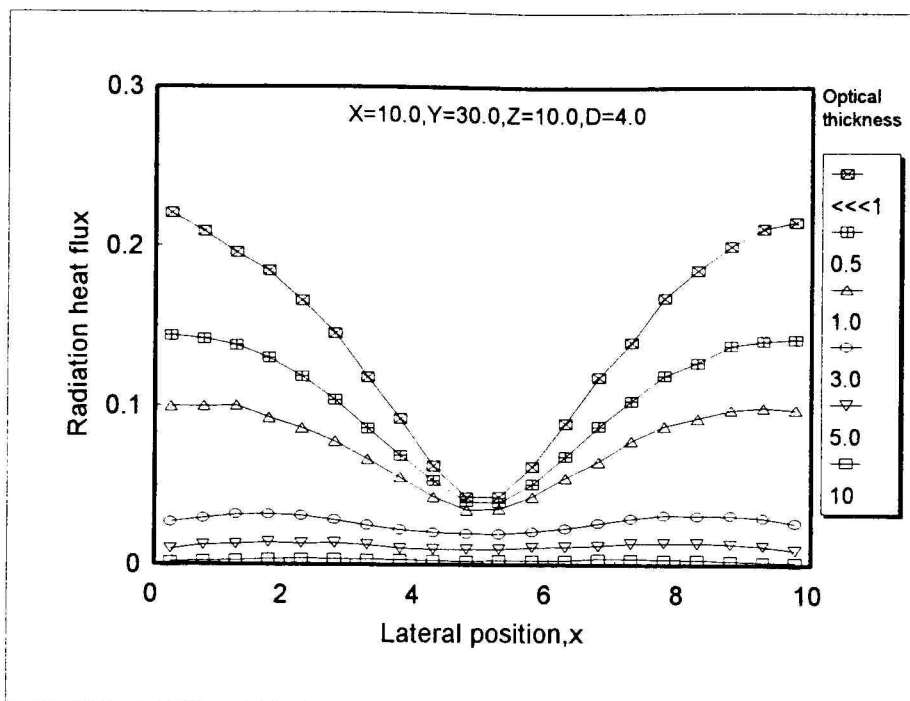


Figure 23. Distribution of radiation heat flux to center line of top surface at  $y = Y/2$  with optical thickness

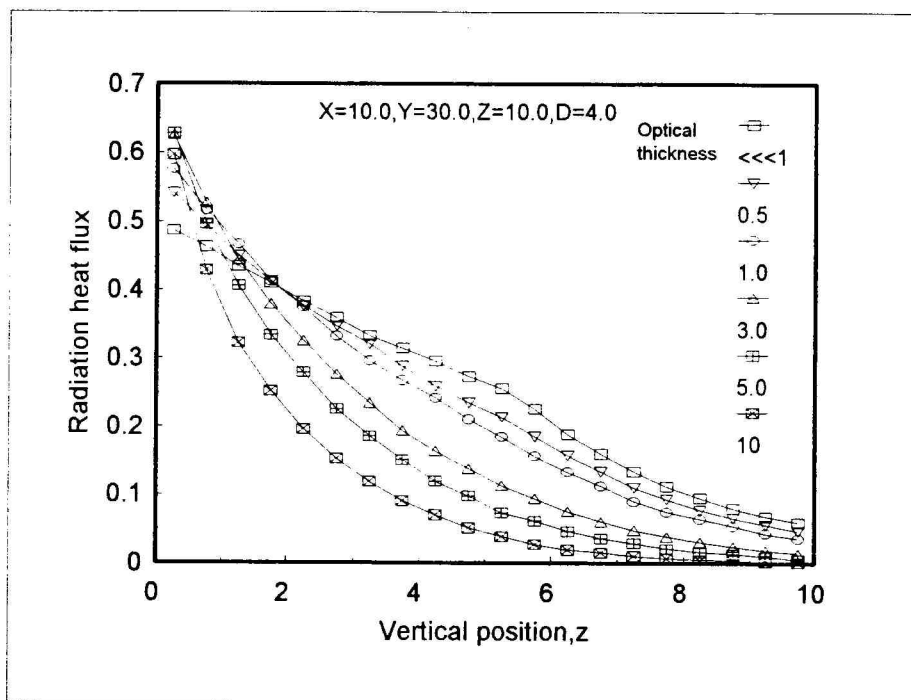


Figure 24. Distribution of radiation heat flux to center line of side wall at  $y = Y/2$  with optical thickness

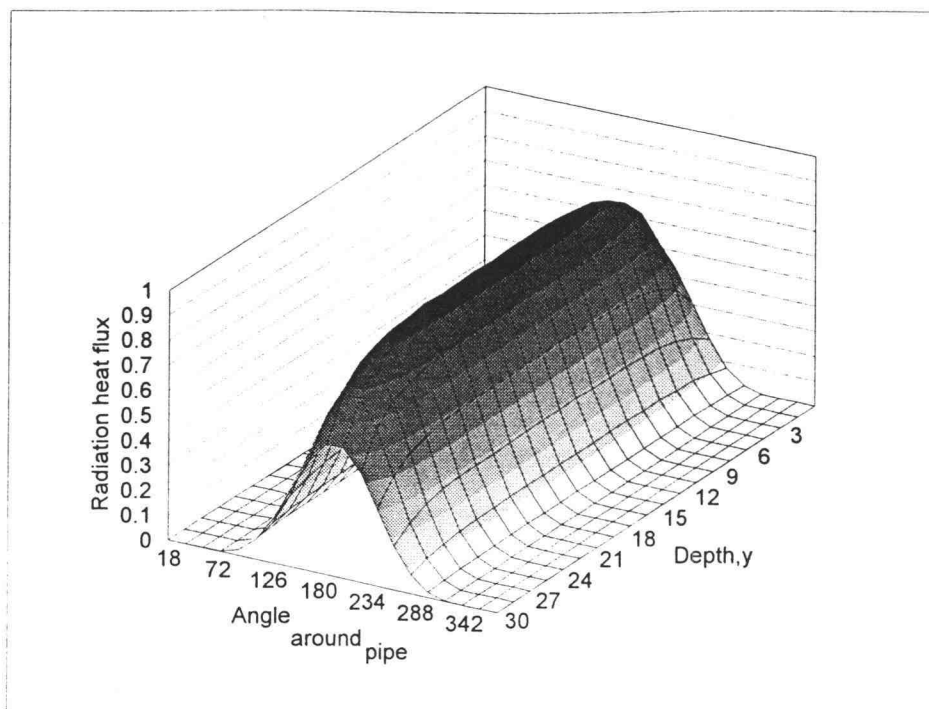
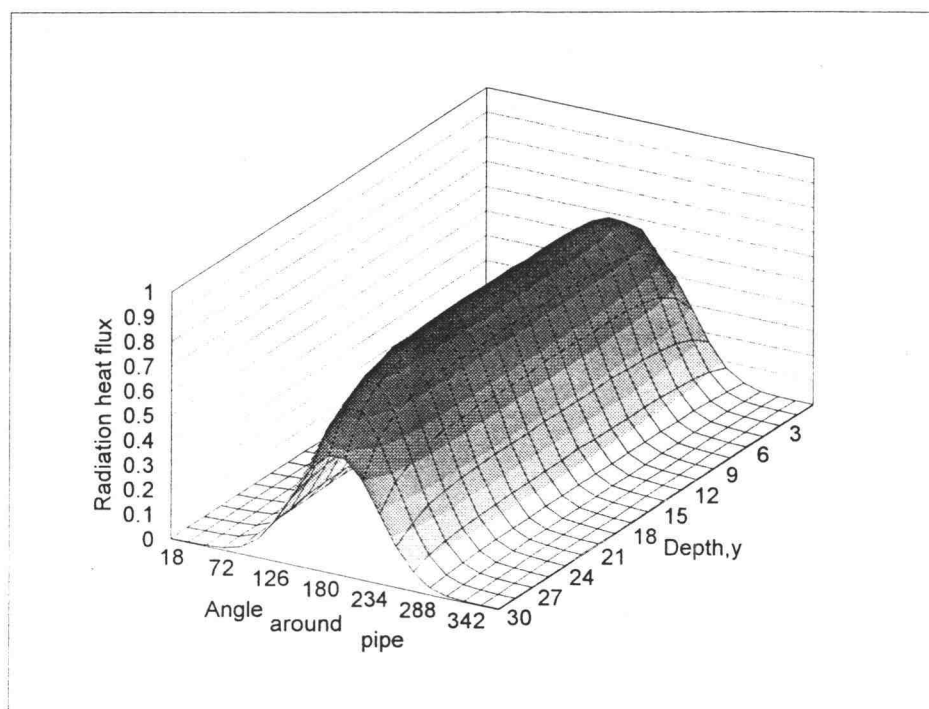
(a)  $\tau \ll 1.0$ (b)  $\tau = 0.5$ 

Figure 25. Distribution of radiation heat flux around pipe surface ( $\tau = \ll 1.0, 0.5, 1.0, 3.0, 5.0, 10.0$ )

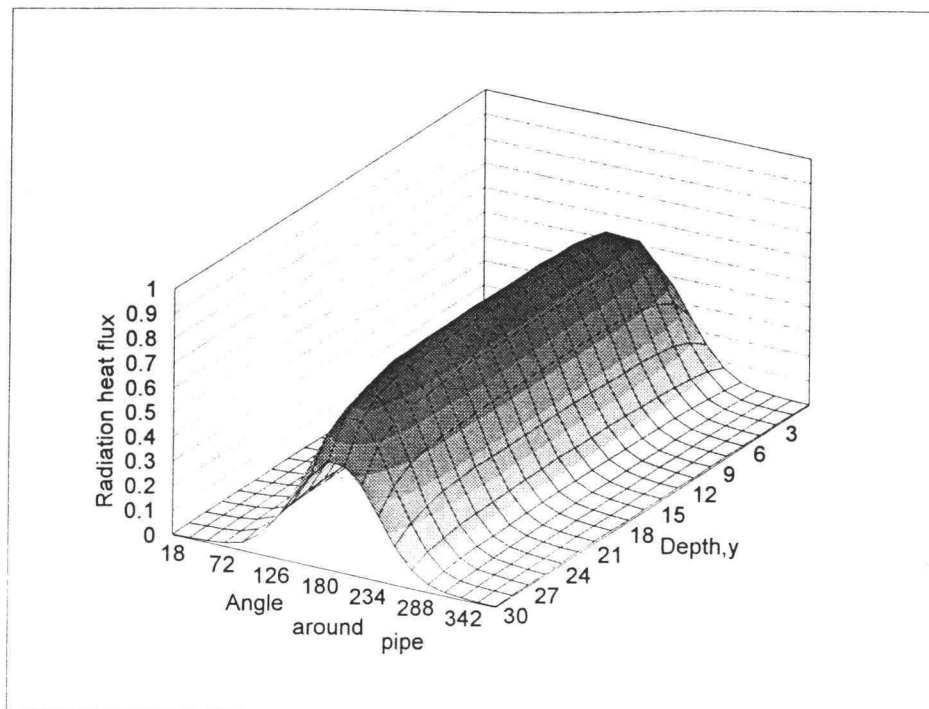
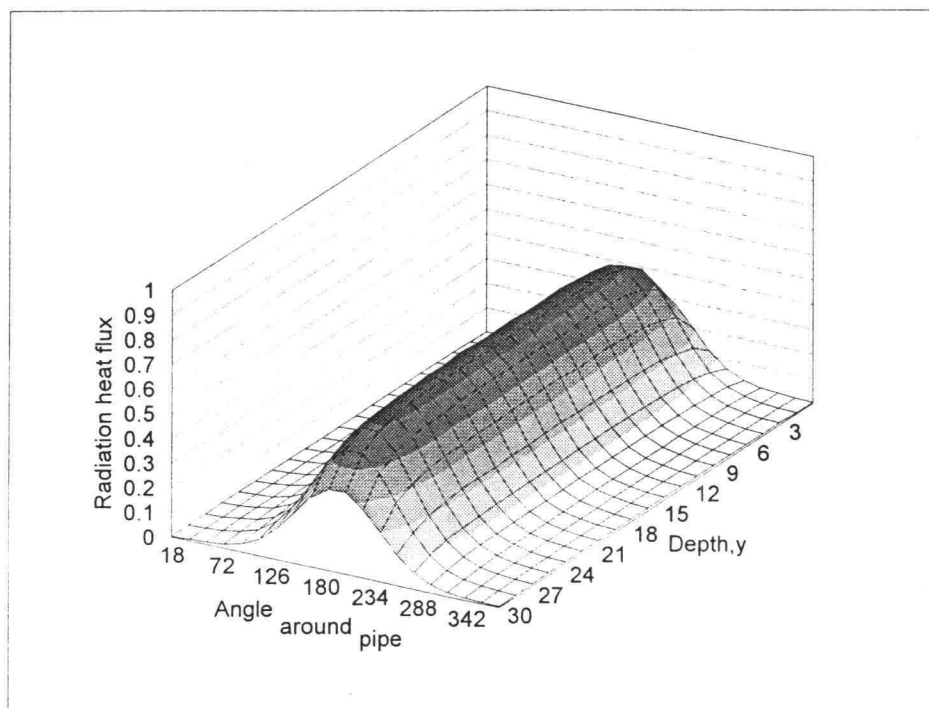
(c)  $\tau = 1.0$ (d)  $\tau = 3.0$ 

Figure 25. (continued)

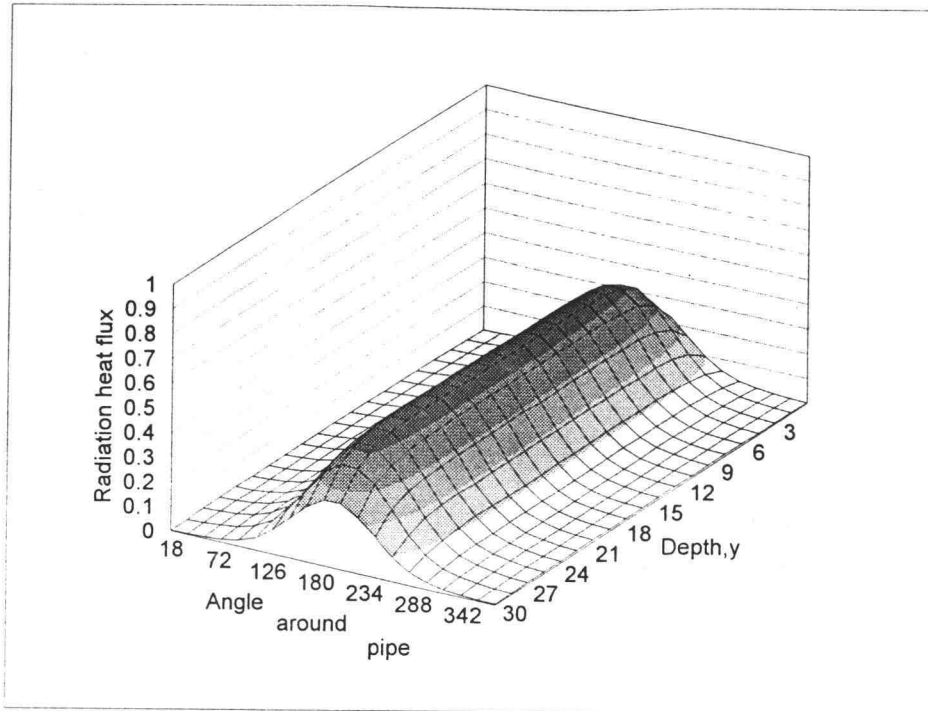
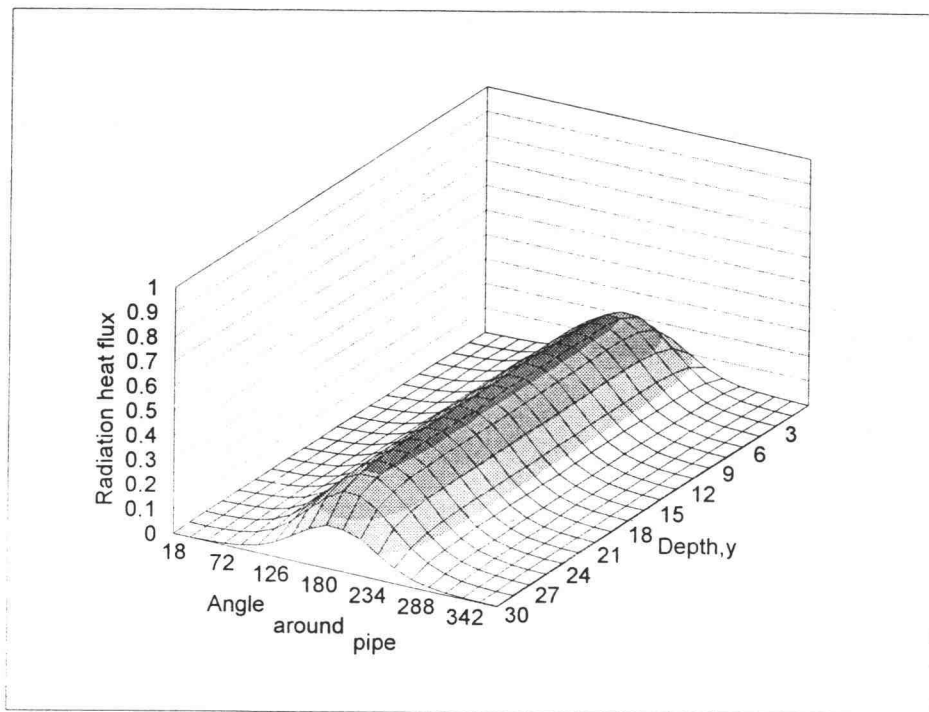
(e)  $\tau = 5.0$ (f)  $\tau = 10.0$ 

Figure 25. (continued)

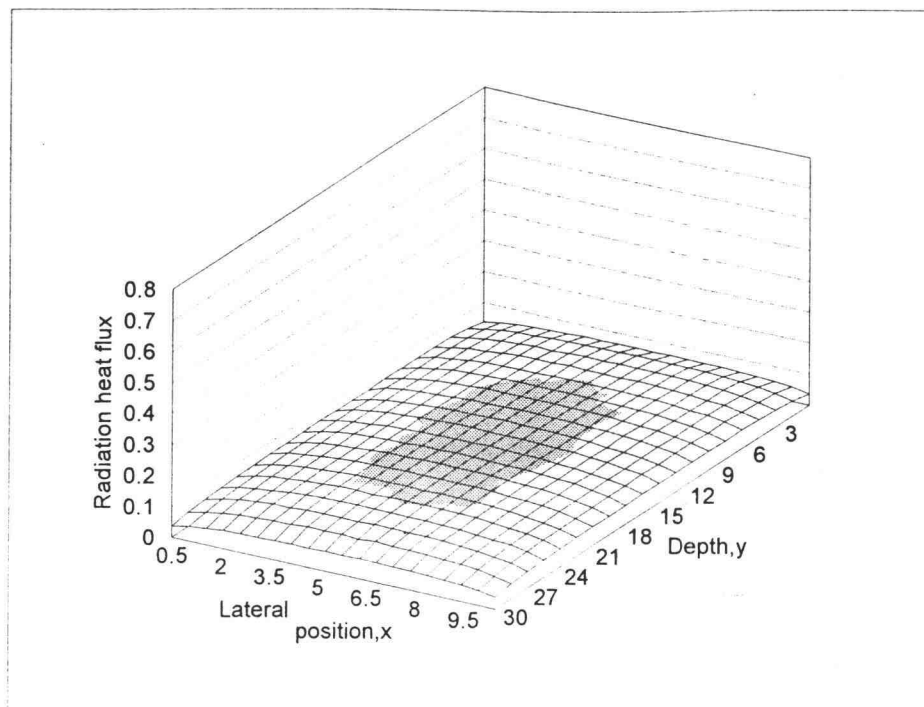
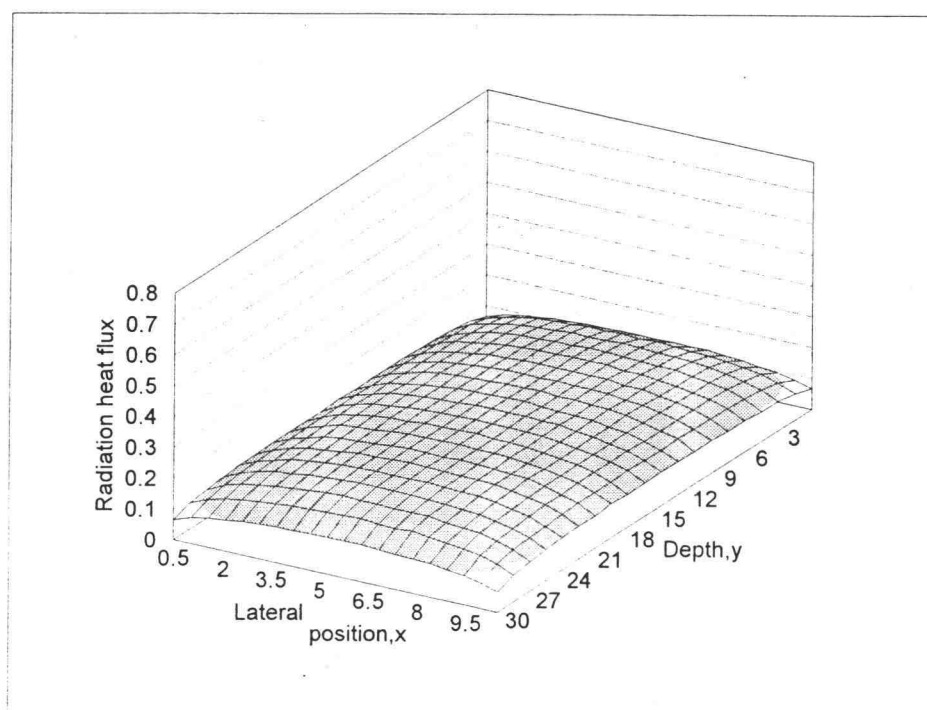
(a)  $\tau = 0.5$ (b)  $\tau = 1.0$ 

Figure 26. Distribution of radiation heat flux on bottom surface ( $\tau = 0.5, 1.0, 3.0, 5.0, 10.0$ )

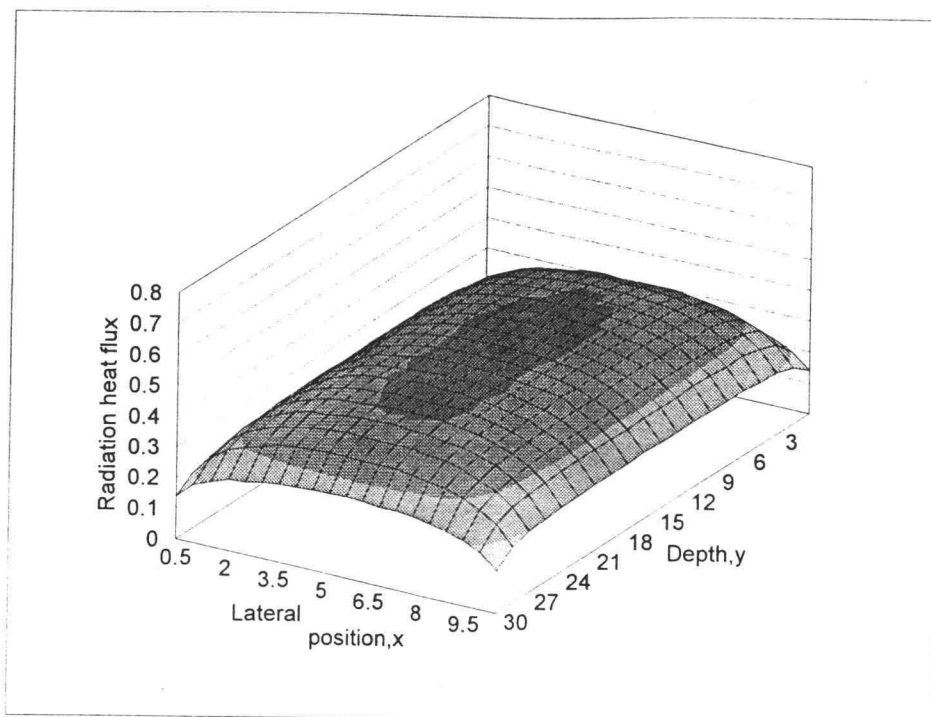
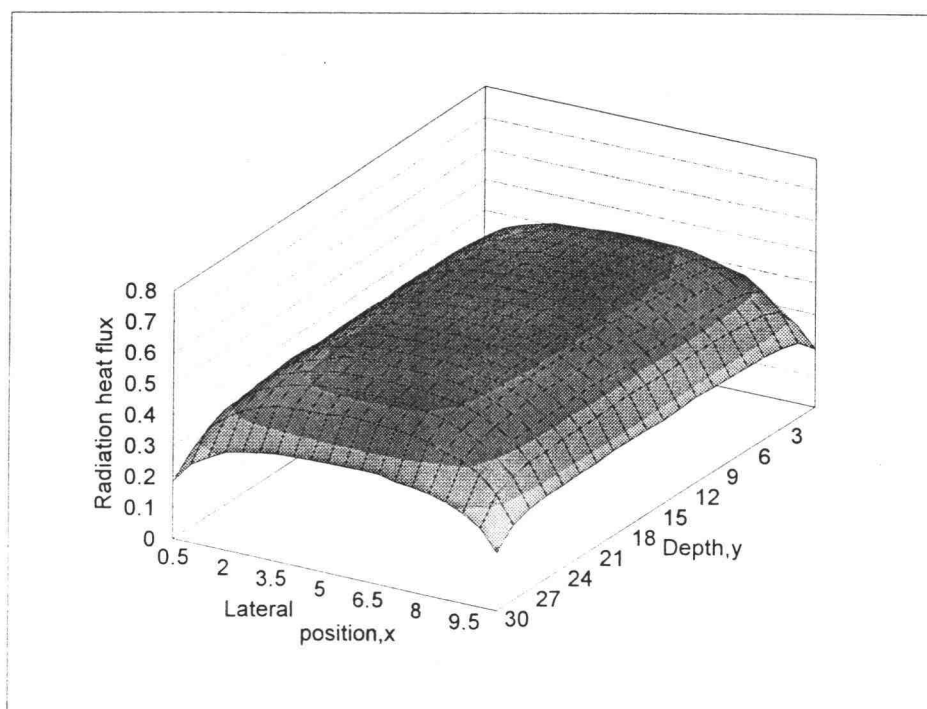
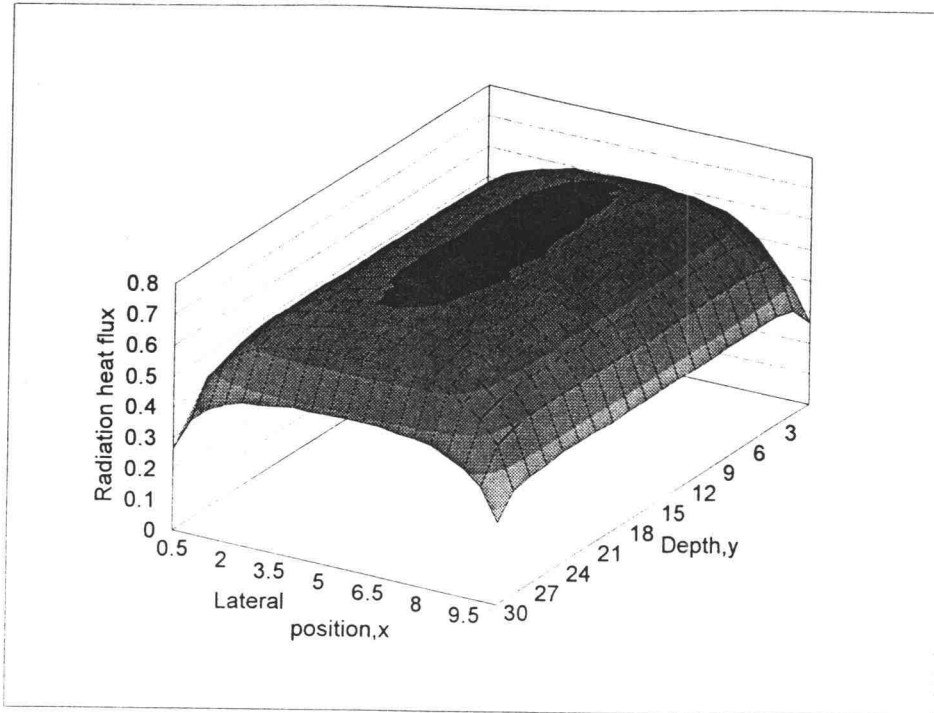
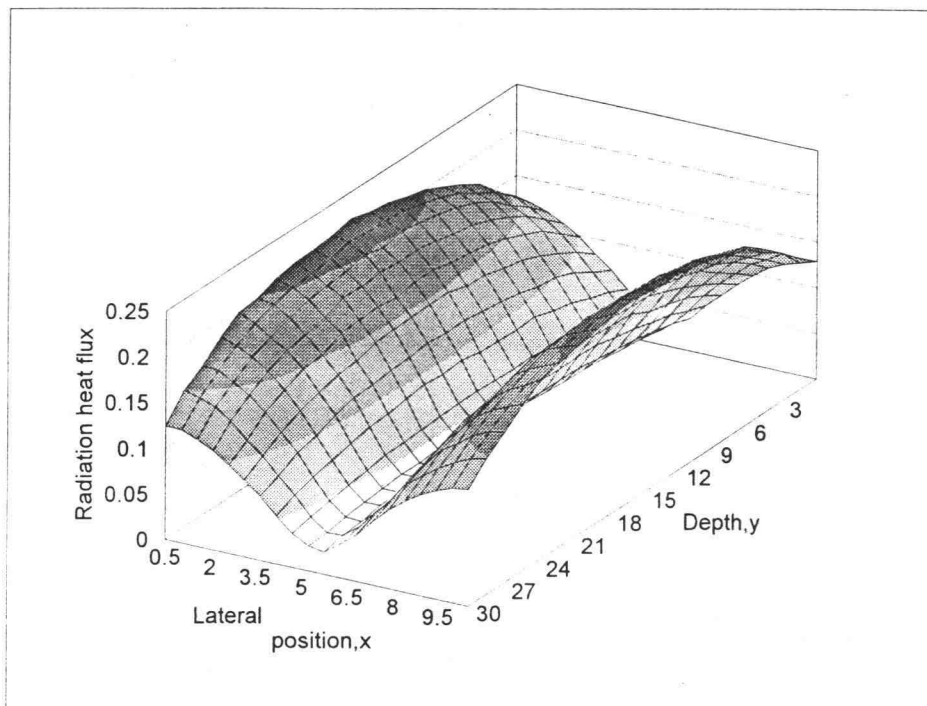
(c)  $\tau = 3.0$ (d)  $\tau = 5.0$ 

Figure 26.(continued)



(e)  $\tau = 10.0$   
Figure 26. (continued)



(a)  $\tau \ll 1.0$   
Figure 27. Distribution of radiation heat flux on top surface ( $\tau = \ll 1.0, 0.5, 1.0, 3.0, 5.0, 10.0$ )

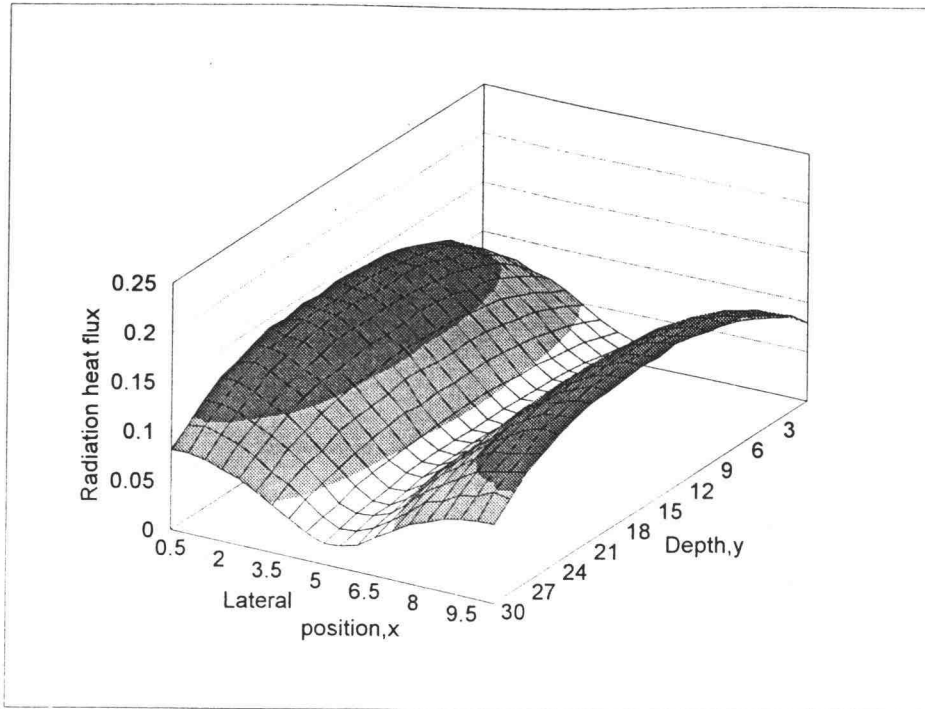
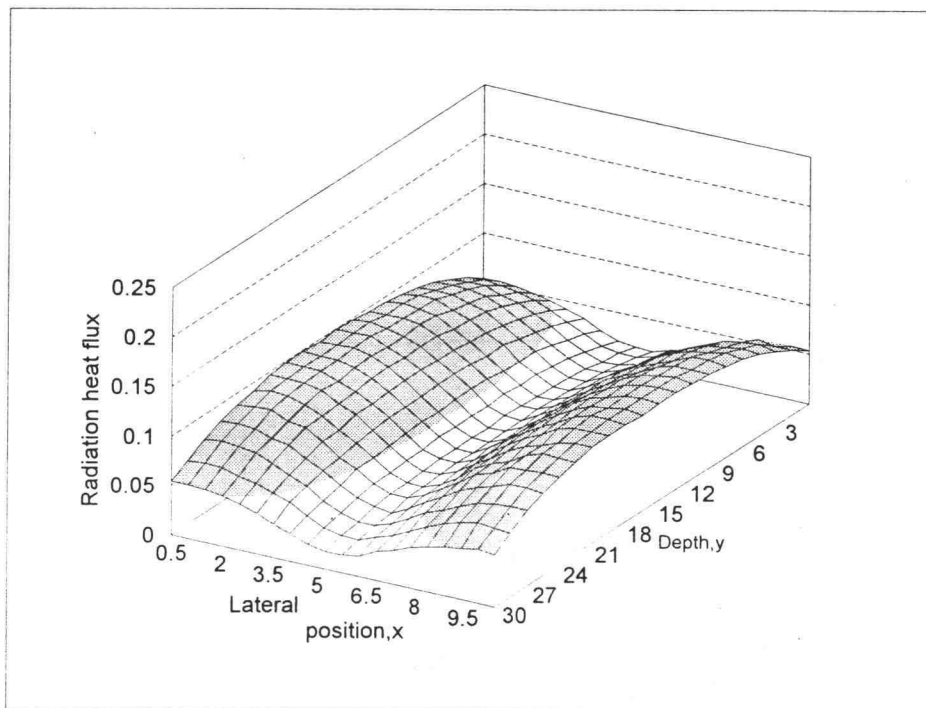
(b)  $\tau = 0.5$ (c)  $\tau = 1.0$ 

Figure 27. (continued)

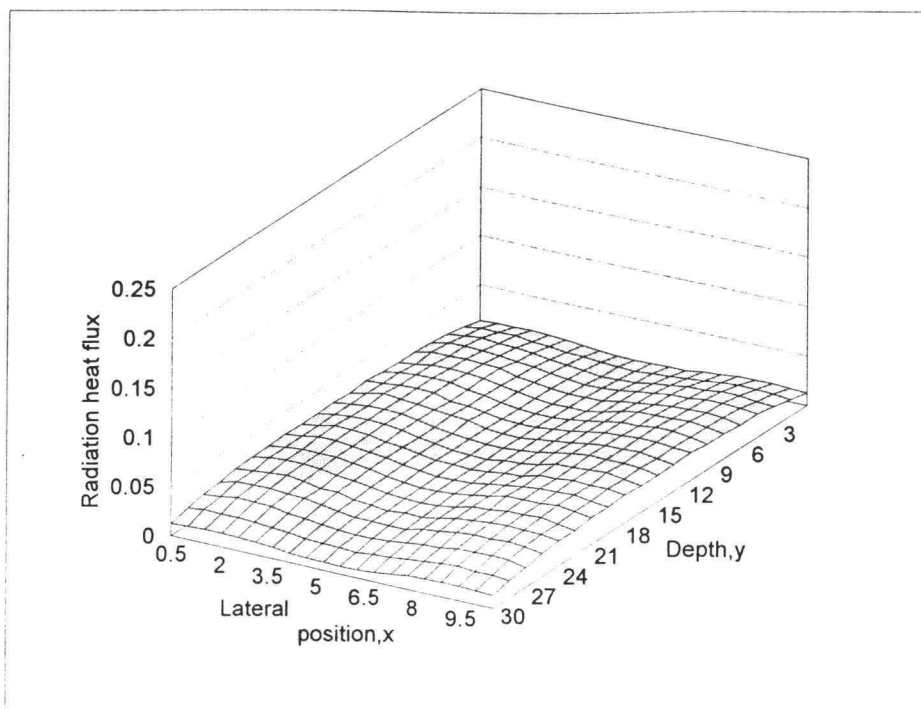
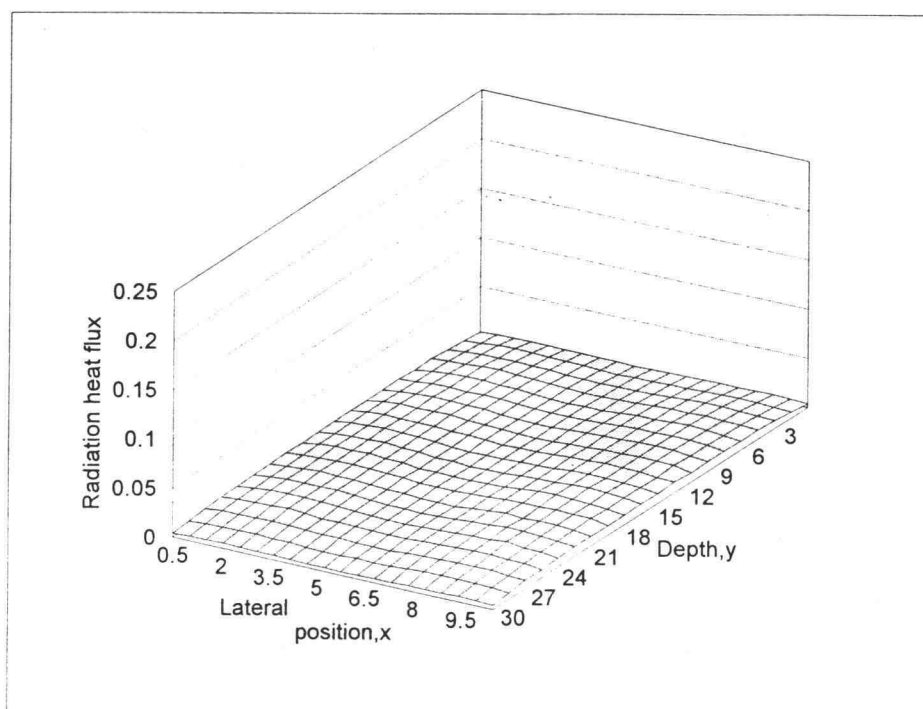
(d)  $\tau = 3.0$ (e)  $\tau = 5.0$ 

Figure 27. (continued)

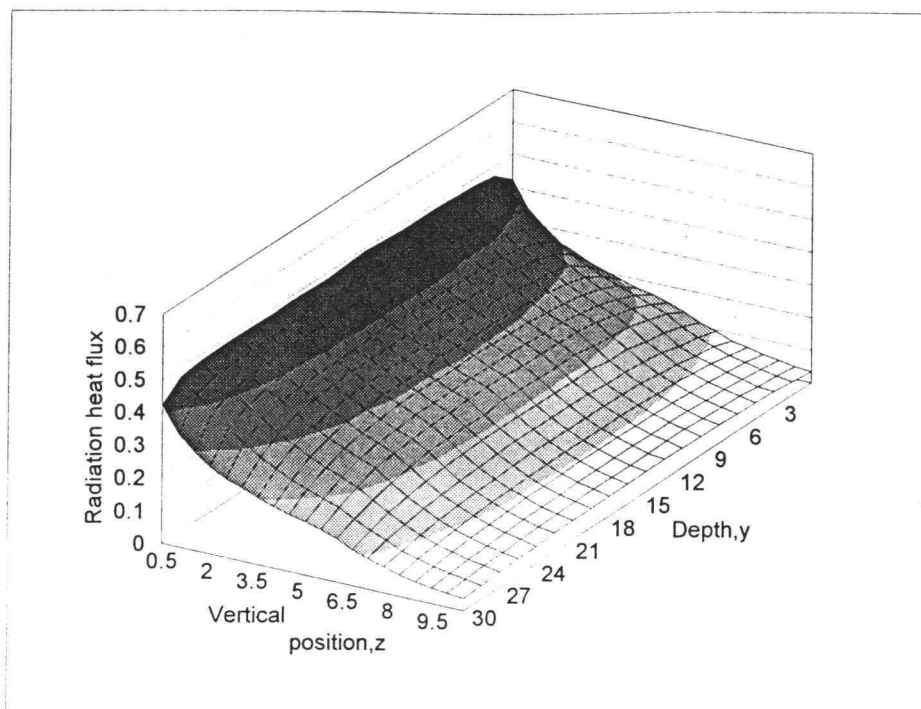
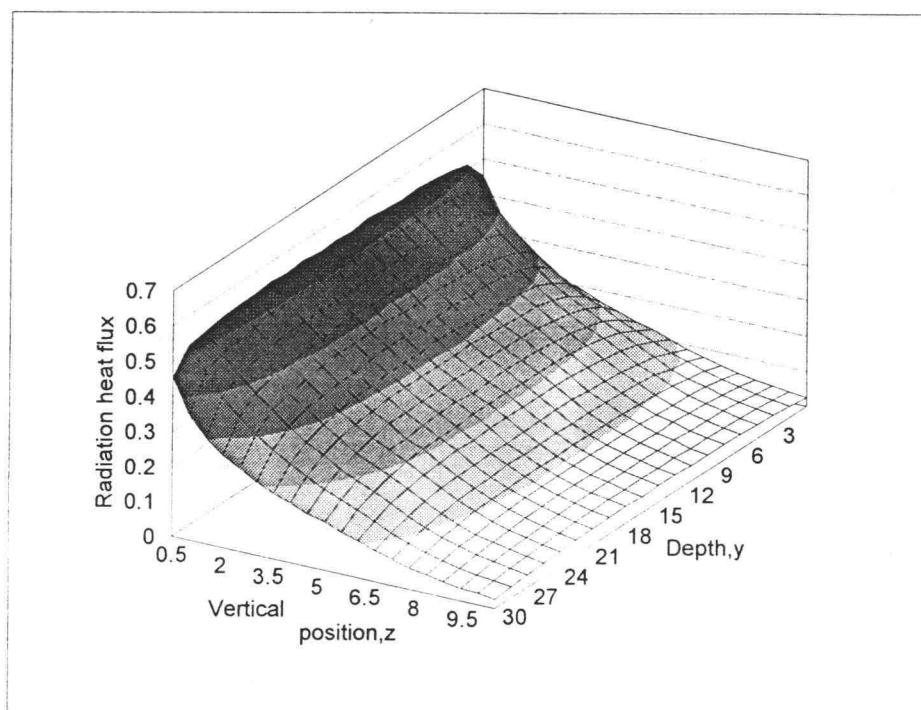
(a)  $\tau < 1.0$ (b)  $\tau = 0.5$ 

Figure 28. Distribution of radiation heat flux on side walls ( $\tau = < 1.0, 0.5, 1.0, 3.0, 5.0, 10.0$ ).

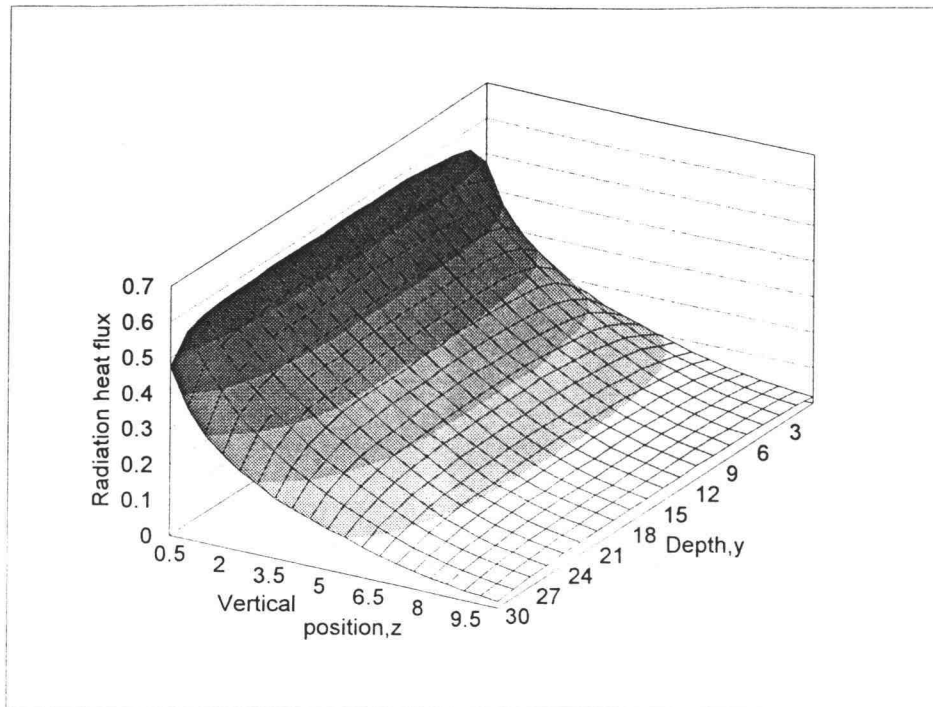
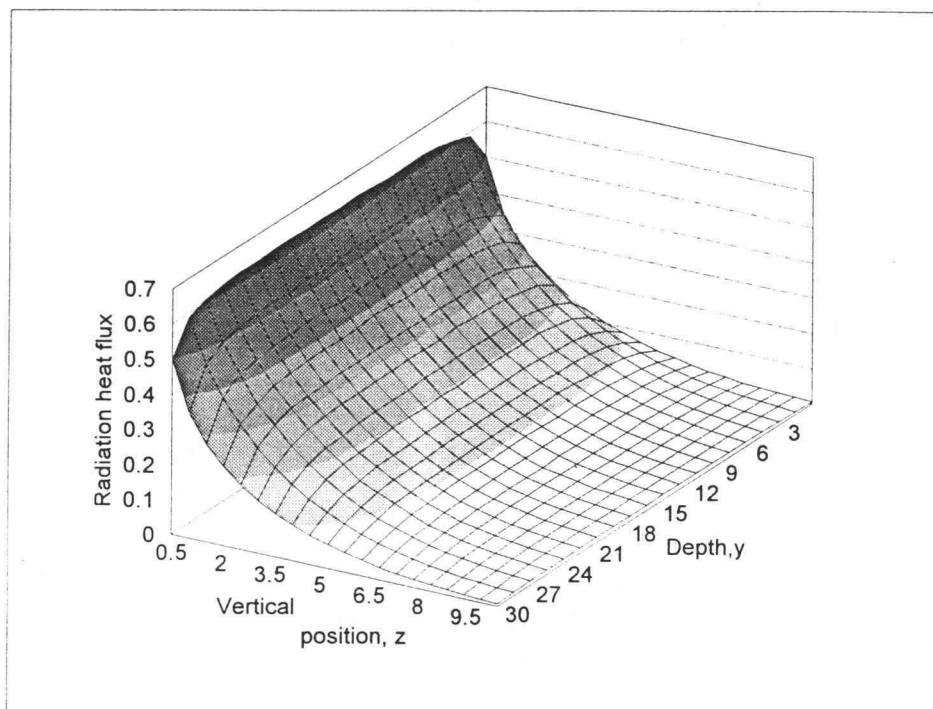
(c)  $\tau = 1.0$ (d)  $\tau = 3.0$ 

Figure 28. (continued)

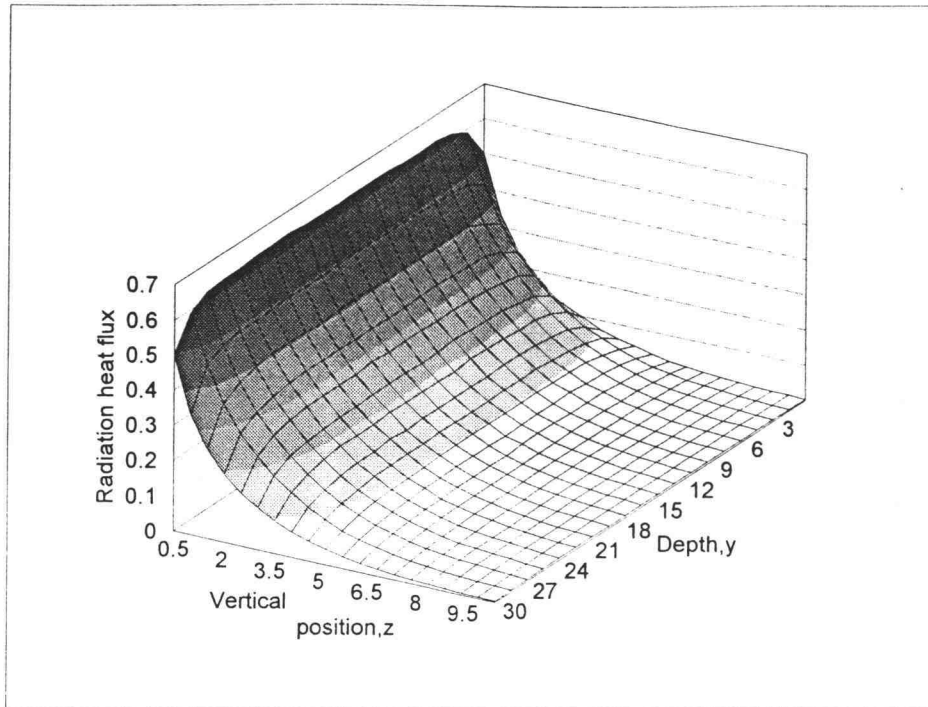
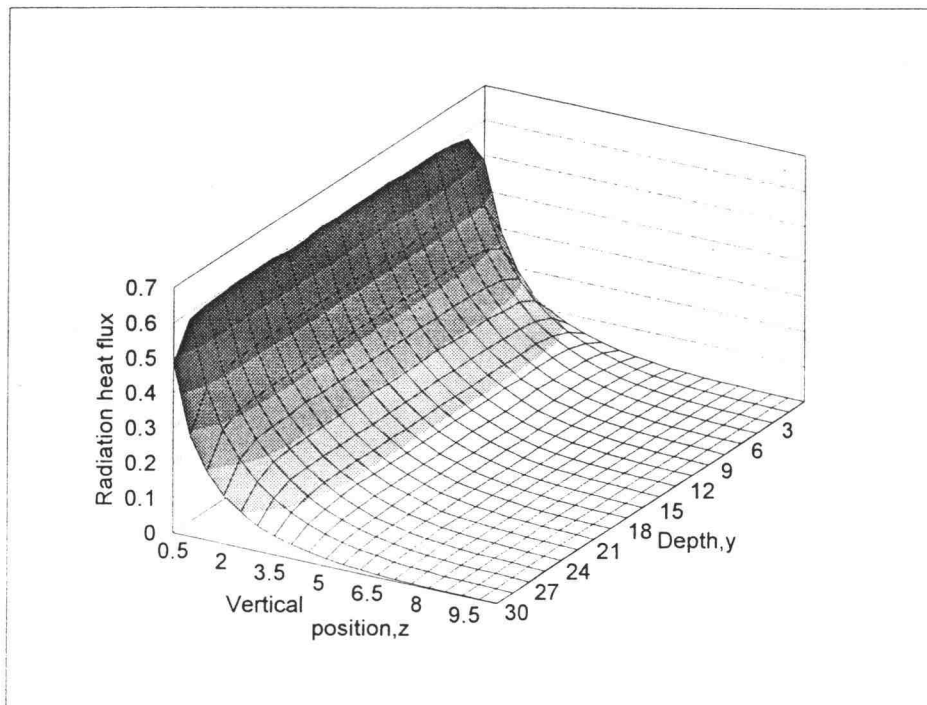
(e)  $\tau = 5.0$ (f)  $\tau = 10.0$ 

Figure 28. (continued)

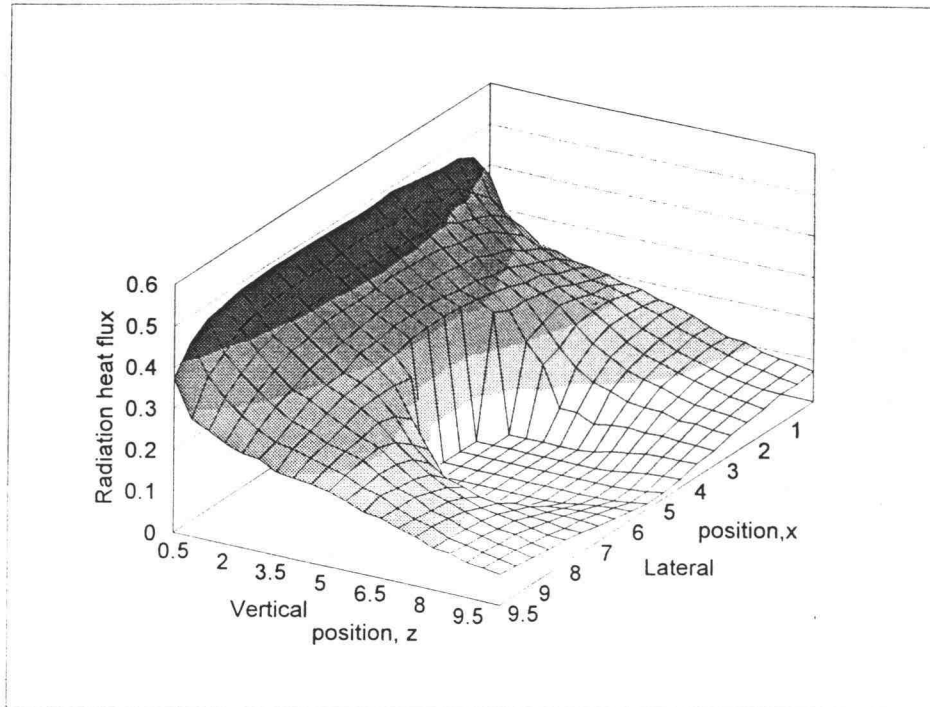
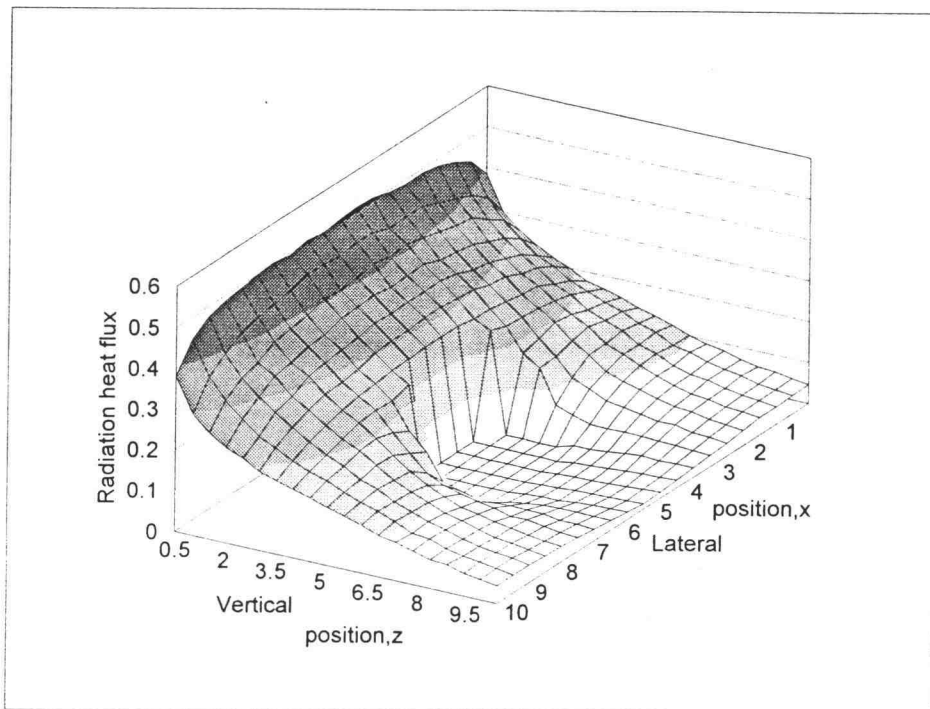
(a)  $\tau < 1.0$ (b)  $\tau = 0.5$ 

Figure 29. Distribution of radiation heat flux on wall 5,6  
 ( $\tau = < 1.0, 0.5, 1.0, 3.0, 5.0, 10.0$ ).

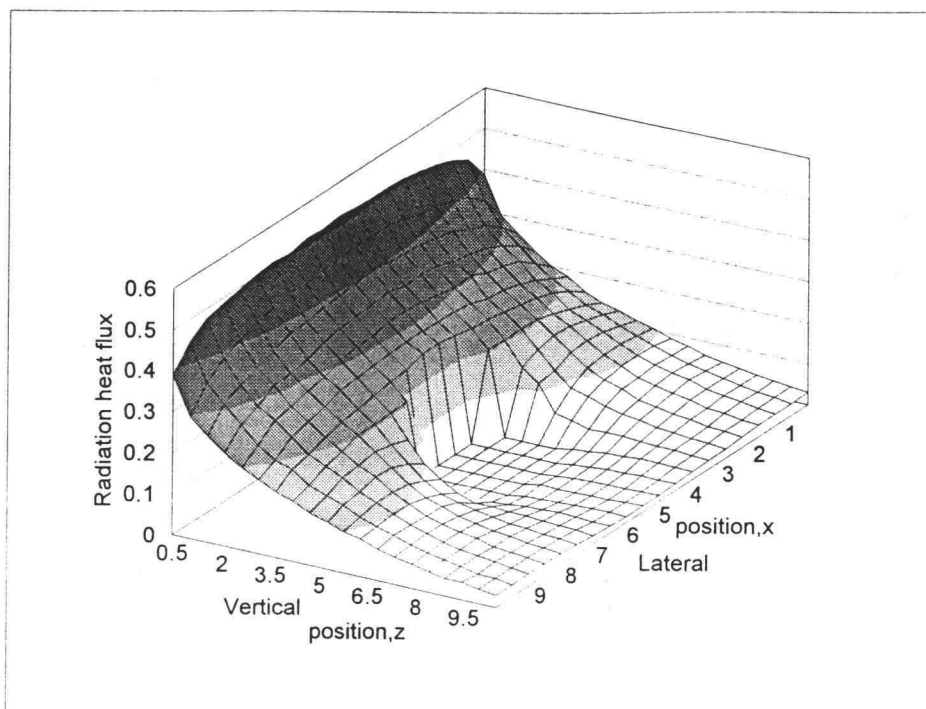
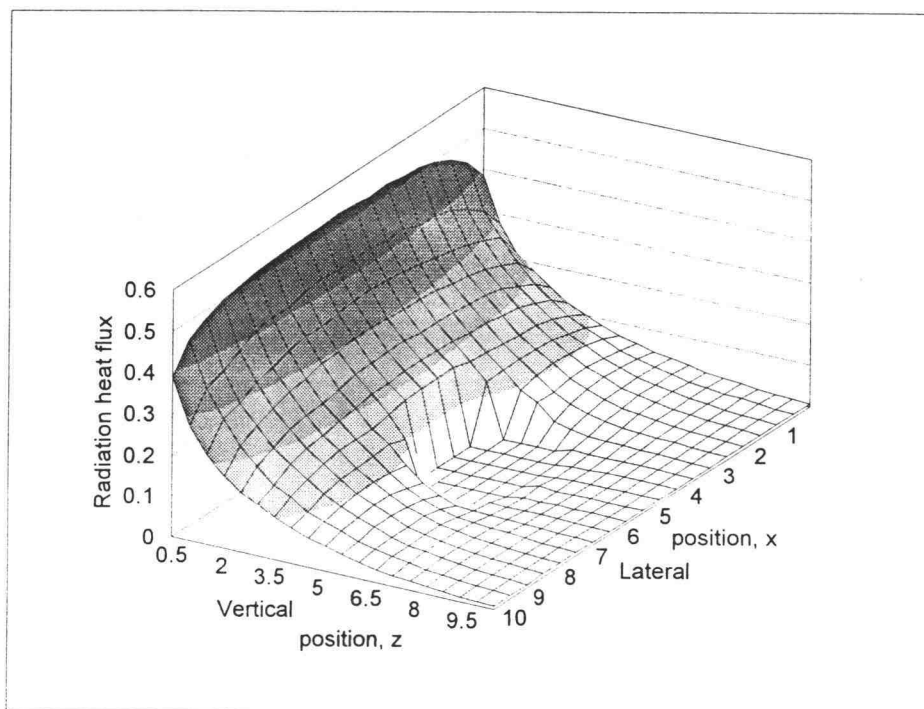
(c)  $\tau = 1.0$ (d)  $\tau = 3.0$ 

Figure 29. (continued)

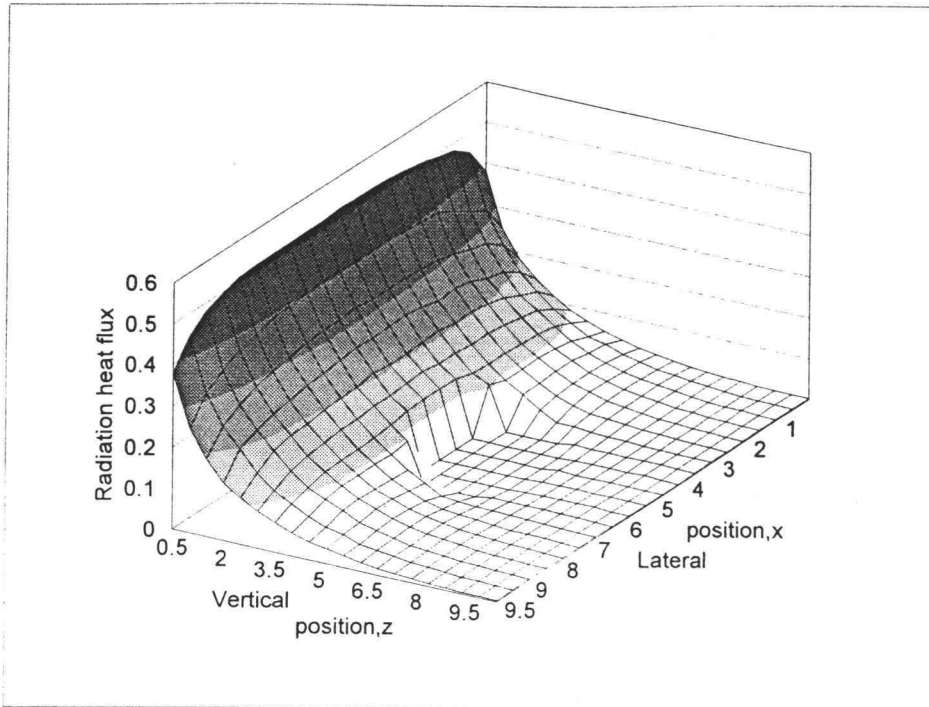
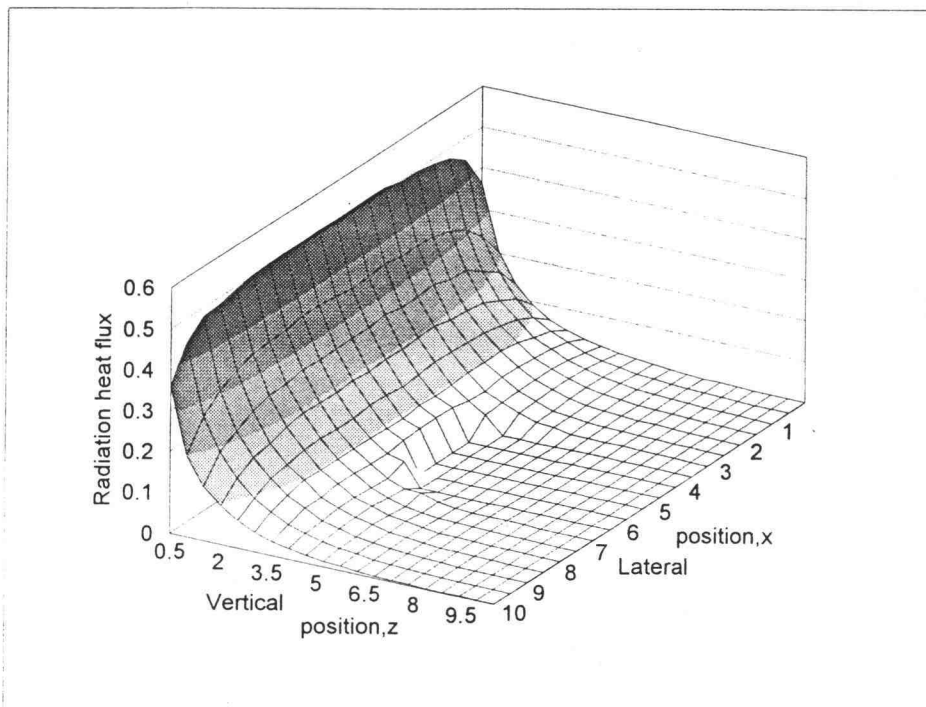
(e)  $\tau = 5.0$ (f)  $\tau = 10.0$ 

Figure 29. (continued)

## CHAPTER 6

### CONCLUSIONS

A Monte Carlo method has been developed and applied to predict the distribution of radiation heat flux within an enclosure containing a horizontal pipe, which also contains a medium which has absorbing, emitting and isotropic scattering characteristics. The MCHO3D Monte Carlo code was developed for this three-dimensional geometry and was applied to one- and two-dimensional cases for validation. The three-dimensional results present useful information for design purposes in readily-usable form.

The amount of radiative energy transferred to the enclosed pipe depends on its location, the optical thickness of the participating medium, and enclosure depth. The maximum radiant transfer to a pipe located in the center of the rectangular enclosure was found to be at a dimensionless enclosure configuration,  $Y/X$ , between 3 and 5. For the optically thin case ( $\tau \ll 1$ ) radiation heat transfer rates can be determined using geometrical view factors.

**BIBLIOGRAPHY**

1. Usiskin, C.M. and Sparrow, E. M. " Thermal Radiation Between Parallel plates Separated by an Absorbing - Emitting Non - Isothermal Gas," International Journal of Heat and Mass Transfer, Vol. 1, June, 1960. pp. 28 - 36.
2. Howell, J. R. and Perlmutter, M. " Monte Carlo Solution of Thermal Transfer Through Radiant Media Between Gray Walls," ASME J. of Heat Transfer, Vol. 86, No. 1, Feb. 1964, pp. 116- 122.
3. Edwards, R. H., and Bobco, R. P., " Radiant Heat Transfer From Isothermal Dispersions with Isotropic Scattering," ASME J. of Heat Transfer, Vol. 89, 1967, pp. 300 - 308.
4. Siegel, R., and Howell, J.R., 1972, Thermal Radiation Heat Transfer (1st ed.), McGraw - Hill, New York.
5. Siegel, R., and Howell, J.R., 1972, Thermal Radiation Heat Transfer, Vol. II: Radiation Exchange Between Surfaces and in Enclosures, NASA, SP-164.
6. Siegel, R., and Howell, J.R., 1972, Thermal Radiation Heat Transfer, Vol. III: Radiation Transfer with Absorbing, Emitting, And Scattering Media, NASA, SP-164
7. Modest, M.F., 1993, Radiative Heat Transfer, McGraw-Hill, New York.
8. Haji - Sheikh, A., " Monte Carlo Methods," in Handbook of Numerical Heat Transfer, W. J. Minkowycz et al. (eds.). pp. 673 - 717, Wiley, New York, 1988.
9. Kahn, Herman, "Application of Monte Carlo," Rept. No. Rm - 1237 - AEC (AEC No. AECU - 3259 ), Rand Corp., April 27, 1956.
10. Perlmutter, M., and Howell, J. R., " Radiant Transfer through a Gray Gas Between Concentric Cylinders Using Monte Carlo," ASME J. of Heat Transfer, Vol. 86, No. 2, pp. 169 - 179, 1964.
11. Fleck, J. A. : " The Calculation of Nonlinear Radiation Transport by a Monte Carlo Method : Statistical Physics," Method in Computational Physics, Vol. 1, pp. 43 - 65, 1961.

12. Howell, J. R., Strite, M. K., and Renkel, H., " Heat Transfer Analysis of Rocket Nozzles Using very High - Temperature Propellants, " *AIAA Journal* Vol. 3, No. 4, April 1965, pp. 669 - 673.
13. Slater, G., Salpeter, G.G., and Wasserman, I., 1982, "Monte Carlo Calculations of Resonance Radiative Transfer Through a Semi-Infinite Medium," *Astrophys. J.*, Vol. 255, pp 293 - 302.
14. Bernes, C., 1979, "A Monte-Carlo Approach to Non-LTE Radiative Transfer Problems," *Astron. Astrophys.*, Vol 73, pp. 67 - 73.
15. Meier, R. R., and Lee, J. -S., 1978, "A Monte Carlo Study of Frequency Redistribution in an Externally Excited Medium," *Astrophys. J.*, Vol. 219, pp. 262 - 273.
16. Katkovskii, L. V., Khodyko, Yu. V., and Leparskaya, L. V., 1983, "Monte Carlo Calculation of Outgoing Radiation in Vibrational-Rotational Band of CO from a Cylindrical Supersonic Molecular Gas Jet in the Absence of Local Thermodynamic Equilibrium," trans. from *Zh. Prikladnoi Spektroskopii*, Vol. 38, No. 2, pp. 256 - 262.
17. Vlasov, Yu, P., and Titarchuk, L. G., 1982, "Monte Carlo Calculations of Resonance-Line Formation in a Plane Layer, " *Sov. Astron.*, Vol 8, No. 5, pp.304 - 307.
18. Carter, L. L., Horak, H. G., and Sandford, M. T., III, 1978, " An Adjoint Monte Carlo Treatment of the Equations of Transfer for Polarized Light," *J. Com. Phys.*, Vol. 26, pp. 119 - 128.
- 19 Egan, W. G., and Hilgeman, T., 1978, " Spectral Reflectance of Particulate Materials: A Monte Carlo Model Including Asperity Scattering," *Applied Optics*, Vol. 17, No. 2, pp. 245 - 252.
- 20 Dunn, W. L.,1981, " Inverse Monte Carlo Analysis," *J. Comput. Phys.* 41, pp. 154 - 166.
21. Gupta, R. P., Wall, T. F., and Truelove, J. S., 1983, "Radiative Scatter by Fly Ash in Pulverized-Coal-Fired Furnaces: Application of the Monte Carlo Method to Anisotropic Scatter," *Int. J. Heat Mass Transfer*, Vol. 26, No. 11, pp. 1649 - 1660.
22. Lewis, E. E., and Miller, W. F., Jr., 1984, Computational Methods of Neutron Transport, Wiley, New York.

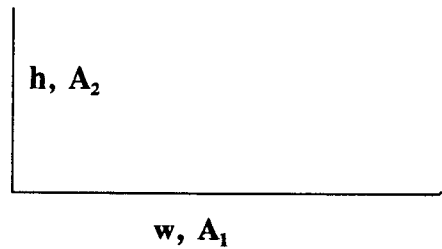
23. Meier, R. R., Lee, J. -S., and Anderson, D. E., 1987, "Atmospheric Radiation of Middle UV Radiation From an Internal Source," *Applied Optics*, Vol. 17, No. 20, pp. 3216 - 3225.
24. Howell, J. R., 1988, "Thermal Radiation in Participation Media : The Past, the Present, and Some Possible Futures," *ASME J. of Heat Transfer*, Vol. 110, pp. 1220 - 1229.
25. Tae-Kuk Kim, and Haeok Lee, " Effect of anisotropic scattering on radiative heat transfer in tow-dimensional rectangular enclosures," *Int. J. Heat Mass Transfer*, Vol.31, No. 8, pp. 1711 -1721, 1988,
26. Heaslet, M. A., and Warming, R. F., "Radiative Trandfer and Wall Temperature slip in and Absorbing Planar Medium," *International J. of Heat and Mass Transfer*, Vol. 8, pp. 979-994, 1965.
27. Thynell and Özisik, M. N., "Radiation transfer in isotropically scattering rectangular enclosures," *J. Thermophys*, Vol. 1, No. 1, Jan. 1987.
28. Kantorovich, L. V., and Krylov, V. I., Approximate Methods of Higher Analysis, John Wiley & Sons, New York, 1964.
29. Chu, C. M. and churchill, S. W., "Representation of and Angular Distribution of Radiation Scatterde by a Spherical Particle," *J. of the Optical Society of America*, Vol. 45, pp 958-962, 1955.
30. Jakob, M. Heat Transfer, Vol.1, John Wiley & Sons, Inc., New York, N.Y., 1949.
31. Wiebelt, J. A. and Ruo, S. Y., "Radiant-Interchange configuration factors for finite right circular cylinder to rectangular," *Int. J. Heat and Mass Transfer*, Vol. 6, pp. 143-146, 1963.

## **APPENDICES**

## APPENDIX 1

### Radiative heat flux between perpendicular surfaces

The geometric view factor for two infinitely long plates of unequal widths,  $h$ , and,  $w$ , having one common edge and oriented  $90^\circ$  to each other, is [7]



$$F_{1-2} = \frac{1}{2} \left[ 1 + \frac{h}{w} - \sqrt{1 - \left(\frac{h}{w}\right)^2} \right] \quad (\text{A-1})$$

Where  $w$  is the unit length,  $n$  is the number of segments in unit length  $w$  giving  $h = w / n$ . In Monte Carlo method the energy per bundle is constant and the view factor is the ratio of bundles absorbed at  $A_2$  to the total number of bundles emitted from  $A_1$ . The dimensionless radiative heat flux on  $A_2$  then becomes

$$q_{A_2} = nF_{1-2} = \frac{1}{2} (n + 1 - \sqrt{n^2 + 1}) \quad (\text{A-2})$$

The dimensionless radiative heat flux  $q_{A_2}$  approaches 0.5 when  $n \rightarrow \infty$ .

## APPENDIX 2

## Program listing for MCHO3D

```

c-----
c          *** MCHO3D ***
c
c  This program calculate the radiative heat transfer in the
c  configuration system participation media shown in Fig.1.1
c          by the Monte Carlo method.
c          Hong, Seung-Ho
c          Oregon State Univ..Mechanical Eng..
c          (09/06/'93)
c-----
c  program mcho3d
c
c  include 'com.for'
c
c  open(unit = 6,file = 'out3d.out',status = 'old')
c  call input
c
c  Define initial condition of variables.
c  absco : absorbtion coefficient of media
c
c  pi = 4.0d00 * atan(1.0d00)
c  absco = ot/hig
c
c  do 30 i = 1,kx
c    do 10 j = 1,ky
c      ns1(i,j) = 0
c      ns4(i,j) = 0
10  continue
c    do 20 j = 1,kz
c      ns5(i,j) = 0
c      ns6(i,j) = 0
20  continue
30  continue
c  do 50 i = 1,ky
c    do 40 j = 1,kz
c      ns2(i,j) = 0
c      ns3(i,j) = 0
40  continue
50  continue

```

```

do 80 i = 1,kx
  do 70 j = 1,ky
    do 60 k = 1,kz
      nsa(i,j,k) = 0
60    continue
70  continue
80  continue
do 100 i = 1,kz
  do 90 j = 1,ky
    nsp(i,j) = 0
90  continue
100 continue
c-----
c          ***** MCHO3D start *****
c-----

x = ran3(-74432333)
c
do 999 ii = 0, nuemy - 1
c
  print*,ii

  buny = (2*ii+1)*alen/2.0/nuemy
c
do 888 jj = 0, nuemx - 1
c
  bunx = (2*jj+1) * width / 2.0 / nuemx
  do 777 kk = 1, npn
c
    x = bunx
    y = buny
    z = 0.0d00
    eta = 0.0d00
c
c Initial direction of bundle from the source
c
  theta = asin(sqrt(ran3(0)))
  phi = 2.0d00 * pi * ran3(0)
  rx = sin(theta)*cos(phi)
  ry = sin(theta)*sin(phi)
  rz = cos(theta)
  call caleta(eta,rx,rz)
c
c Path length of emitting bundle through the media
c

```

```

1000    s = -1.0d00 / absco * dlog(ran3(0))
c
c start from pipe.If the direction of bundle is not pipe
c the direction will be walls
c
c ixx = 1 means that bundle is absobed by wall
c ixx = 2 means that bundle is reflected
c ixx = 3 means that bundle dosen't reach to the wall
c
666    rxnew = sin(eta)
        rynew = sin(phi)
        rznew = cos(eta)
        sdc = sqrt((dx-x)**2+(dz-z)**2)
        sig2 = asin(dia/2.0d00/sdc)
c
        if(x.ge.dx.and.z.ge.dz) then
            if((dx-x).eq.0.0d00) then
                sigma = pi
                sig3 = pi + sig2
                sig4 = pi - sig2
            else
                if((dz-z).eq.0.0d00) then
                    sigma = 1.5d00 * pi
                else
                    sigma = 1.5d00 * pi - atan((dz-z)/(dx-x))
                endif
                sig3 = sigma + sig2
                sig4 = sigma - sig2
            endif
c
        rdz3 = cos(sig3)
        rdx4 = sin(sig4)
c
        if(rznew.lt.rdz3.and.rxnew.lt.rdx4) then
            call pipe
            goto(777,666,1000)ixx
        else
            call wall
            goto(777,666,1000)ixx
        endif
c
        elseif(x.lt.dx.and.z.gt.dz) then
            sigma = pi/2.0d00 + atan(abs((dz-z)/(dx-x)))
            sig3 = sigma - sig2
            sig4 = sigma + sig2

```

```

rdz3 = cos(sig3)
rdx4 = sin(sig4)
c
if(rznew.lt.rdz3.and.rxnew.gt.rdx4) then
  call pipe
  goto(777,666,1000)ixx
else
  call wall
  goto(777,666,1000)ixx
endif
c
elseif(x.le.dx.and.z.le.dz) then
c
  if((dx-x).eq.0.0d00) then
    sigma = 0.0d00
    sig3 = sig2
    sig4 = 2.0d00 * pi - sig2
  else
    if((dz-z).eq.0.0d00) then
      sigma = pi/2.0d00
    else
      sigma = atan((dx-x)/(dz-z))
    endif
    sig3 = sigma + sig2
    sig4 = 2.0d00 * pi + sigma - sig2
  endif
c
  rdz3 = cos(sig3)
  rdx4 = sin(sig4)
c
  if(rznew.gt.rdz3.and.rxnew.gt.rdx4) then
    call pipe
    goto(777,666,1000)ixx
  else
    call wall
    goto(777,666,1000)ixx
  endif
c
  elseif(x.gt.dx.and.z.lt.dz) then
    sigma = 1.5d00 * pi + atan(abs((dz-z)/(dx-x)))
    sig3 = sigma - sig2
    sig4 = sigma + sig2
    rdz3 = cos(sig3)
    rdx4 = sin(sig4)
c

```

```

        if(rznew.gt.rdz3.and.rxnew.lt.rdx4) then
            call pipe
            goto(777,666,1000)ixx
        else
            call wall
            goto(777,666,1000)ixx
        endif
c
        else
            print*, 'something wrong in celecting hitting direction'
            goto 555
        endif
c
777 continue
888 continue
999 continue
c
        call output

555 stop
end

```

```

c-----
c This subroutine calculate the bundle history. The bundle is
c moving toward pipe. So after the bundle impacts with pipe
c two cases will be occur in pipe, absorption or reflection.
c-----

```

```

        subroutine pipe
c
        include 'com.for'
c
        xold = x
        yold = y
        zold = z
        sold = s
        sxz = s * sqrt(rx**2 + rz**2)
        sdcold = sqrt((dx-xold)**2+(dz-zold)**2)
        sig2 = asin(dia/2.0d00/sdcold)
        sxznew = sdcold * cos(sig2)
c
        if(sxz.gt.sxznew) then
            sxz = sxznew
        endif
c

```

```

x = xold + sxz * rxnew
z = zold + sxz * rznew
sdc = sqrt((dx-x)**2+(dz-z)**2)

```

c

c Does the bundle impacts with the pipe ?

c

```

if(sdc.lt.dia/2.0d00) then
  ddx = dx - xold
  ddz = dz - zold
  sdotr = rxnew * ddx + rznew * ddz
  rsqr = ddx**2 + ddz**2
  sarg = sdotr**2 - (rsqr - dia**2/4.0d00)
  sxz = sdotr - sqrt(sarg)

```

c

c Calculate impact point of bundle with pipe

c

```

s = sxz / sqrt(rx**2 + rz**2)
x = xold + s * rx
y = yold + s * ry
z = zold + s * rz

```

c

c Does the bundle hit the surface 5 or 6 before hit the pipe ?

c

```

if(y.le.0.0d00) then
  call surface5
elseif(y.gt.alen) then
  call surface6
else

```

c

c The bundle hits the pipe

c

```

rx = (x-dx)/(dia/2.0d00)
rz = (z-dz)/(dia/2.0d00)

```

c

c Change the impact point to angle value(from 0 to 2pi)

c

```

if(rx.ge.0.0d00.and.rz.gt.0.0d00) then
  eta = atan(rx/rz)
elseif(rx.ge.0.0d00.and.rz.eq.0.0d00) then
  eta = pi/2.0d00
elseif(rz.le.0.0d00) then
  if(rx.lt.0.0d00.and.rz.eq.0.0d00) then
    eta = 1.5d00*pi
  else
    eta = pi + atan(rx/rz)

```

```

        endif
    else
        eta = 2.0d00*pi + atan(rx/rz)
    endif
c
c Does the bundle absorb by the pipe ?
c
    if(ran3(0).le.abop) then
        ix = 1
        do 100 i = 1,ky
            if(y.le.alen*i/ky) then
                ni = i
                goto 200
            endif
100        continue
200        do 300 j = 1,kp
            ramda2 = 2.0d00 * pi * j / kp
            if(eta.le.ramda2) then
                nsp(ni,j) = nsp(ni,j) + 1
                goto 400
            endif
300        continue
c
c Because the bundle does not absorbed, it will be reflected. So
c generate new random numbers and calculate "thetap" and "phip"
c for new direction of the bundle emitted from pipe.
c
        else
            ix = 2
            s = sold - s
            theta = asin(sqrt(ran3(0)))
            phi = 2.0d00 * pi * ran3(0)
            rx = sin(theta) * cos(phi)
            ry = sin(theta) * sin(phi)
            rz = cos(theta)
c
c Calculate new direction based on x-z coordinate
c
            sr = sqrt(rx**2 + rz**2)
            pi = 4.0d00 * atan(1.0d00)
c
            if(rx.ge.0.0d00.and.rz.gt.0.0d00) then
                etap = atan(rx/rz)
            elseif(rx.ge.0.0d00.and.rz.eq.0.0d00) then
                etap = pi / 2.0d00

```

```

elseif(rz.le.0.0d00) then
  if(rx.lt.0.0d00.and.rz.eq.0.0d00) then
    etap = 1.5d00 * pi
  else
    etap = pi + atan(rx/rz)
  endif
else
  etap = 2.0d00 * pi + atan(rx/rz)
endif

eta = eta + etap
rx = sin(eta)
rz = cos(eta)

if(rx.ge.0.0d00.and.rz.gt.0.0d00) then
  etap = atan(rx/rz)
elseif(rx.ge.0.0d00.and.rz.eq.0.0d00) then
  etap = pi / 2.0d00
elseif(rz.le.0.0d00) then
  if(rx.lt.0.0d00.and.rz.eq.0.0d00) then
    etap = 1.5d00 * pi
  else
    etap = pi + atan(rx/rz)
  endif
else
  etap = 2.0d00 * pi + atan(rx/rz)
endif

c
  eta = etap
  rx = rx * sr
  rz = rz * sr

c
  s = -1.0d00 / absco * dlog(ran3(0))
  call wall
endif

c
c The bundle doesn't reach to the pipe. It is absorbed in the
c gas and reemitted.
c
  else
    ixx = 3
    call gas
  endif

```

```

400 return
end

```

```

c-----
c This subroutine calculates the bundle historz which hit
c the walls.
c-----

subroutine wall
c
include 'com.for'
c
xold = x
yold = y
zold = z
x = xold + s * rx
y = yold + s * ry
z = zold + s * rz
rxnew = sin(eta)
rynew = sin(phi)
rznew = cos(eta)
c
c Calculate walls position based on old position(xold,zold)
c of bundle.
c
if((xold**2 + (hig - zold)**2).eq.0.0d00) then
r3u = 0.0d00
else
r3u = (hig - zold) / sqrt(xold**2 + (hig - zold)**2)
endif
c
if((xold**2 + zold**2).eq.0.0d00) then
r3d = 0.0d00
else
r3d = -zold / sqrt(xold**2 + zold**2)
endif
c
if(sqrt((width-xold)**2 + (hig-zold)**2).eq.0.0d00) then
r2u = 0.0d00
else
r2u = (hig-zold) / sqrt((width-xold)**2 + (hig-zold)**2)
endif
c
if(sqrt((width-xold)**2 + zold**2).eq.0.0d00) then
r2d = 0.0d00

```

```

else
  r2d = -zold / sqrt((width-xold)**2 + zold**2)
endif
c
c Deside direction of bundle
c
if(rxnew.ge.0.0d00) then
  if(rznew.lt.r2d) then
    call surface1
  elseif(rznew.ge.r2d.and.rznew.lt.r2u) then
    call surface2
  else
    call surface4
  endif
else
  if(rznew.le.r3d) then
    call surface1
  elseif(rznew.gt.r3d.and.rznew.le.r3u) then
    call surface3
  else
    call surface4
  endif
endif
c
return
end

```

```

c-----
c This subroutine calculates the bundle history which hit
c the surface 1.
c-----

```

```

subroutine surface1
c
include 'com.for'
c
if(z.lt.0.0d00) then
  zold2 = z
  tau = zold/abs(rz)
  x = xold + tau * rx
  y = yold + tau * ry
  z = 0.0d00

  if(y.lt.0.0d00) then
    call surface5
  endif
endif

```

```

elseif(y.gt.alen) then
  call surface6
else

  if(ran3(0).le.abopw) then
    ix = 1
    do 10 i=1,kx
      if(x.le.width*i/kx) then
        ni = i
        goto 20
      endif
10    continue
20    do 30 j = 1,ky
      if(y.le.alen*j/ky) then
        ns1(ni,j) = ns1(ni,j) + 1
        goto 40
      endif
30    continue

c
c   The bundle is reflected
c
    else
      ix = 2
      s = s-abs(zold*s/(zold2-zold))

c
c   Diffuse reflection
c
      if(ran3(0).gt.specu) then
        eta = 0.0d00
        theta = asin(sqrt(ran3(0)))
        phi = 2.0d00 * pi * ran3(0)
        rx = sin(theta) * cos(phi)
        ry = sin(theta) * sin(phi)
        rz = cos(theta)
        call caleta(eta,rx,rz)

c
c   Specular reflection
c
      else
        rx = rx
        ry = ry
        rz = -rz
        if(rx.ge.0.0d00) then
          eta = pi - eta
        else

```

```

        eta = 3.0d00 * pi - eta
    endif
endif
endif
endif
c
c Does the bundle hit the surface 5 or 6 ?
c
    elseif(y.lt.0.0d00) then
        call surface5
    elseif(y.gt.alen) then
        call surface6
c
c The bundle is located in gas
c
    else
        ix = 3
        call gas
    endif
c
40 return
end

c-----
c This subroutine calculates the bundle historz which hit
c the surface 2.
c-----

subroutine surface2
c
include 'com.for'
c
if(x.gt.width) then
    xold = x
    tau = (width-xold) / abs(rx)
    x = width
    y = yold + tau * ry
    z = zold + tau * rz

    if(y.lt.0.0d00) then
        call surface5
    elseif(y.gt.alen) then
        call surface6
    else
c

```

```

    if(ran3(0).le.abopw) then
      ix = 1
      do 10 i=1,kz
        if(z.le.hig*i/kz) then
          ni = i
          goto 20
        endif
10      continue
20      do 30 j = 1,ky
        if(y.le.alen*j/ky) then
          ns2(j,ni) = ns2(j,ni) + 1
          goto 40
        endif
30      continue
c
c    The bundle is reflected
c
      else
        ix = 2
        s = s - abs((xold-width)*s/(xold2-xold))
c
c    Diffuse reflection
c
        if(ran3(0).gt.specu) then
          eta = 1.5d00 * pi
          theta = asin(sqrt(ran3(0)))
          phi = 2.0d00 * pi * ran3(0)
          rx = -cos(theta)
          ry = sin(theta) * sin(phi)
          rz = sin(theta) * cos(phi)
          call caleta(eta,rx,rz)
c
c    Specular reflection
c
          else
            rx = -rx
            ry = ry
            rz = rz
            eta = 2.0d00 * pi - eta
          endif
        endif
      endif
c
c    Does the bundle hit the surface 5 or 6 ?
c

```

```

elseif(y.lt.0.0d00) then
  call surface5
elseif(y.gt.alen) then
  call surface6
c
c The bundle is located in gas
c
  else
    ixx = 3
    call gas
  endif
c
40 return
end

c-----
c This subroutine calculates the bundle history which hit
c the surface 3.
c-----

subroutine surface3
c
include 'com.for'
c
if(x.lt.0.0d00) then
  xold2 = x
  tau = xold / abs(rx)
  x = 0.0d00
  y = yold + tau * ry
  z = zold + tau * rz
c
  if(y.lt.0.0d00) then
    call surface5
  elseif(y.gt.alen) then
    call surface6
  else
    if(ran3(0).le.abopw) then
      ixx = 1
      do 10 i=1,kz
        if(z.le.hig*i/kz) then
          ni = i
          goto 20
        endif
10      continue
20      do 30 j = 1,ky

```

```

        if(y.le.alen*j/ky) then
            ns3(j,ni) = ns3(j,ni) + 1
            goto 40
        endif
30    continue
c
c    The bundle is reflected
c
        else
            ix = 2
            s = s - abs(xold*s/(xold2-xold))
c
c    Diffuse reflection
c
            if(ran3(0).gt.specu) then
                eta = pi / 2.0d00
                theta = asin(sqrt(ran3(0)))
                phi = 2.0d00 * pi * ran3(0)
                rx = cos(theta)
                ry = sin(theta) * sin(phi)
                rz = -sin(theta) * cos(phi)
                call caleta(eta,rx,rz)
c
c    Specular reflection
c
            else
                rx = -rx
                ry = ry
                rz = rz
                eta = 2.0d00 * pi - eta
            endif
        endif
    endif
c
c    Does the bundle hit the surface 5 or 6 ?
c
        elseif(y.lt.0.0d00) then
            call surface5
        elseif(y.gt.alen) then
            call surface6
c
c    the bundle is located in gas
c
        else
            ix = 3

```

```

        call gas
    endif
c
    40 return
    end

c-----
c   This subroutine calculates the bundle history which hit
c           the surface 4.
c-----

    subroutine surface4
c
    include 'com.for'
c
    if(z.gt.hig) then
        zold2 = z
        tau = (hig - zold) / abs(rz)
        x = xold + tau * rx
        y = yold + tau * ry
        z = hig
c
    if(y.lt.0.0d00) then
        call surface5
    elseif(y.gt.alen) then
        call surface6
    else

        if(ran3(0).le.abopw) then
            ixx = 1
            do 10 i = 1,kx
                if(x.le.width*i/kx) then
                    ni = i
                    goto 20
                endif
            10 continue
            20 do 30 j = 1,ky
                if(y.le.alen*j/ky) then
                    ns4(ni,j) = ns4(ni,j) + 1
                    goto 40
                endif
            30 continue
c
c   The bundle is reflected
c

```

```

    else
      ix = 2
      s = s-abs((hig-zold)*s/(zold2-zold))
c
c   Diffuse reflection
c
      if(ran3(0).gt.specu) then
        eta = pi
        theta = asin(sqrt(ran3(0)))
        phi = 2.0d00 * pi * ran3(0)
        rx = -sin(theta) * cos(phi)
        ry = sin(theta) * sin(phi)
        rz = -cos(theta)
        call caleta(eta,rx,rz)
c
c   Specular reflection
c
      else
        rx = rx
        ry = ry
        rz = -rz
        if(rx.ge.0.0d00) then
          eta = pi - eta
        else
          eta = 3.0d00 * pi - eta
        endif
      endif
    endif
  endif
c
c   Does the bundle hit the surface 5 or 6 ?
c
  elseif(y.lt.0.0d00) then
    call surface5
  elseif(y.gt.alen) then
    call surface6
c
c   The bundle is located in gas
c
  else
    ix = 3
    call gas
  endif
c
40 return

```

end

```

c-----
c This subroutine calculates the bundle history which hit
c the surface 5.
c-----

```

```

subroutine surface5
c
c include 'com.for'
c
yold2 = y
tau = yold/abs(ry)
x = xold + tau * rx
z = zold + tau * rz
y = 0.0d00

if(ran3(0).le.abopw) then
  ix = 1
  do 10 i = 1,kx
    if(x.le.width*i/kx) then
      ni = i
      goto 20
    endif
10  continue
20  do 30 j = 1,kz
    if(z.le.hig*j/kz) then
      ns5(ni,j) = ns5(ni,j) + 1
      goto 40
    endif
30  continue
  else
    ix = 2
    s = s - abs(yold*s/(yold2-yold))
    if(ran3(0).gt.specu) then
      theta = asin(sqrt(ran3(0)))
      phi = 2.0d00 * pi * ran3(0)
      rx = sin(theta) * cos(phi)
      ry = cos(theta)
      rz = -sin(theta) * sin(phi)
      call caleta(eta,rx,rz)
    else
      rx = rx
      ry = -ry
      rz = rz

```

```

        eta = eta
    endif
endif

40 return
end

c-----
c  This subroutine calculates the bundle history which hit
c          the surface 6.
c-----

subroutine surface6
c
c  include 'com.for'
c
yold2 = y
tau = (alen-yold)/abs(ry)
x = xold + tau * rx
z = zold + tau *rz
y = alen
c
if(ran3(0).le.abopw) then
    ix = 1
    do 10 i = 1,kx
        if(x.le.width*i/kx) then
            ni = i
            goto 20
        endif
10    continue
20    do 30 j = 1,kz
        if(z.le.hig*j/kz) then
            ns6(ni,j) = ns6(ni,j) + 1
            goto 40
        endif
30    continue
    else
        ix = 2
        s = s - abs((yold-alen)*s/(yold2-yold))
        if(ran3(0).gt.specu) then
            theta = asin(sqrt(ran3(0)))
            phi = 2.0d00 * pi * ran3(0)
            rx = - sin(theta) * cos(phi)
            ry = - cos(theta)
            rz = - sin(theta) * sin(phi)

```

```

        call caleta(eta,rx,rz)
    else
        rx = rx
        ry = -ry
        rz = rz
        eta = eta
    endif
endif

40 return
end

```

```

c-----
c   This subroutine caleta calculates new directions based on
c           X - z coordinate.
c-----

```

```

subroutine caleta(eta,rx,rz)
real*8 eta,rx,rz,pi

pi = 4.0d00 * atan(1.0d00)
c
if(rx.ge.0.0d00.and.rz.gt.0.0d00) then
    etap = atan(rx/rz)
elseif(rx.ge.0.0d00.and.rz.eq.0.0d00) then
    etap = pi / 2.0d00
elseif(rz.le.0.0d00) then
    if(rx.lt.0.0d00.and.rz.eq.0.0d00) then
        etap = 1.5d00 * pi
    else
        etap = pi + atan(rx/rz)
    endif
else
    etap = 2.0d00 * pi + atan(rx/rz)
endif
eta = etap
c
return
end

```

```

c-----
c   This function program generates random number.
c
c-----

```

```

function ran3(idum)
c
c implicit real*4(m)
c parameter (mbig=4000000.,mseed=1618033.,mz=0.,fac=2.5e-7)
c
implicit real*8 (a-h,o-z)
parameter (mbig=1000000000,mseed=161803398,mz=0,fac=1.e-9)
dimension ma(55)
data iff /0/
if(idum.lt.0.or.iff.eq.0)then
  iff=1
  mj=mseed-iabs(idum)
  mj=mod(mj,mbig)
  ma(55)=mj
  mk=1
  do 11 i=1,54
    ii=mod(21*i,55)
    ma(ii)=mk
    mk=mj-mk
    if(mk.lt.mz)mk=mk+mbig
    mj=ma(ii)
11 continue
  do 13 k=1,4
    do 12 i=1,55
      ma(i)=ma(i)-ma(1+mod(i+30,55))
      if(ma(i).lt.mz)ma(i)=ma(i)+mbig
12 continue
13 continue
  inext=0
  inextp=31
endif
inext=inext+1
if(inext.eq.56)inext=1
inextp=inextp+1
if(inextp.eq.56)inextp=1
mj=ma(inext)-ma(inextp)
if(mj.lt.mz)mj=mj+mbig
ma(inext)=mj
ran3=mj*fac
return
end

```

```

c-----
c This subroutine calculate new direction of bundles emitted
c from medium and counts bundle numbers

```

```
c-----  
  
      subroutine gas  
c  
      include 'com.for'  
c  
      pi = 3.141592654  
      theta = acos(1.0d00 - 2.0d00 * ran3(0))  
      phi = 2.0d00 * pi * ran3(0)  
      rx = sin(theta) * cos(phi)  
      ry = sin(theta) * sin(phi)  
      rz = cos(theta)  
c  
      call caleta(eta,rx,rz)  
c  
      do 20 i = 1,kz  
        if(z.le.hig*i/kz) then  
          ni = i  
          goto 25  
        endif  
      20 continue  
      25 do 30 j = 1,ky  
        if(y.le.alen*j/ky) then  
          nj = j  
          goto 40  
        endif  
      30 continue  
      40 do 45 k = 1,kx  
        if(x.le.width*k/kx) then  
          nsa(k,nj,ni) = nsa(k,nj,ni) + 1  
          goto 50  
        endif  
      45 continue  
c  
      50 return  
      end  
  
c-----  
c   This subroutine read in all information necessarz to perform  
c   the simulation.  
c-----  
  
      subroutine input  
c  
      include 'com.for'
```

```
c
  open(unit=5,file='input3d.dat',status='old')
c
c   Line 1 : read the dimension of model
c
c   width(real) : width of  enclouser
c   alen(real): length of enclouser
c   hig(real) : hight of  enclouser
c   dia(real) : diameter of the pipe
c   dx(real)  : distance from left of the enclouser to the center
c               of the pipe
c   dz(real)  : distance from bottom of the enclouser to the center
c               of the pipe
c
c   read(5,*) width,alen,hig,dia,dx,dz
c
c   Line 2
c
c   kx  : number of strip in x-direction
c   ky  : number of strip in y-direction
c   kz  : number of strip in z-direction
c   kp  : number of segment through the circumference of circle
c   nuemx : number of emitting sources in x direction
c   nuemy : number of emitting sources in y direction
c   npn  : total number of bundles at each emitting source
c
c   read(5,*) kx,ky,kz,kp,nuemx,nuemy,npn
c
c   Line 3 : read each properties
c
c   abopw : absorptivitz of walls(Assume that all surfaces except
c           the circle have same surface properties)
c   specu : specularitz of wall surfaces
c   abop  : absorptivitz of circle surface
c
c   read(5,*) abopw,specu,abop
c
c   Line 4
c
c   ot  : optical thickness of media
c
c   read(5,*) ot
c   close(5)
c
c   Write out setup information of given model
```

c

```

write(6,2000)
write(6,2010) width
write(6,2015) alen
write(6,2020) hig
write(6,2030) dia
write(6,2040) dx
write(6,2050) dz
write(6,2060) kx
write(6,2065) ky
write(6,2070) kz
write(6,2080) kp
write(6,2090) nuemx
write(6,2095) nuemy
write(6,2100) npn
write(6,2110) abopw
write(6,2120) specu
write(6,2130) abop
write(6,2140) ot

```

c

```

2000 format(7x,'Dimension and properties of given model')
2010 format(7x,'width of rectangular enclouser           :',f7.3)
2015 format(7x,'length of rectangular enclouser        :',f7.3)
2020 format(7x,'hight of rectangular enclouser         :',f7.3)
2030 format(7x,'diameter of the circle                  :',f7.3)
2040 format(7x,'distance from left of the enclouser to '/
+ '                the center of circle           :',f7.3)
2050 format(7x,'distance from bottom of the enclouser to '/
+ '                the center of circle           :',f7.3)
2060 format(7x,'number of strips in x-direction         :',i4)
2065 format(7x,'number of strips in y-direction        :',i4)
2070 format(7x,'number of strips in z-direction        :',i4)
2080 format(7x,'number of strips in circumference of circle :',i4)
2090 format(7x,'number of emitting sources in x direction :',i4)
2095 format(7x,'number of emitting sources in y direction :',i4)
2100 format(7x,'number of bundles at each emitting'/
+ '                source                          :',i6)
2110 format(7x,'absorptivitz of walls                   :',f7.3)
2120 format(7x,'specularitz of wall surfaces             :',f7.3)
2130 format(7x,'absorptivitz of circle surface          :',f7.3)
2140 format(7x,'optical thickness of media               :',f7.3)

```

c

```

return
end

```

```

c-----
c           This subroutine print out the results
c-----

      subroutine output
c
c      include 'com.for'
c
c      delx = width/kx
c      dely = alen/ky
c      delz = hig/kz
c      totaln = npn * nuemx * nuemy
c
c      open(unit=7,file='medium.dat',status='old')
c      write(7,*)'This is the distribution of bundle fraction in medium'
c      write(7,*)'-----'
c      write(7,*)'          Position          Fraction'
c      write(7,*)'          (x,y,z)          N(xyz)/N(total)'
c      write(7,*)'-----'
c      do 200 i=1,kx
c          sum = 0.0d00
c          do 100 j=1,ky
c              do 50 k = 1,kz
c                  frac = nsa(i,j,k)/totaln
c                  px = width / kx * i - width / 2.0d00 / kx
c                  py = alen / ky * j - alen / 2.0d00 / ky
c                  pz = hig / kz * k - hig / 2.0d00 / kz
c                  sum = sum + frac
c                  write(7,1000) px,py,pz,frac
c      50      continue
c              write(7,*)
c      100     continue
c              write(7,1100) i,sum
c              write(7,*)
c      200     continue
c              close(7)
c
c
c      open(unit=7,file='wall14.dat',status='old')
c      write(7,*)' Distribution of bundle fraction in wall-1,4'
c      write(7,*)'-----'
c      write(7,*)'          Position(y,z)          Wall - 1          Wall - 4'
c      write(7,*)'-----'
c      sum1 = 0.0d00
c      sum4 = 0.0d00

```

```

do 300 i=1,kx
  do 250 j = 1,ky
    fra1 = ns1(i,j)/delx/dely/(totaln/width/alen)
    fra4 = ns4(i,j)/delx/dely/(totaln/width/alen)
    px = width / kx * i
    py = alen / ky * j
    sum1 = sum1 + ns1(i,j)/totaln
    sum4 = sum4 + ns4(i,j)/totaln
    write(7,1200) px,py,fra1,fra4
250  continue
    write(7,*)
300  continue
    write(7,1300) sum1,sum4
    close(7)
c
c
open(unit=7,file='wall23.dat',status='old')
write(7,*)'   Distribution of bundle fraction in Wall-2,3'
write(7,*)'   -----'
write(7,*)'   Position(z)      Wall - 2      Wall - 3'
write(7,*)'   -----'
sum2 = 0.0d00
sum3 = 0.0d00
do 400 i=1,ky
  do 350 j=1,kz
    fra2 = ns2(i,j)/dely/delz/(totaln/width/alen)
    fra3 = ns3(i,j)/dely/delz/(totaln/width/alen)
    py = alen / ky * i
    pz = hig / kz * j
    sum2 = sum2 + ns2(i,j)/totaln
    sum3 = sum3 + ns3(i,j)/totaln
    write(7,1200) py,pz,fra2,fra3
350  continue
    write(7,*)
400  continue
    write(7,1300) sum2,sum3
    close(7)
c
c
open(unit=7,file='pipe.dat',status='old')
write(7,*)'   Distribution of bundle fraction in Pipe'
write(7,*)'   -----'
write(7,*)'   Position      Fraction'
write(7,*)'   (y,angle)      N(y,angle)/N(total)'
write(7,*)'   -----'

```

```

sum = 0.0d00
do 500 i=1,ky
  do 450 j=1,kp
    frac = nsp(i,j)/dely/(pi*dia/kp)/(totaln/width/alen)
    py = alen / ky * i
    pd = 360.0d00 / kp * j
    sum = sum + nsp(i,j)/totaln
    write(7,1400) py,pd,frac
450  continue
    write(7,*)
500  continue
    write(7,1500) sum
    close(7)
c
open(unit=7,file='wall56.dat',status='old')
write(7,*)'  Distribution of bundle fraction in Wall-5,6'
write(7,*)'  -----'
write(7,*)'      Position(x,z)      Wall - 5      Wall - 6'
write(7,*)'  -----'
sum5 = 0.0d00
sum6 = 0.0d00
do 510 i=1,kx
  do 510 j=1,kz
    a56(i,j)=0.25d00
510  continue

a56(8,8)=0.015
a56(13,8)=0.015
a56(8,13)=0.015
a56(13,13)=0.015
a56(7,8)=0.209945
a56(8,7)=0.209945
a56(13,7)=0.209945
a56(14,8)=0.209945
a56(13,14)=0.209945
a56(14,13)=0.209945
a56(7,13)=0.209945
a56(8,14)=0.209945
a56(7,9)=0.077207
a56(9,7)=0.077207
a56(12,7)=0.077207
a56(14,9)=0.077207
a56(14,12)=0.077207
a56(12,14)=0.077207
a56(7,12)=0.077207

```

```

a56(9,14)=0.077207
a56(7,10)=0.00957
a56(10,7)=0.00957
a56(7,11)=0.00957
a56(11,7)=0.00957
a56(14,10)=0.00957
a56(14,11)=0.00957
a56(10,14)=0.00957
a56(11,14)=0.00957

do 600 i=1,kx
  do 550 j=1,kz

    fra5 = ns5(i,j)/a56(i,j)/(totaln/width/alen)
    fra6 = ns6(i,j)/a56(i,j)/(totaln/width/alen)
    px = width / kx * i
    pz = hig / kz * j
    sum5 = sum5 + ns5(i,j)/totaln
    sum6 = sum6 + ns6(i,j)/totaln
    write(7,1200) px,pz,fra5,fra6
550  continue
    write(7,*)
600  continue
    write(7,1300) sum5,sum6
    close(7)
c
1000 format(3x,3f7.2,f18.6)
1100 format('    Total fraction in column(',i3,') : ',f9.6)
1200 format(4x,2f7.2,2f16.6)
1300 format('    Total fractions :',f9.6,f16.6)
1400 format(6x,2f8.2,f20.6)
1500 format('    Total fraction in pipe : ',f8.6)
c
    write(6,1800) akkk(jk)/10.0,sum,sum4,sum2,sum5
1800 format(2x,f7.2,4f9.5)
    return
    end
c-----

```

```
c-----  
c           Cmomon block for hong3d.for  
c-----  
  implicit real*8(a-h,o-z)  
  integer ns1(30,30),ns2(30,30),ns3(30,30),ns4(30,30),  
+      ns5(30,30),ns6(30,30),nsp(30,36),nsa(30,30,30)  
  real*8 a56(20,20),otp(20),akkk(20)  
  common /proper/ specu,abopw,abop,ot,absco  
  common /bundle/ nuemx,nuemy,npn  
  common /locate/ x,y,z,xold,yold,zold,rx,ry,rz,dx,dz,kx,ky,kz,kp  
  common /shape/ width,alen,hig,dia  
  common /surface/ ix,x,ns1,ns2,ns3,ns4,ns5,ns6,nsp,nsa,a56  
  common /angle/ pi,s,eta,phi  
  common /new/ rxnew,rynew,rznew,otp,akkk,jk  
c-----
```